Introduction to optical/IR interferometry

History and basic principles

J. Surdej

Institute of Astrophysics and Geophysics
Liège University
Allée du 6 Août 19c, 4000 Liège, Belgium

E-mail: jsurdej@ulg.ac.be

IUCAA (India), 17-25 April 2018

Table of Contents

LIÈGE université

Table of Contents

LIÈGE université

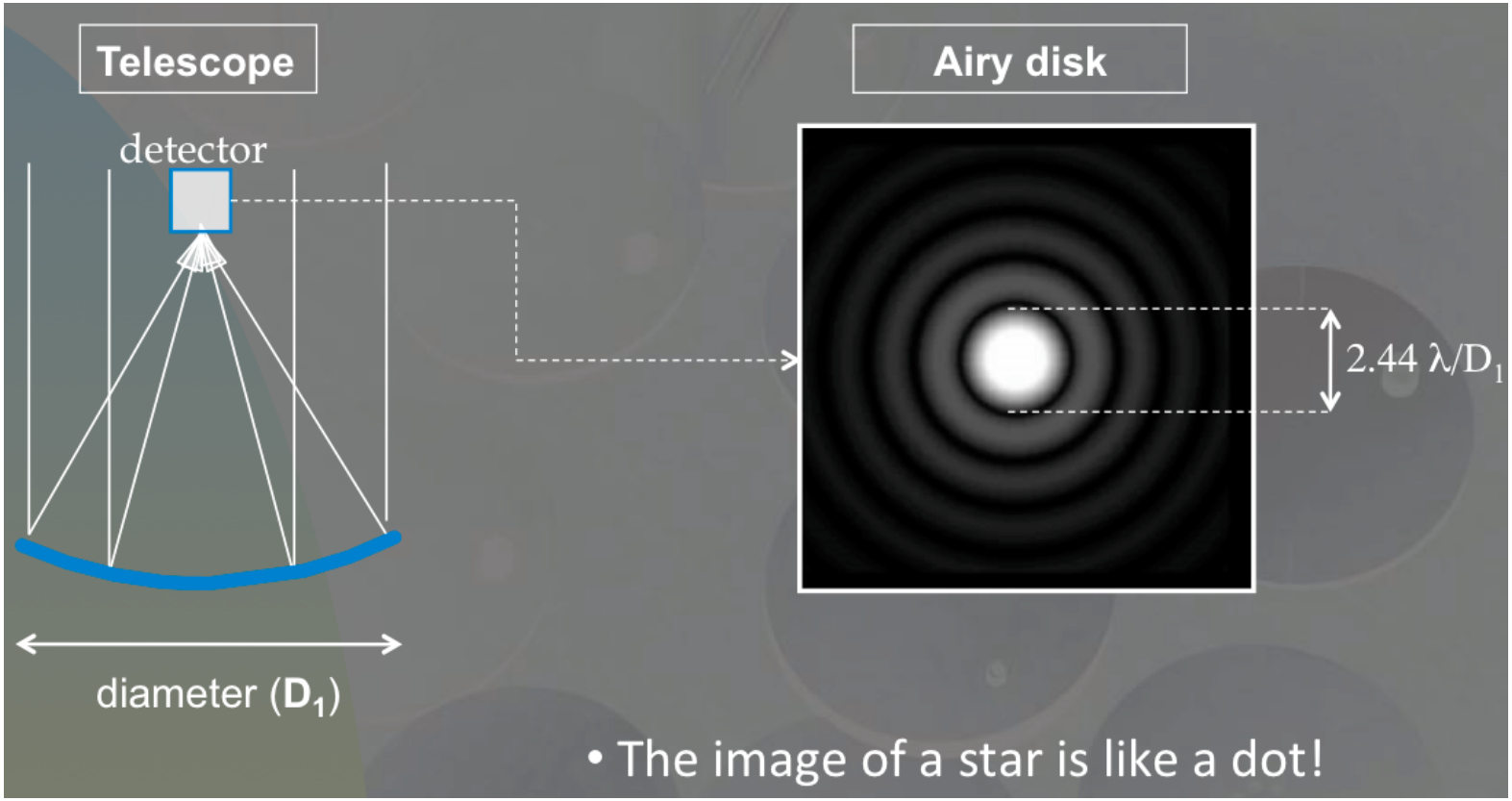

Figure: Airy disk of a point-like star recorded in the focal plane of a telescope with diameter D_1. The angular diameter of the Airy disk is 2.44 λ/D_1.

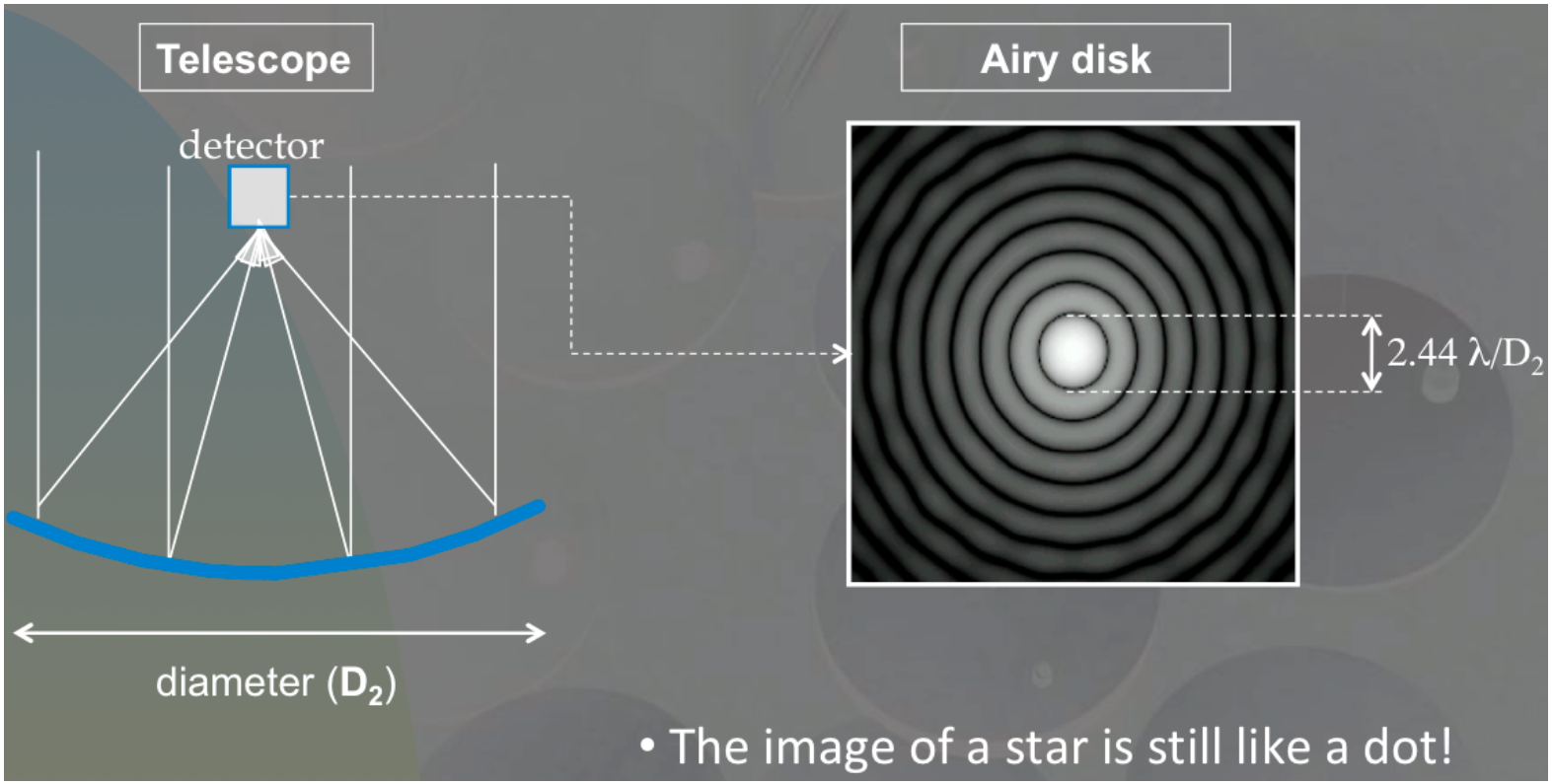

Figure: As the diameter of a telescope increases ($D_2 > D_1$), the Airy disk of a point-like star gets smaller.

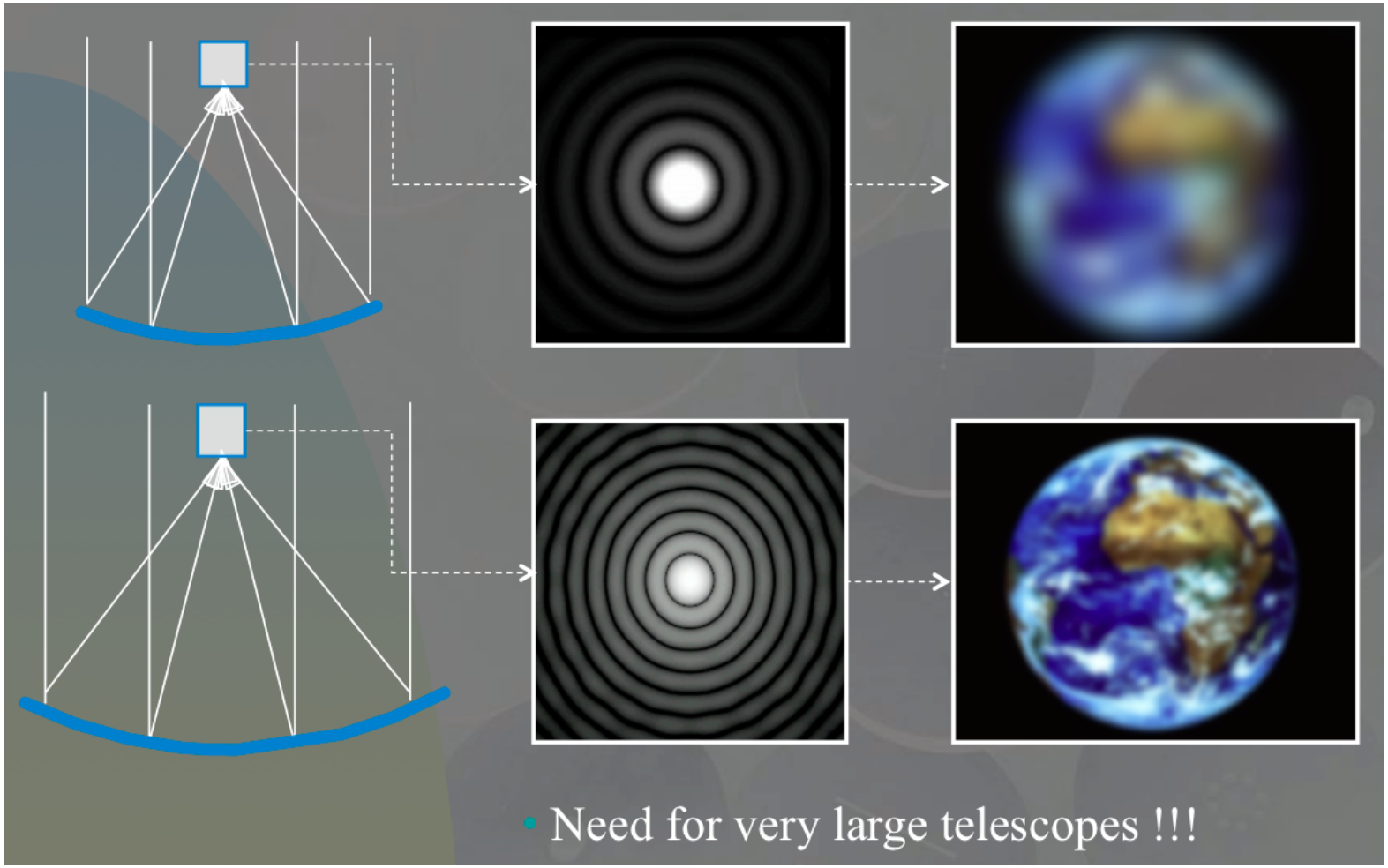

Figure: While observing an extended celestial object (cf. an Earth-like planet) above the atmosphere, we see more details as the diameter of the telescope increases.

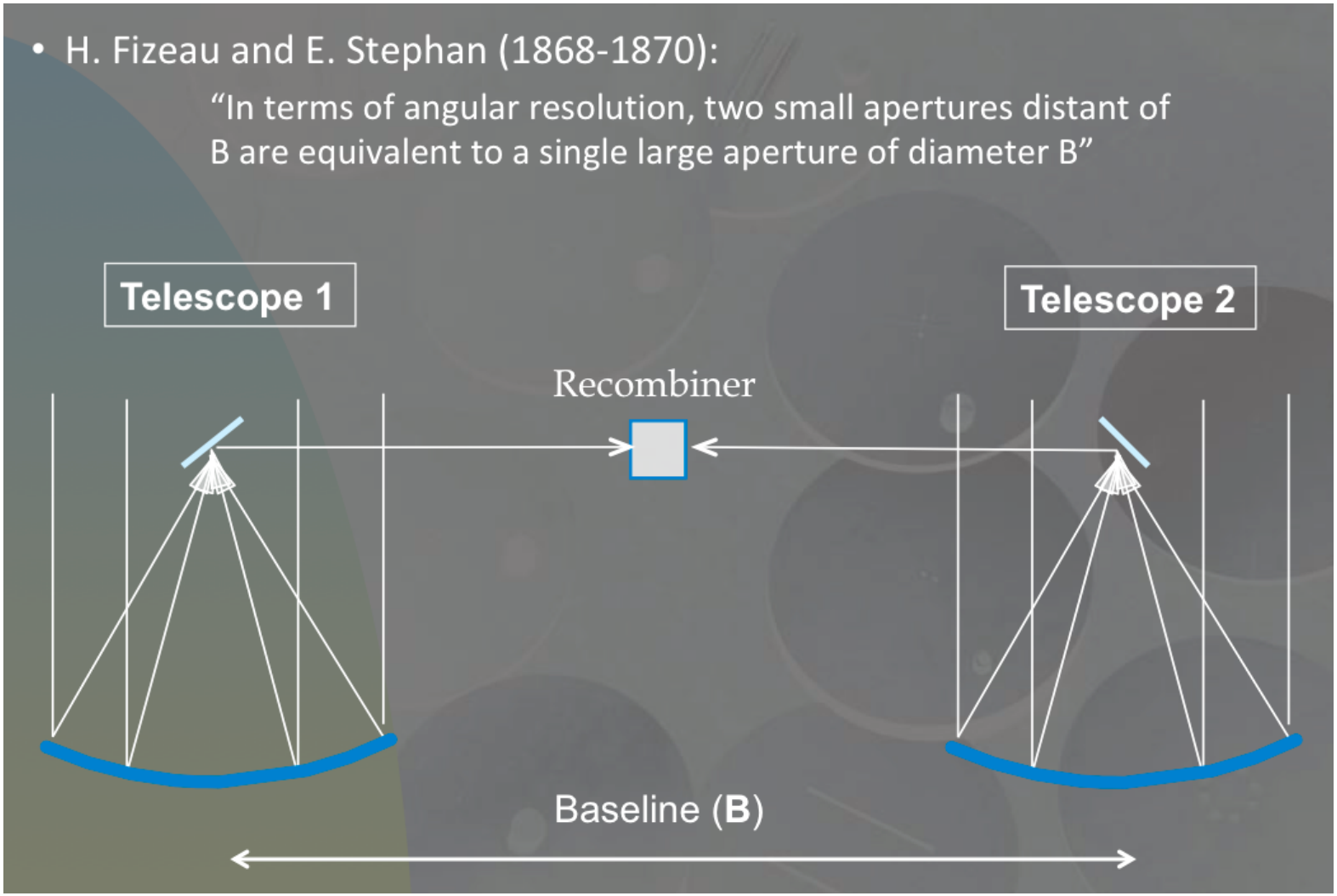

Figure: Fizeau and Stephan proposed to recombine the light from two independent telescopes separated by a baseline B to recover the same angular resolution as that given by a single dish telescope having a diameter B.

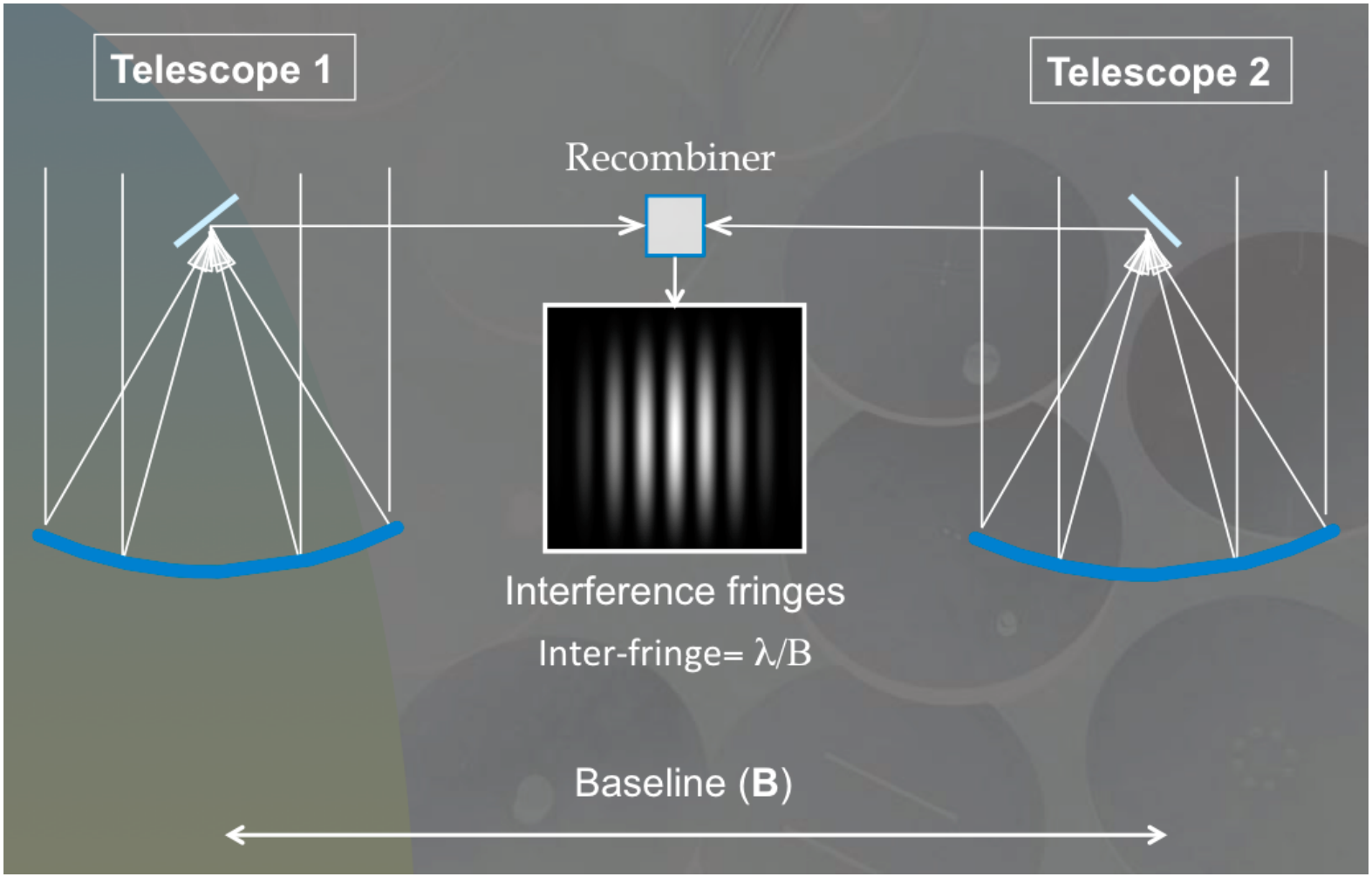

Figure: When recombining the monochromatic light of two independent telescopes, there results the formation of a pattern of bright and dark fringes superimposed over the combined Airy disk. The angular inter-fringe separation is equal to λ/B.

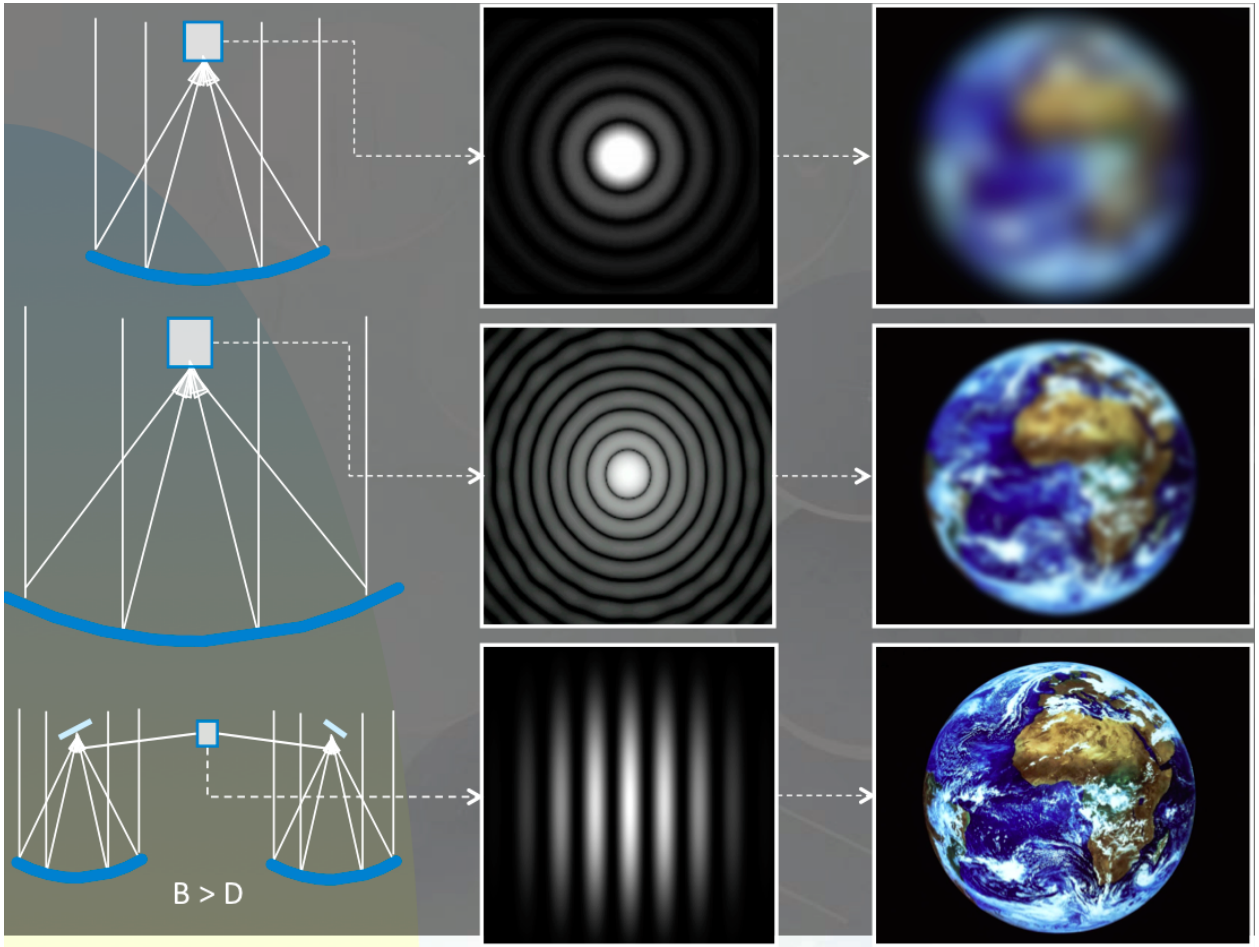

Figure: Improvement expected in angular resolution while observing an extended celestial source (cf. an Earth-like planet) with telescopes of increasing size ($D_2 > D_1$) and with an interferometer composed of two telescopes separated by a baseline $B > D$.

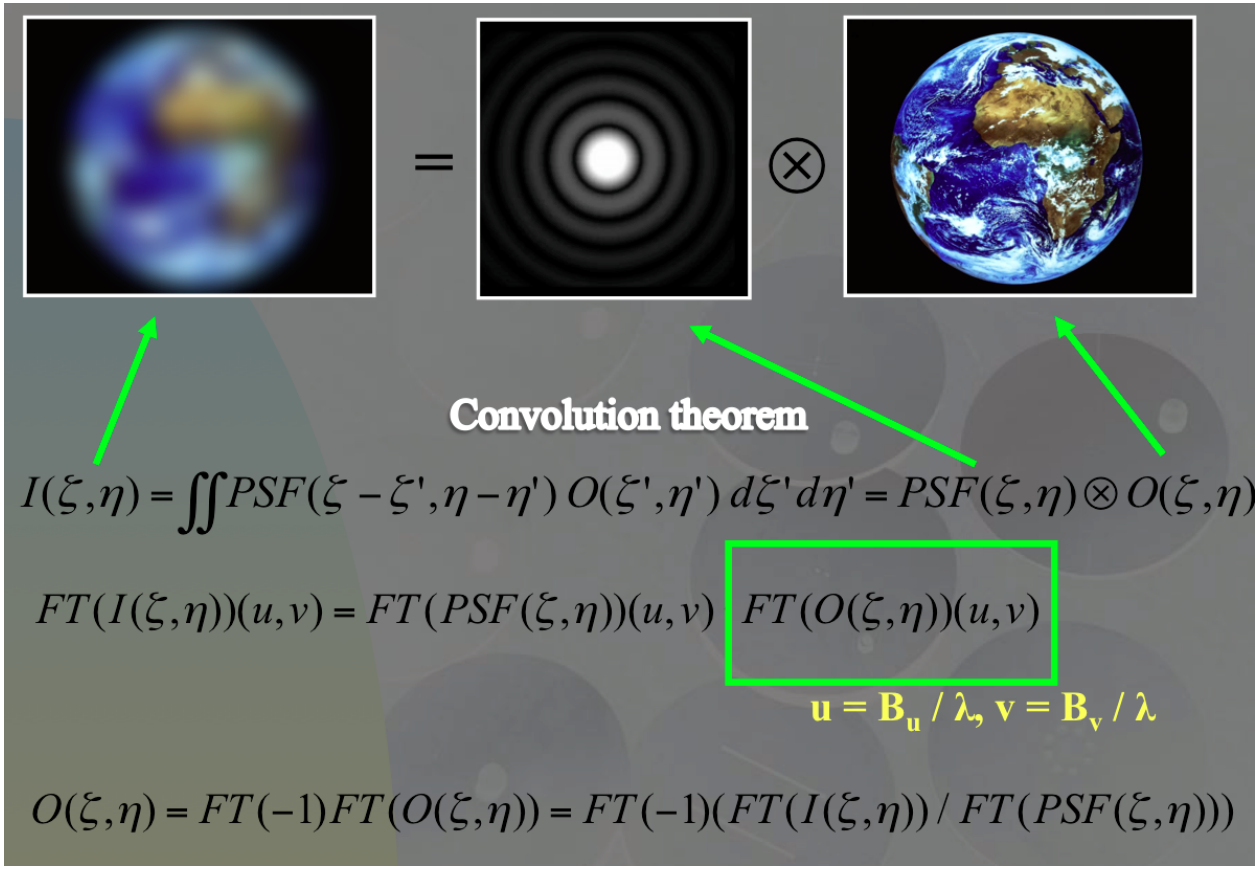

Figure: The image $I(\zeta,\eta)$ we observe in the focal plane of an instrument (cf. single dish telescope) from a distant extended source as a function of its angular coordinates ζ,η is the convolution product of the real source image (cf. the extended Earth-like planet, $O(\zeta,\eta)$) by the point spread function $PSF(\zeta,\eta)$ of the telescope.

$$O(\zeta,\eta) = FT_{-}^{-1}(FT_{-}(O(\zeta,\eta))(u,v))(\zeta,\eta) =$$
$$\mathrm{FT}_{-}^{-1}\left(\frac{FT_{-}(I(\zeta,\eta))(u,v)}{FT_{-}(PSF(\zeta,\eta))(u,v)}\right)(\zeta,\eta). \quad (1)$$

Table of Contents

LIÈGE université

Some reminders

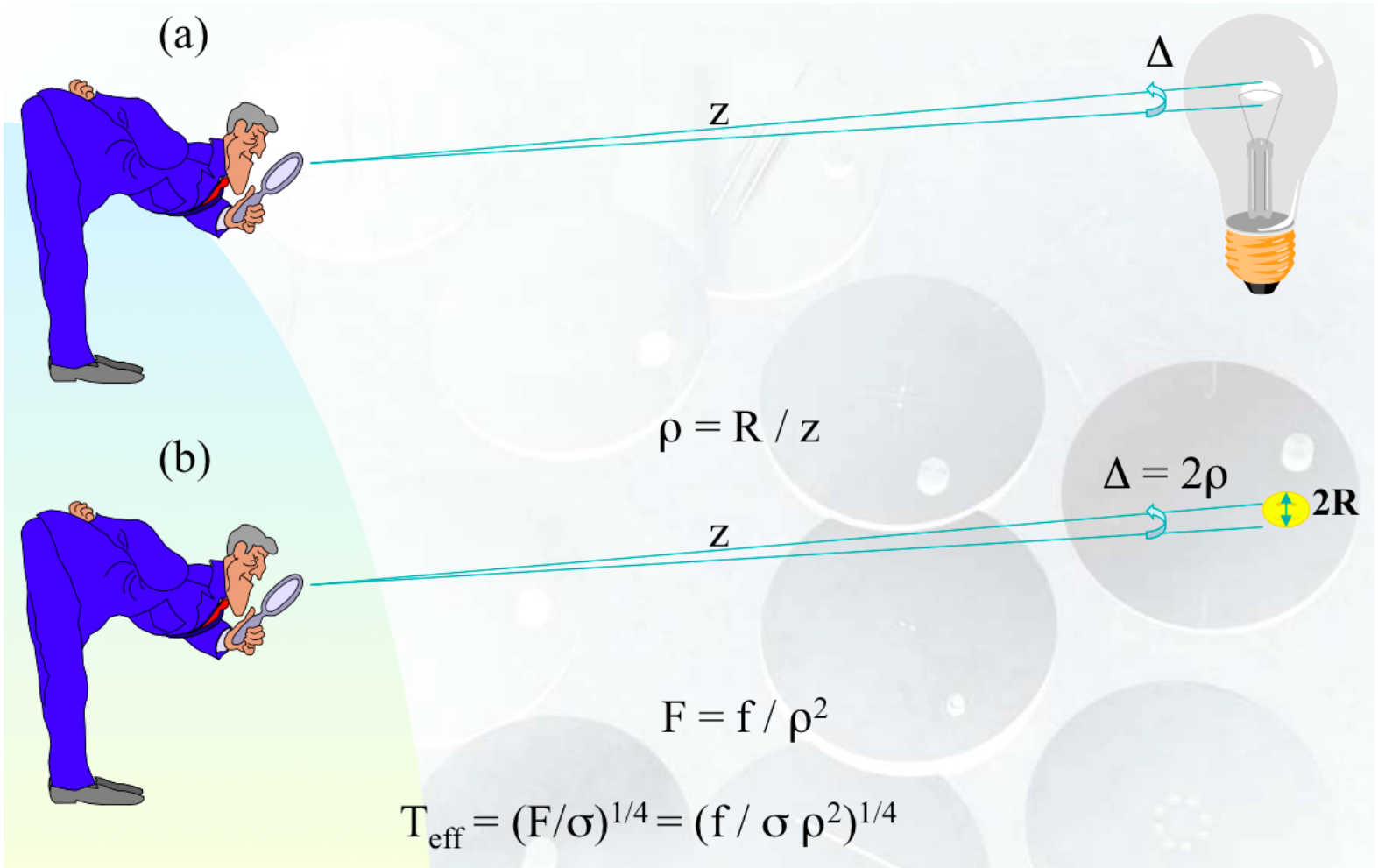

Figure: Resolving the angular diameter of a star (b) is alike trying to estimate the angular size of the filament of a light bulb (a).

Some reminders: Complex representation of an electromagnetic wave

$$E = a\ cos(2\pi(\nu t - z/\lambda)) \tag{2}$$

where

$$\lambda = c\ T = c/\nu \tag{3}$$

c, λ, ν, T and a representing the speed of light, the wavelength, the frequency, the period and the amplitude of the electromagnetic vibrations, respectively (see Figure 9).

Some reminders: Complex representation of an electromagnetic wave

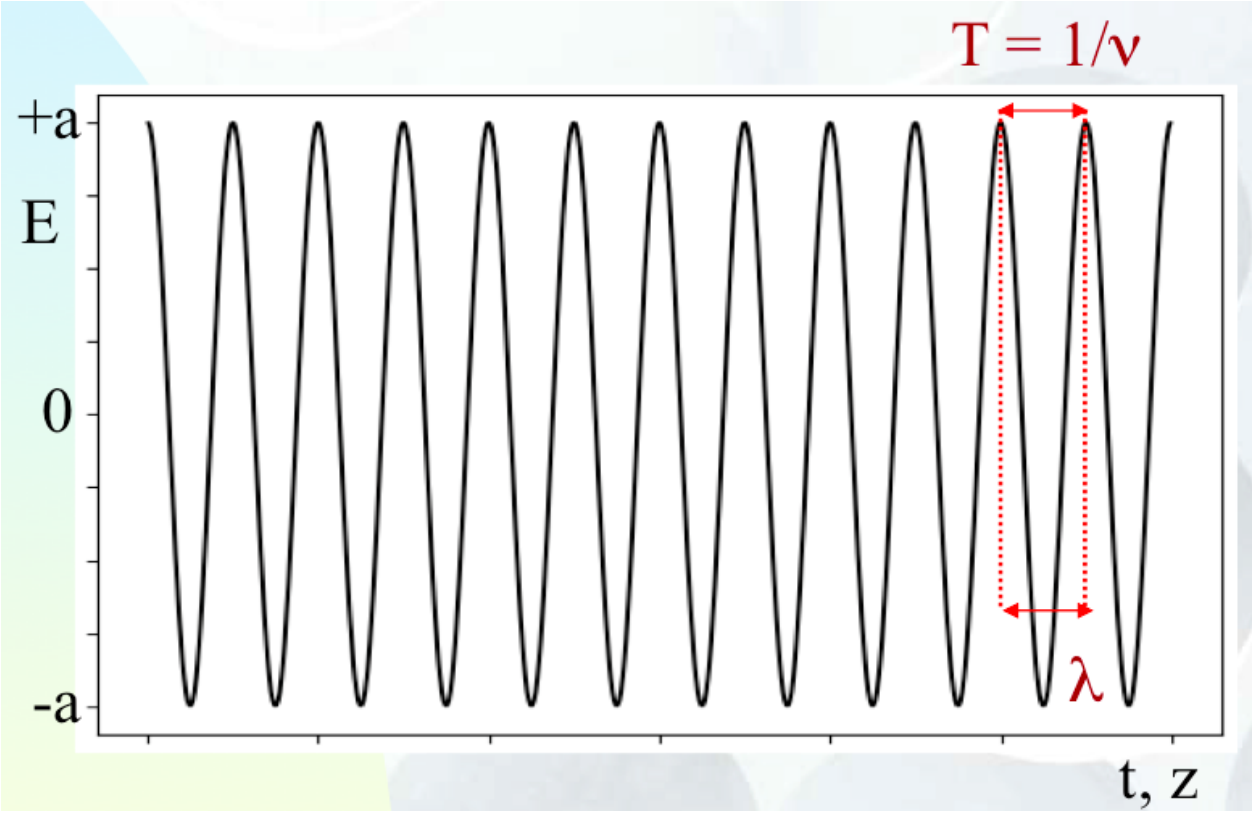

Figure: Representation of an electromagnetic wave.

Some reminders: Complex representation of an electromagnetic wave

We know how convenient it is to rewrite the previous relation in complex notation:

$$E = Re\{a \exp[i2\pi(\nu t - z/\lambda)]\} \tag{4}$$

where Re represents the real part of the expression between the two curly braces.

Some reminders: Complex representation of an electromagnetic wave

We know how convenient it is to rewrite the previous relation in complex notation:

$$E = Re\{a \exp[i2\pi(\nu t - z/\lambda)]\} \tag{4}$$

where Re represents the real part of the expression between the two curly braces.

$$E = a \exp(-i\phi) \exp(i2\pi\nu t) \tag{5}$$

where

$$\phi = 2\pi z/\lambda. \tag{6}$$

Some reminders: Complex representation of an electromagnetic wave

We know how convenient it is to rewrite the previous relation in complex notation:

$$E = Re\{a \exp[i2\pi(\nu t - z/\lambda)]\} \tag{4}$$

where Re represents the real part of the expression between the two curly braces.

$$E = a \exp(-i\phi) \exp(i2\pi\nu t) \tag{5}$$

where

$$\phi = 2\pi z/\lambda. \tag{6}$$

We can then rewrite the previous equation as follows:

$$E = A \exp(i2\pi\nu t), \tag{7}$$

Some reminders: Complex representation of an electromagnetic wave

We know how convenient it is to rewrite the previous relation in complex notation:

$$E = Re\{a \exp[i2\pi(\nu t - z/\lambda)]\} \tag{4}$$

where Re represents the real part of the expression between the two curly braces.

$$E = a \exp(-i\phi) \exp(i2\pi\nu t) \tag{5}$$

where

$$\phi = 2\pi z/\lambda. \tag{6}$$

We can then rewrite the previous equation as follows:

$$E = A \exp(i2\pi\nu t), \tag{7}$$

where

$$A = a \exp(-i\phi) \tag{8}$$

Some reminders: Complex representation of an electromagnetic wave

We know how convenient it is to rewrite the previous relation in complex notation:

$$E = Re\{a \exp[i2\pi(\nu t - z/\lambda)]\} \tag{4}$$

where Re represents the real part of the expression between the two curly braces.

$$E = a \exp(-i\phi) \exp(i2\pi\nu t) \tag{5}$$

where

$$\phi = 2\pi z/\lambda. \tag{6}$$

We can then rewrite the previous equation as follows:

$$E = A \exp(i2\pi\nu t), \tag{7}$$

where

$$A = a \exp(-i\phi) \tag{8}$$

with A representing the complex amplitude of the vibration.

The intensity I is proportional to the temporal average of the square of the electric field:

$$\left\langle E^2 \right\rangle = lim_{T\to\infty} \frac{1}{2T} \int_{-T}^{+T} E^2 dt, \tag{9}$$

The intensity I is proportional to the temporal average of the square of the electric field:

$$\left\langle E^2 \right\rangle = lim_{T\to\infty} \frac{1}{2T} \int_{-T}^{+T} E^2 dt, \tag{9}$$

which is reduced to (e.g. replace in the previous relation E by Eq.(2))

$$\left\langle E^2 \right\rangle = \frac{a^2}{2}, \tag{10}$$

where a is the real amplitude of the electric field.

The intensity I is proportional to the temporal average of the square of the electric field:

$$\left\langle E^2 \right\rangle = lim_{T\to\infty} \frac{1}{2T} \int_{-T}^{+T} E^2 dt, \tag{9}$$

which is reduced to (e.g. replace in the previous relation E by Eq.(2))

$$\left\langle E^2 \right\rangle = \frac{a^2}{2}, \tag{10}$$

where a is the real amplitude of the electric field.
By convention, the intensity of the radiation is defined by the following relation:

$$I = A\ A^* = |A|^2 = a^2. \tag{11}$$

Some reminders: Principle of Huygens-Fresnel

$\sigma = 2.44\ \lambda / d$

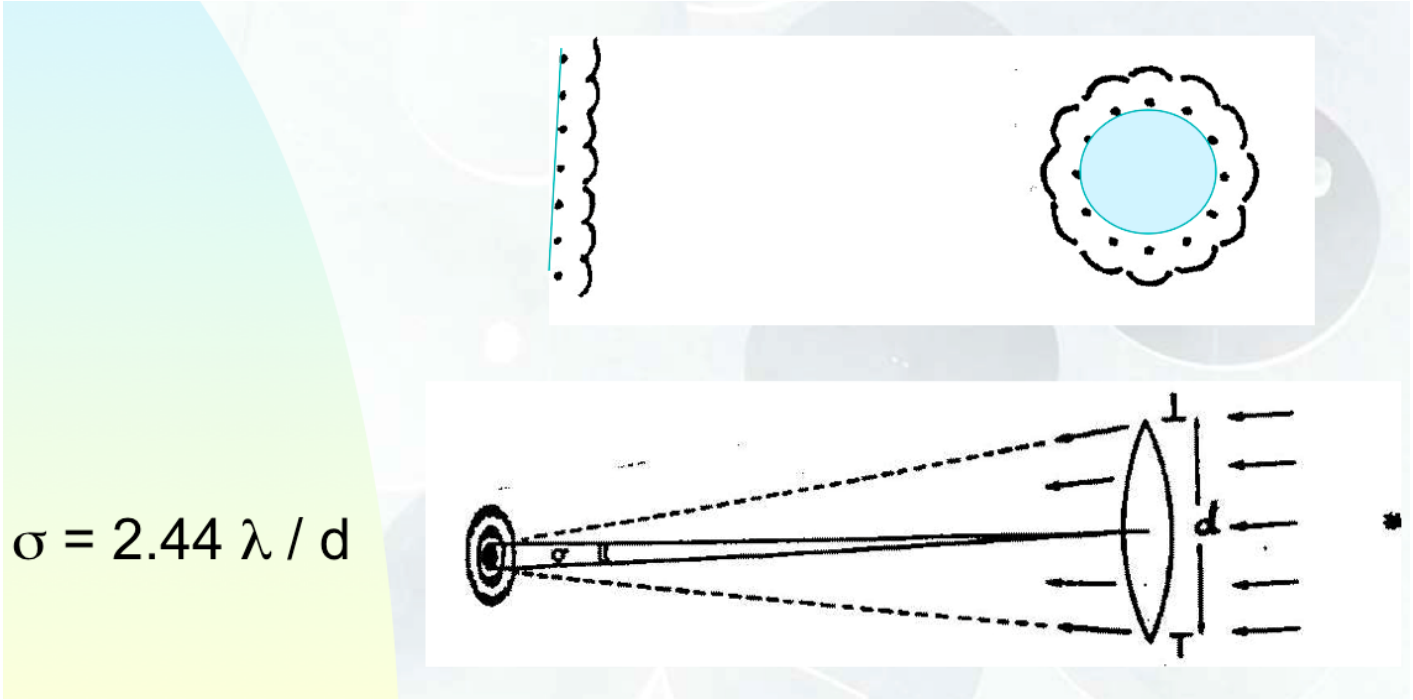

Figure: Illustration of the Huygens-Fresnel principle during the propagation of a plane or circular wavefront and diffraction of light which encounters a converging lens.

Some reminders: Principle of Huygens-Fresnel

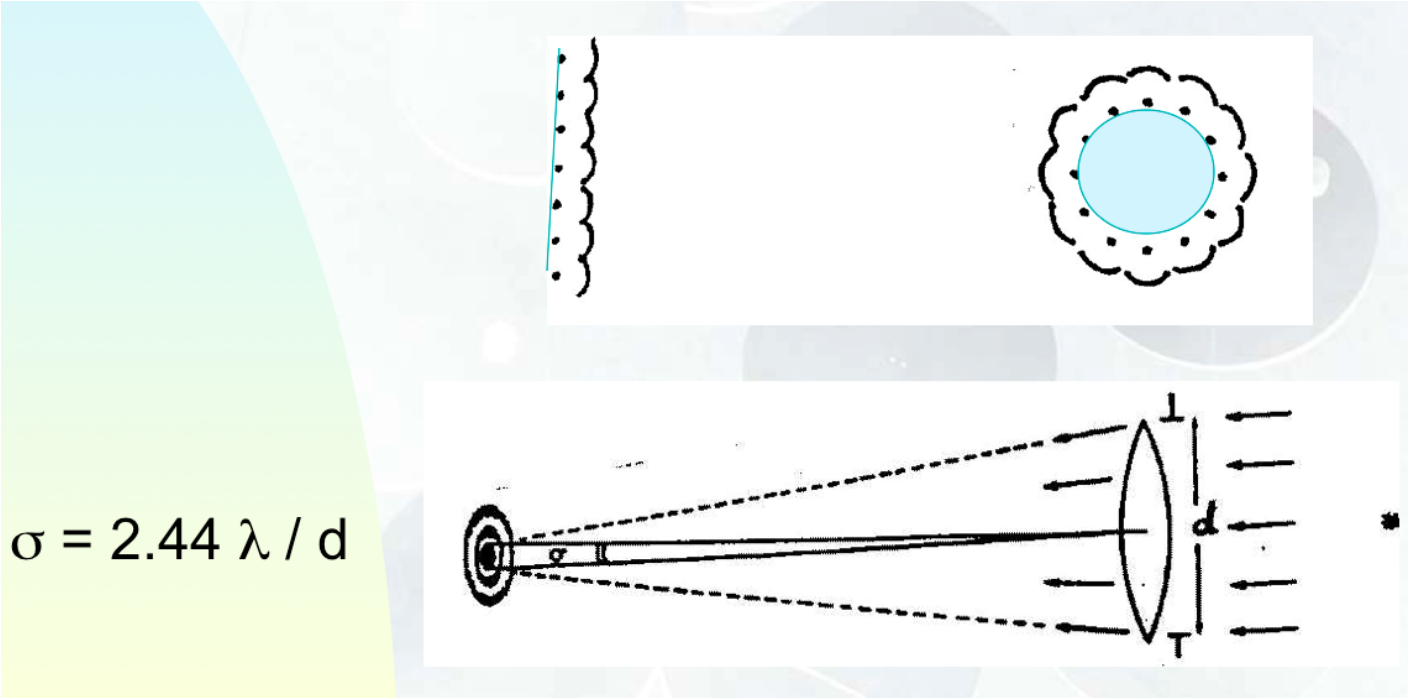

Figure: Illustration of the Huygens-Fresnel principle during the propagation of a plane or circular wavefront and diffraction of light which encounters a converging lens.

$$\sigma = 2.44\,\lambda/d \tag{12}$$

where λ is the wavelength of light and d is the linear diameter of the aperture.

Some reminders: Principle of Huygens-Fresnel

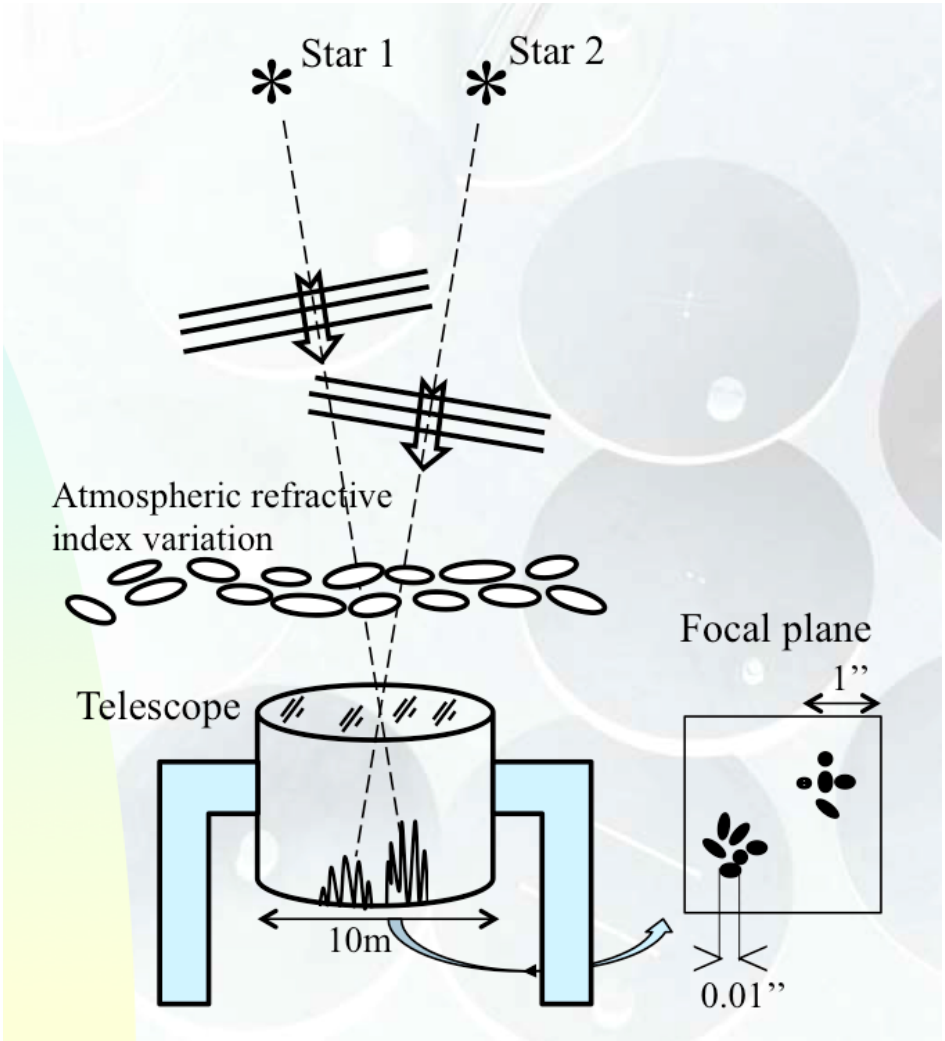

Figure: Atmospheric agitation above the objective of a large telescope causing the seeing effects seen in its focal plane.

Table of Contents

LIÈGE université

Brief history about the measurements of stellar diameters: Galileo

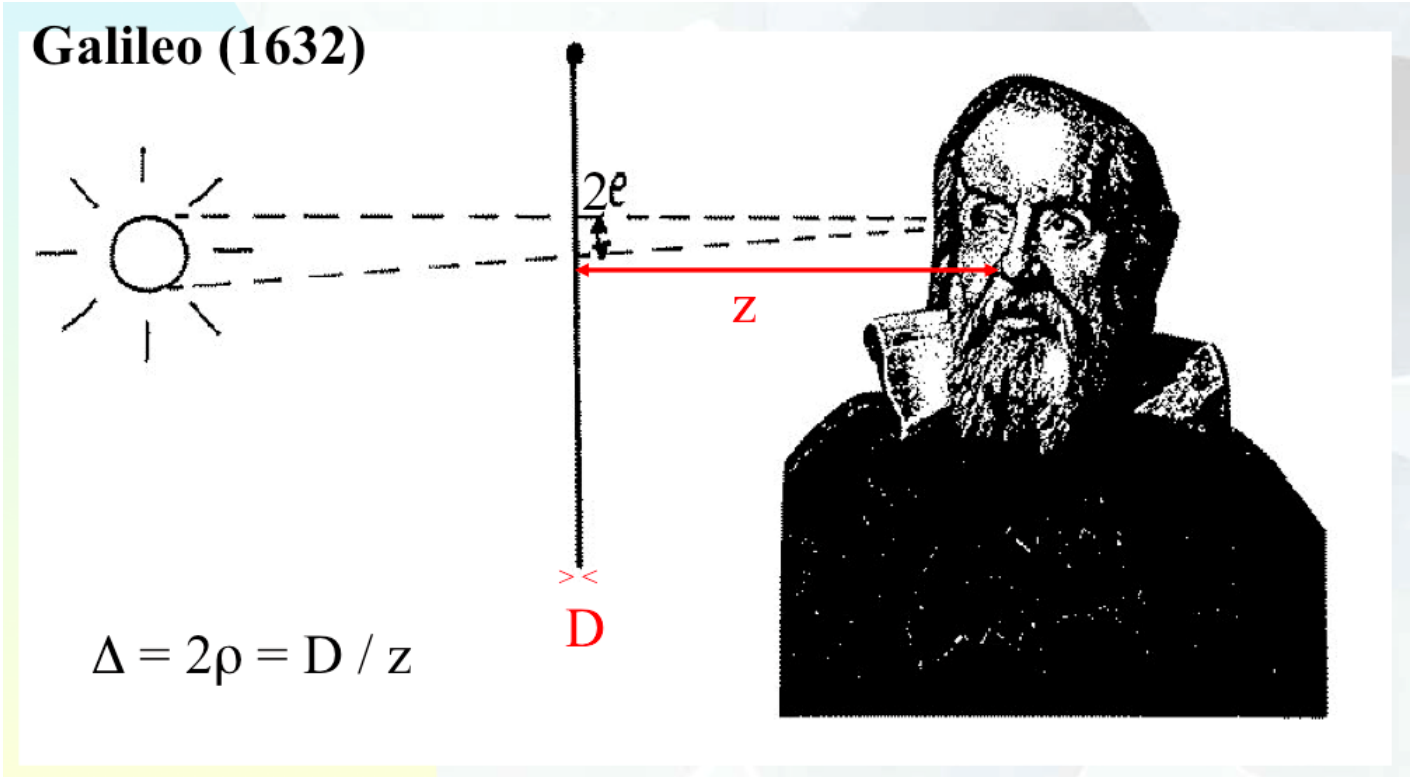

Figure: Experimental measurement by Galileo of the angular diameter of a star (see text).

Brief history about the measurements of stellar diameters: Newton

The angular diameter Δ of the Sun should be of the order of $2\,10^{-3}$" (with the current value of the visual apparent magnitude of the Sun, $V_\odot$ = -26.7, we find $\sim 8\,10^{-3}$"). It should be noted that the value currently established for the star Vega with modern interferometers is $3\,10^{-3}$". The formula to be used to establish this result can be obtained as follows: the angular diameter of the Sun Δ placed at the distance of Vega ($V = 0$) is given by the product of the apparent angular diameter of the Sun $\Delta_\odot$ times the factor $10^{V_\odot/5}$. As a reminder, the apparent diameter of the Sun is about 30'.

Brief history about the measurements of stellar diameters: Fizeau-type interferometry

Let us first remind the results obtained in the Young double hole experiment (1803, see Fig. 13).

Brief history about the measurements of stellar diameters: Fizeau-type interferometry

Let us first remind the results obtained in the Young double hole experiment (1803, see Fig. 13).

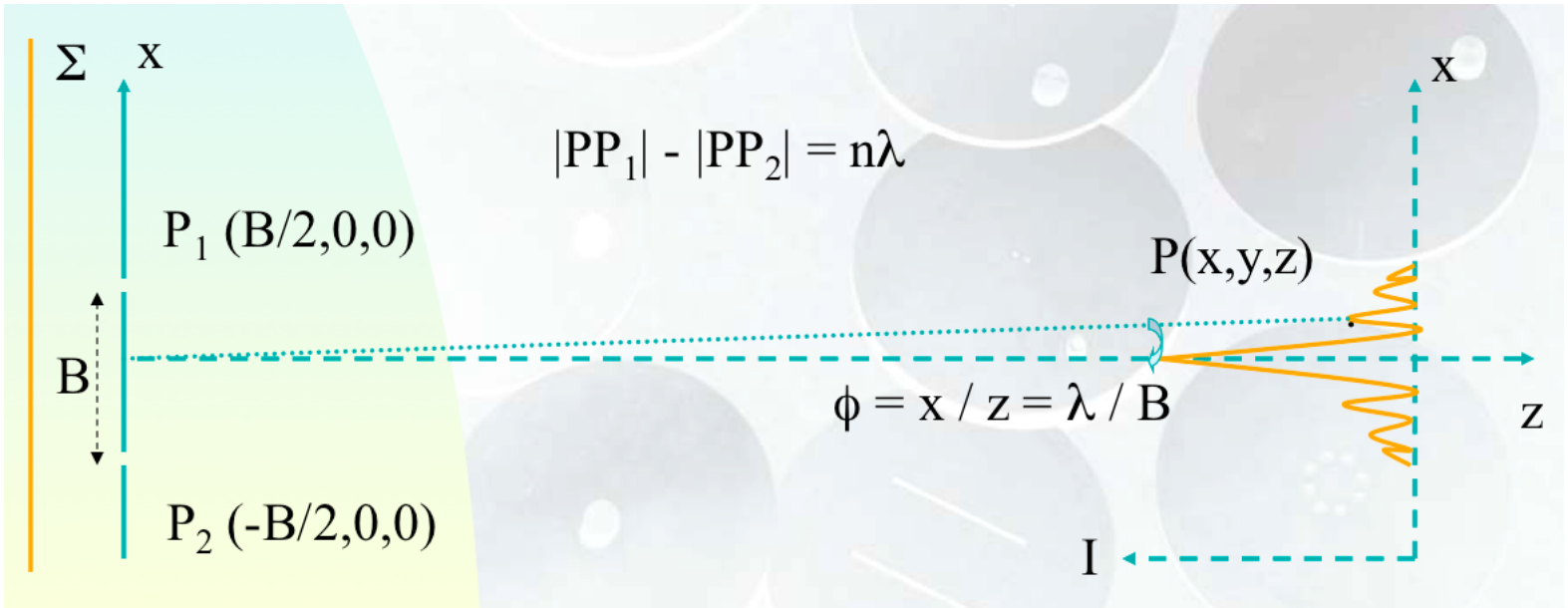

Figure: The double hole experiment of Young (see text).

Brief history about the measurements of stellar diameters: Fizeau-type interferometry

The locus of points $P(x, y, z)$ with cartesian coordinates x, y, z (see Fig. 13) where there will be a constructive interference is thus given by

$$|P_1P| - |P_2P| = n\lambda \tag{13}$$

with $n = 0, \pm 1, \pm 2$, etc.

The locus of points $P(x, y, z)$ with cartesian coordinates x, y, z (see Fig. 13) where there will be a constructive interference is thus given by

$$|P_1P| - |P_2P| = n\lambda \tag{13}$$

with $n = 0, \pm 1, \pm 2$, etc.
Let the points $P_i(x_i, y_i, 0)$ in the screen plane and $P(x, y, z)$ in the observer plane be such that $|x_i|, |y_i|, |x|, |y| << |z|$. We then find that

$$|P_iP| = \{(x - x_i)^2 + (y - y_i)^2 + z^2\}^{1/2} \tag{14}$$

The locus of points $P(x, y, z)$ with cartesian coordinates x, y, z (see Fig. 13) where there will be a constructive interference is thus given by

$$|P_1P| - |P_2P| = n\lambda \tag{13}$$

with $n = 0, \pm 1, \pm 2$, etc.
Let the points $P_i(x_i, y_i, 0)$ in the screen plane and $P(x, y, z)$ in the observer plane be such that $|x_i|, |y_i|, |x|, |y| << |z|$. We then find that

$$|P_iP| = \{(x - x_i)^2 + (y - y_i)^2 + z^2\}^{1/2} \tag{14}$$

which can be simplified at first order (given the above conditions) as follows:

$$|P_iP| = z\{1 + \frac{(x - x_i)^2 + (y - y_i)^2}{2z^2}\}. \tag{15}$$

Considering the two points P_1 and P_2 in the Young's screen, Eq. (13) reduces to

$$z\{1+\frac{(x+B/2)^2+y^2)}{2z^2}\}-z\{1+\frac{(x-B/2)^2+y^2}{2z^2}\}=n\lambda \tag{16}$$

Considering the two points P_1 and P_2 in the Young's screen, Eq. (13) reduces to

$$z\{1+\frac{(x+B/2)^2+y^2)}{2z^2}\}-z\{1+\frac{(x-B/2)^2+y^2}{2z^2}\}=n\lambda \tag{16}$$

and finally

$$\frac{xB}{z}=n\lambda \tag{17}$$

Considering the two points P_1 and P_2 in the Young's screen, Eq. (13) reduces to

$$z\{1+\frac{(x+B/2)^2+y^2)}{2z^2}\}-z\{1+\frac{(x-B/2)^2+y^2}{2z^2}\}=n\lambda \tag{16}$$

and finally

$$\frac{xB}{z}=n\lambda \tag{17}$$

or else

$$\Phi=\frac{x}{z}=n\frac{\lambda}{B}. \tag{18}$$

Brief history about the measurements of stellar diameters: Fizeau-type interferometry

If $\Delta \geq \phi/2 = \lambda / (2B)$,

fringe disappearance!

Fringe visibility:

$$v = \left(\frac{I_{max} - I_{min}}{I_{max} + I_{min}} \right)$$

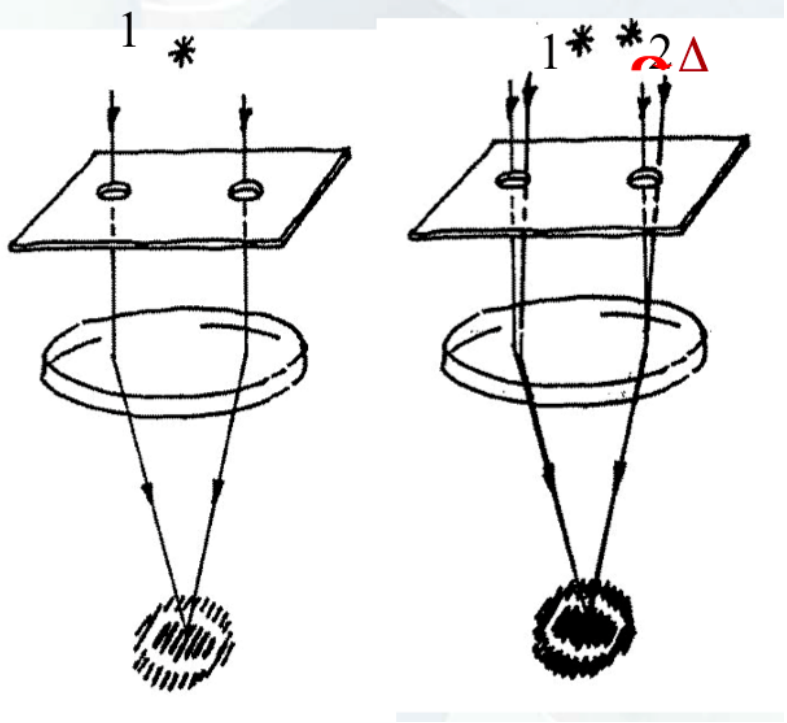

Figure: Fizeau, the father of stellar interferometry (1868; see text).

Brief history about the measurements of stellar diameters: Fizeau-type interferometry

If $\Delta \geq \phi/2 = \lambda / (2B)$,

fringe disappearance!

Fringe visibility:

$$v = \left(\frac{I_{max} - I_{min}}{I_{max} + I_{min}} \right)$$

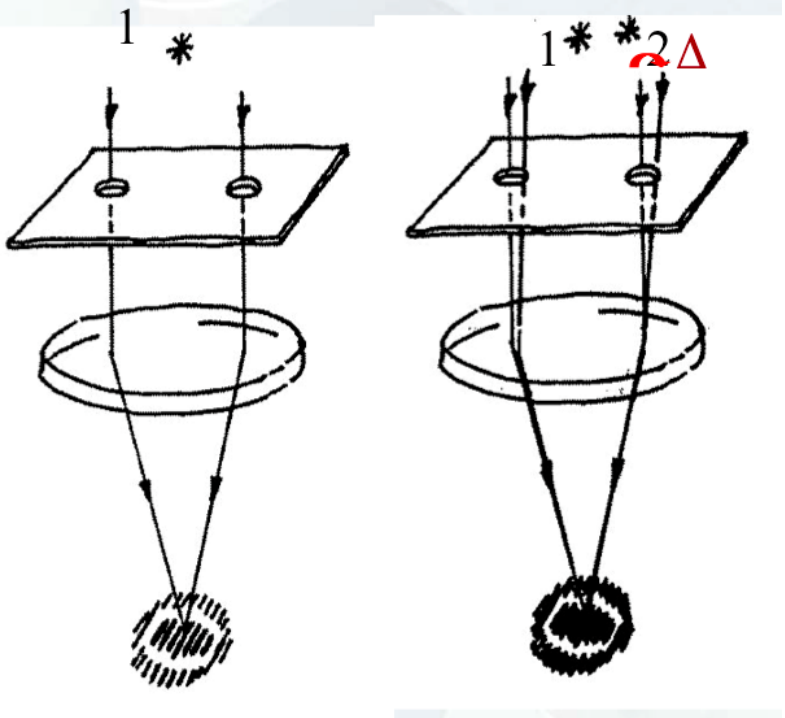

Figure: Fizeau, the father of stellar interferometry (1868; see text).

From Fig. 14, it is clear that the visibility of the fringes will significantly decrease whenever the following condition takes place

$$\Delta > \frac{\Phi}{2} = \frac{\lambda}{2B}. \quad (19)$$

Brief history about the measurements of stellar diameters: Fizeau-type interferometry

A quantity that objectively measures the contrast of the fringes is called the visibility.

Brief history about the measurements of stellar diameters: Fizeau-type interferometry

A quantity that objectively measures the contrast of the fringes is called the visibility. It is defined by the following expression:

$$v = \left(\frac{I_{\max} - I_{\min}}{I_{\max} + I_{\min}} \right). \tag{20}$$

Brief history about the measurements of stellar diameters: Fizeau-type interferometry

A quantity that objectively measures the contrast of the fringes is called the visibility. It is defined by the following expression:

$$v = \left(\frac{I_{\max} - I_{\min}}{I_{\max} + I_{\min}} \right). \tag{20}$$

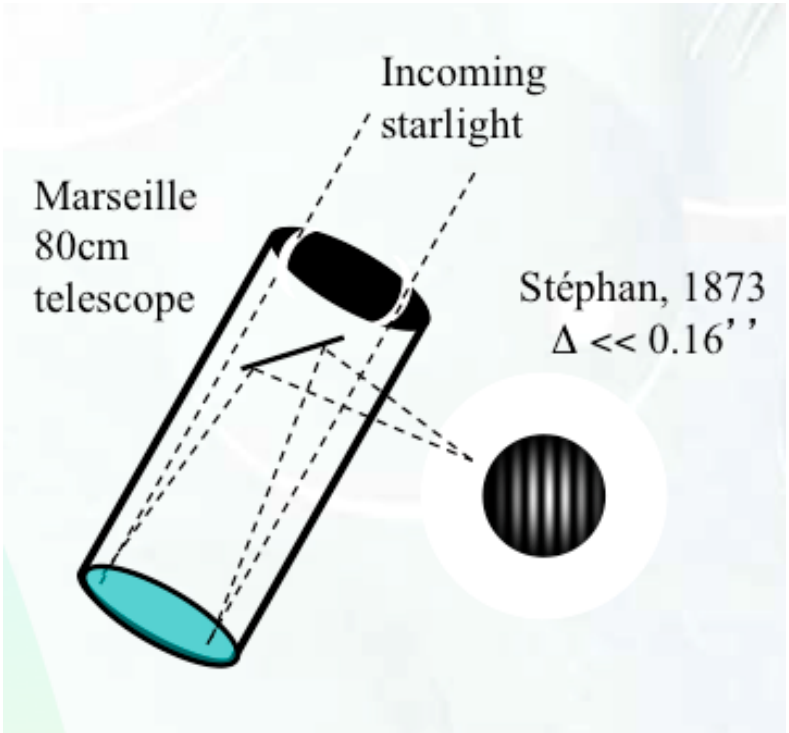

Figure: Diagram illustrating the way Fizeau and Stephan proceeded in order to measure the angular diameters of stars with the interferometric technique.

Brief history about the measurements of stellar diameters: Fizeau-type interferometry

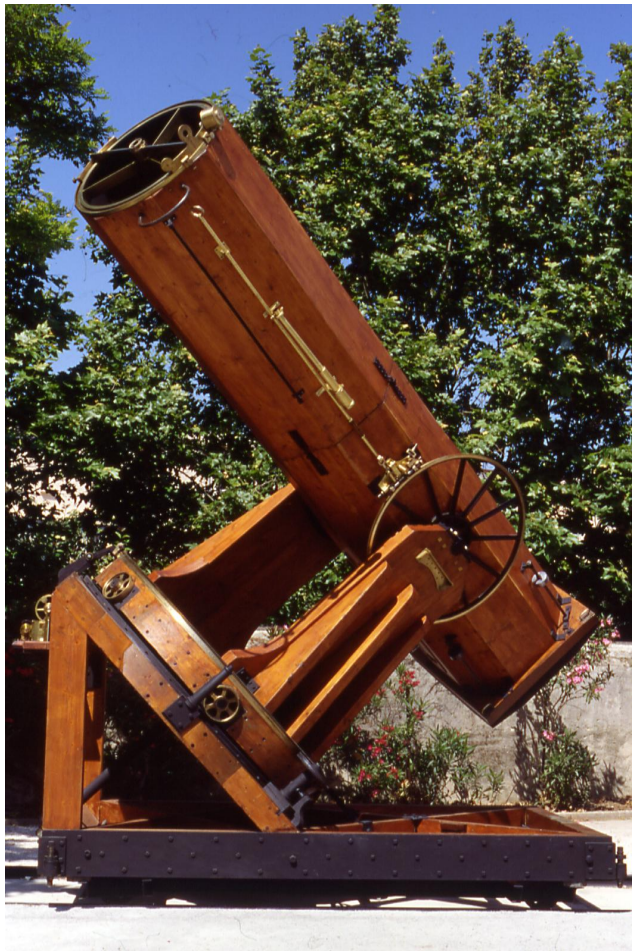

Figure: The 80cm Marseille telescope used by Fizeau and Stephan. © Michel Marcelin.

Brief history about the measurements of stellar diameters: Fizeau-type interferometry

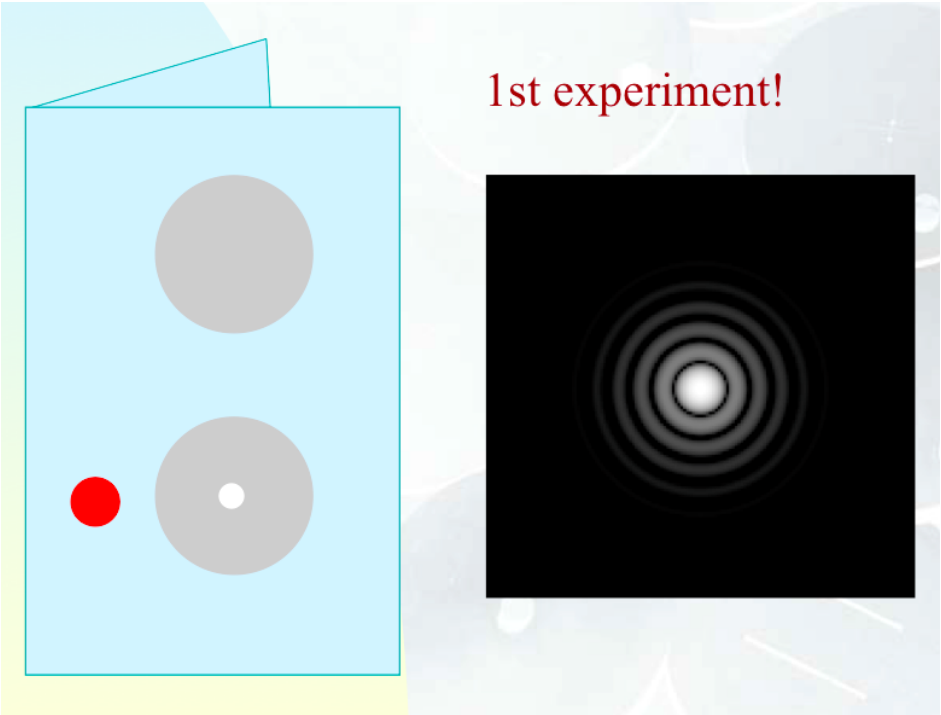

Figure: The one hole screen experiment: the small circular hole drilled in the aluminium paper is visible inside the lower bigger hole perforated in the cartoon screen. When looking through this hole at a distant light bulb, you perceive a nice Airy disk (cf. right image).

Brief history about the measurements of stellar diameters: Fizeau-type interferometry

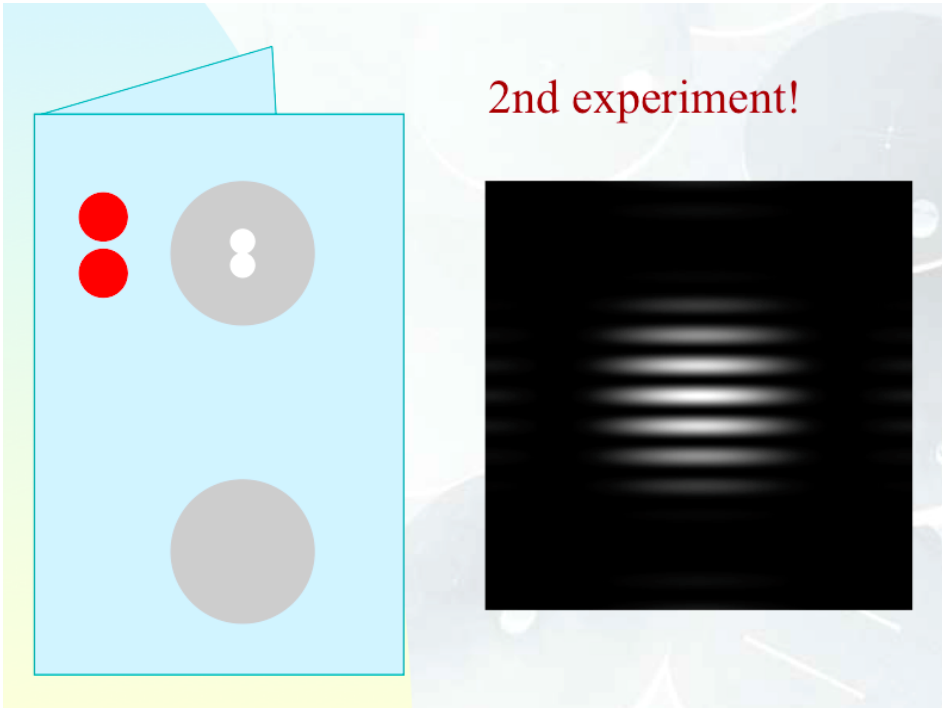

Figure: The two hole screen experiment: the two small circular holes drilled in the aluminium paper are visible inside the upper bigger hole perforated in the cartoon screen. When looking through these two holes at a distant light bulb, you perceive a nice Airy disk superimposed by a pattern of bright and dark fringes (cf. right image).

Brief history about the measurements of stellar diameters: Fizeau-type interferometry

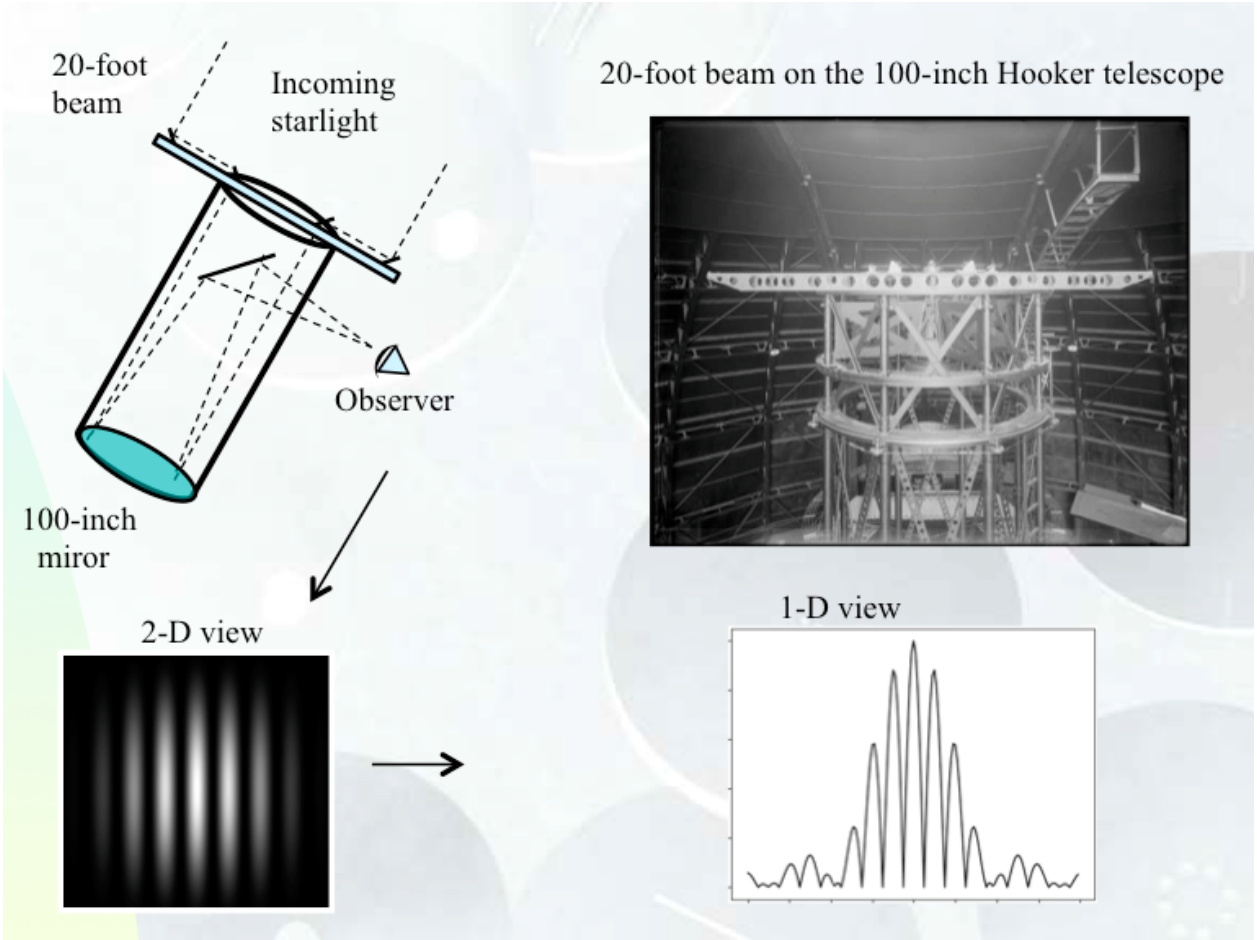

Figure: The stellar interferometer of Michelson-Pease set on top of the 2.5m Mount Wilson telescope. © The Observatories of the Carnegie Institution.

Different possible recombination schemes

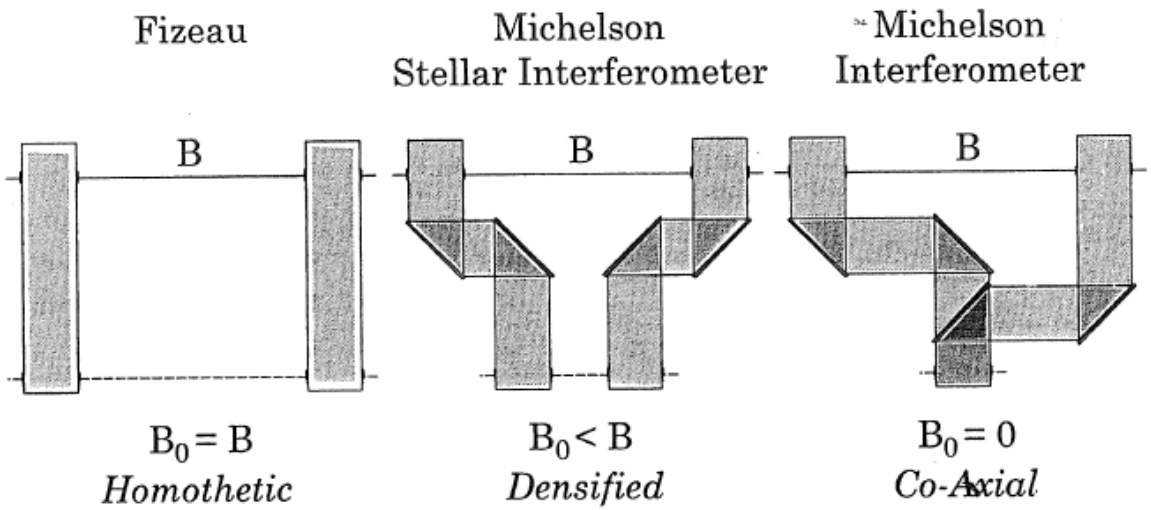

Figure: This illustration represents different possibilities for exit pupil placement, for a general exit baseline B_0.

Table of Contents

LIÈGE université

Light coherence: quasi-monochromatic light

This theory consists essentially in a statistical description of the properties of the radiation field in terms of the correlation between electromagnetic vibrations at different points in the field.

Light coherence: quasi-monochromatic light

This theory consists essentially in a statistical description of the properties of the radiation field in terms of the correlation between electromagnetic vibrations at different points in the field.
The light emitted by a real source (see Fig. 21) is of course not monochromatic. As in the case of a monochromatic wave, the intensity of such a radiation field at any point in space is defined by

$$I = \langle V(t)V(t)^* \rangle . \tag{21}$$

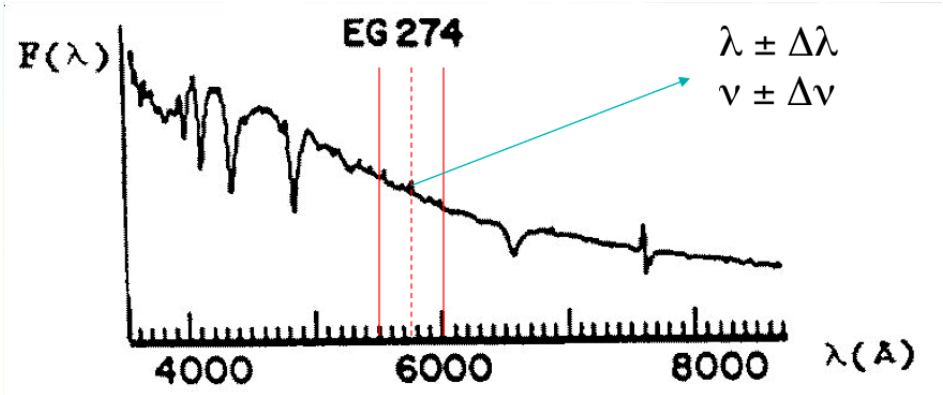

Figure: Stars do not emit monochromatic light. Quasi monochromatic light is assumed to be emitted at the wavelength λ (resp. the frequency ν) within the bandwidth $\pm\Delta\lambda$ (resp. $\pm\Delta\nu$).

Light coherence: quasi-monochromatic light

In order to determine the electric field created by such a source, emitting within a certain frequency range $\pm\Delta\nu$, we must sum up the fields due to all the individual monochromatic components such that the resulting electric field $V(z,t)$ is given by the real part of the following expression:

$$V(z,t) = \int_{\nu-\Delta\nu}^{\nu+\Delta\nu} a(\nu') \exp[i2\pi(\nu' t - z/\lambda')] d\nu'. \tag{22}$$

Light coherence: quasi-monochromatic light

In order to determine the electric field created by such a source, emitting within a certain frequency range $\pm\Delta\nu$, we must sum up the fields due to all the individual monochromatic components such that the resulting electric field $V(z,t)$ is given by the real part of the following expression:

$$V(z,t) = \int_{\nu-\Delta\nu}^{\nu+\Delta\nu} a(\nu') \exp[i2\pi(\nu' t - z/\lambda')] d\nu'. \tag{22}$$

While a monochromatic beam of radiation corresponds to an infinitely long wave train, it can easily be shown that the superposition of multiple infinitely long wave trains, with nearly similar frequencies, results in the formation of wave groups.

In order to determine the electric field created by such a source, emitting within a certain frequency range $\pm\Delta\nu$, we must sum up the fields due to all the individual monochromatic components such that the resulting electric field $V(z,t)$ is given by the real part of the following expression:

$$V(z,t) = \int_{\nu-\Delta\nu}^{\nu+\Delta\nu} a(\nu') \exp[i2\pi(\nu' t - z/\lambda')] d\nu'. \tag{22}$$

While a monochromatic beam of radiation corresponds to an infinitely long wave train, it can easily be shown that the superposition of multiple infinitely long wave trains, with nearly similar frequencies, results in the formation of wave groups.
Indeed, we find that Eq. (22) may be rewritten as

$$V(z,t) = A(z,t) \exp[i2\pi(\nu t - z/\lambda)] \tag{23}$$

where

$$A(z,t) = \int_{\nu-\Delta\nu}^{\nu+\Delta\nu} a(\nu') \exp\{i2\pi[(\nu'-\nu)t - z(1/\lambda' - 1/\lambda)]\} d\nu'. \tag{24}$$

Light coherence: quasi-monochromatic light

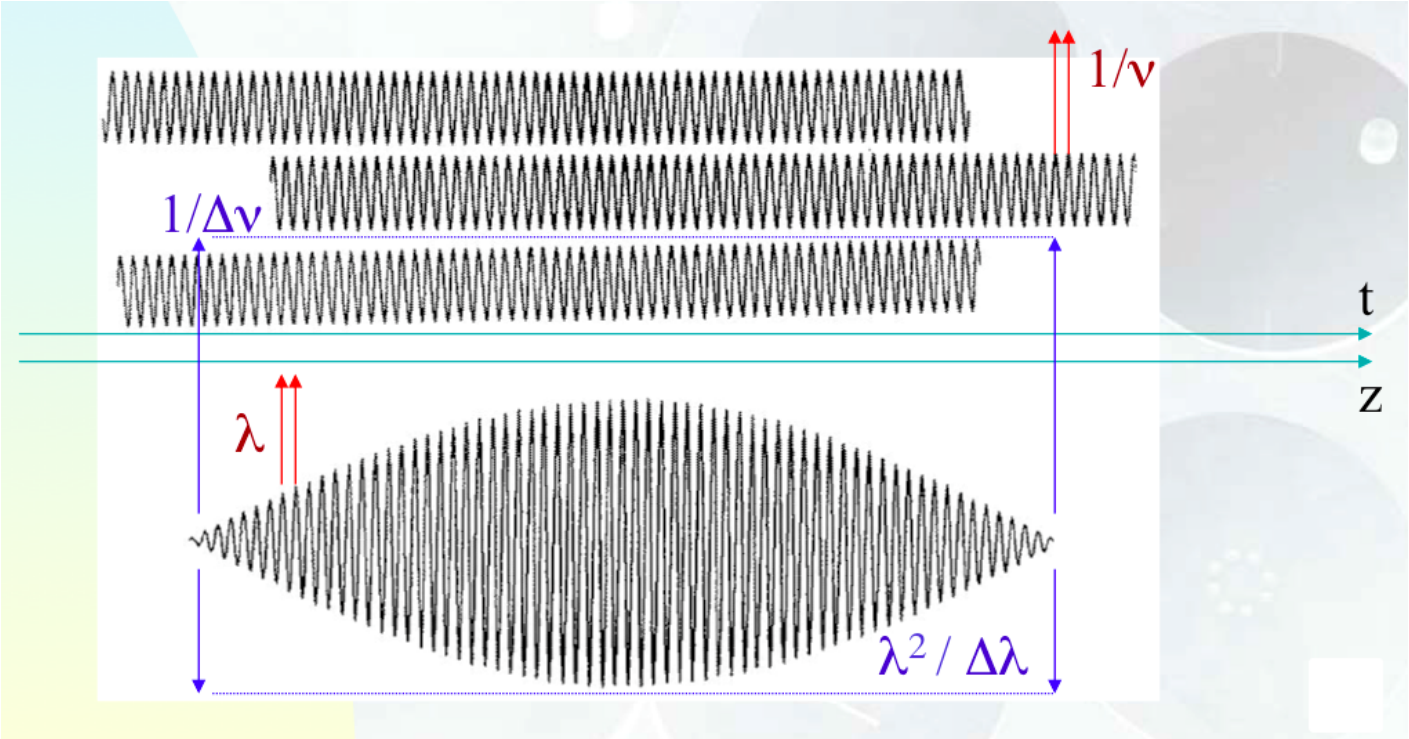

Figure: Superposition of long wave trains having quite similar frequencies ν' in the range $\nu \pm \Delta\nu$ (resp. wavelengths λ' in the range $\lambda \pm \Delta\lambda$) results in the propagation of a long wave train with the frequency ν (resp. wavelength λ) but which amplitude $A(z,t)$ is varying with a lower frequency $\Delta\nu$ (resp. longer wavelength $\lambda^2/\Delta\lambda$).

Light coherence: visibility of the interference fringes

What becomes the visibility of the interference fringes in the Young's hole experiment for the case of a quasi-monochromatic source having a finite dimension?

Light coherence: visibility of the interference fringes

What becomes the visibility of the interference fringes in the Young's hole experiment for the case of a quasi-monochromatic source having a finite dimension?

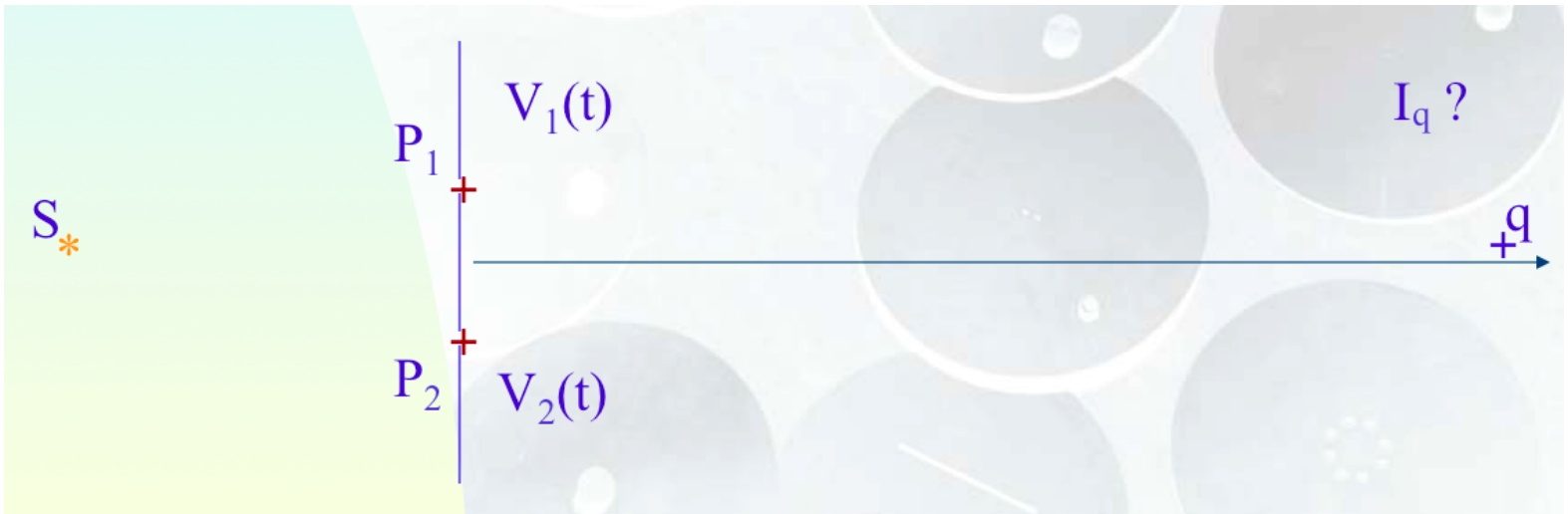

Figure: Assuming an extended source S which quasi monochromatic light passes through the two holes P_1 and P_2, I_q represents the intensity distribution at the point q which accounts for the formation of the interference fringes.

Light coherence: visibility of the interference fringes

We can re-write the expression of the intensity I_q at point q as indicated below (see Eqs. (25)-(28)). It is assumed that the holes placed at the points P_1, P_2 in the Young plane have the same aperture size (i.e. $V_1(t) = V_2(t)$) and that the propagation times of the light between P_1 (resp. P_2) and q are t_{1q} (resp. t_{2q}, see Fig. 23) :

$$I_q = \left\langle V_q^*(t) V_q(t) \right\rangle , \tag{25}$$

We can re-write the expression of the intensity I_q at point q as indicated below (see Eqs. (25)-(28)). It is assumed that the holes placed at the points P_1, P_2 in the Young plane have the same aperture size (i.e. $V_1(t) = V_2(t)$) and that the propagation times of the light between P_1 (resp. P_2) and q are t_{1q} (resp. t_{2q}, see Fig. 23) :

$$I_q = \left\langle V_q^*(t) V_q(t) \right\rangle, \tag{25}$$

$$V_q(t) = V_1(t - t_{1q}) + V_2(t - t_{2q}) \tag{26}$$

Light coherence: visibility of the interference fringes

We can re-write the expression of the intensity I_q at point q as indicated below (see Eqs. (25)-(28)). It is assumed that the holes placed at the points P_1, P_2 in the Young plane have the same aperture size (i.e. $V_1(t) = V_2(t)$) and that the propagation times of the light between P_1 (resp. P_2) and q are t_{1q} (resp. t_{2q}, see Fig. 23) :

$$I_q = \left\langle V_q^*(t) V_q(t) \right\rangle, \tag{25}$$

$$V_q(t) = V_1(t - t_{1q}) + V_2(t - t_{2q}) \tag{26}$$

and after a mere change of the time origin

$$V_q(t) = V_1(t) + V_2(t - \tau) \tag{27}$$

where we have defined

$$\tau = t_{2q} - t_{1q}. \tag{28}$$

Light coherence: visibility of the interference fringes

It follows that Eq. (25) can be easily transformed into (29) where (30) represents the complex degree of mutual coherence, and the intensity $I = < V_1 V_1^* > = < V_2 V_2^* >$.

$$I_q = I + I + 2I\,Re[\gamma_{12}(\tau)], \tag{29}$$

$$\gamma_{12}(\tau) = \langle V_1^*(t) V_2(t-\tau) \rangle / I. \tag{30}$$

It follows that Eq. (25) can be easily transformed into (29) where (30) represents the complex degree of mutual coherence, and the intensity $I = < V_1 V_1^* > = < V_2 V_2^* >$.

$$I_q = I + I + 2I\, Re[\gamma_{12}(\tau)], \tag{29}$$

$$\gamma_{12}(\tau) = \langle V_1^*(t) V_2(t-\tau) \rangle / I. \tag{30}$$

By means of (23), this function $\gamma_{12}(\tau)$ can still be expressed as (31), and if $\tau << 1/\Delta\nu$ (i.e. the difference between the arrival times of the two light rays is less than the beat period $1/\Delta\nu$), we can give it the form (32):

$$\gamma_{12}(\tau) = \langle A_1^*(z,t) A_2(z, t-\tau) \rangle \, \exp(-i2\pi\nu\tau)/I, \tag{31}$$

and if $\tau << 1/\Delta\nu$

$$\gamma_{12}(\tau) = |\gamma_{12}(\tau = 0)| \, \exp(i\beta_{12} - i2\pi\nu\tau). \tag{32}$$

Light coherence: visibility of the interference fringes

Equation (29) can then be rewritten as (33) and in this case the visibility v of the interference fringes is $|\gamma_{12}(\tau = 0)|$ (see Eq. (34)), I_{max} and I_{min} representing the brightest and weakest fringe intensities.

$$I_q = I + I + 2I\,|\gamma_{12}(\tau = 0)|\,cos(\beta_{12} - 2\pi\nu\tau) \tag{33}$$

Light coherence: visibility of the interference fringes

Equation (29) can then be rewritten as (33) and in this case the visibility v of the interference fringes is $|\gamma_{12}(\tau = 0)|$ (see Eq. (34)), I_{max} and I_{min} representing the brightest and weakest fringe intensities.

$$I_q = I + I + 2I\,|\gamma_{12}(\tau = 0)|\,cos(\beta_{12} - 2\pi\nu\tau) \tag{33}$$

and

$$v = \left(\frac{I_{\max} - I_{\min}}{I_{\max} + I_{\min}}\right) = |\gamma_{12}(\tau = 0)|. \tag{34}$$

Light coherence: visibility of the interference fringes

Equation (29) can then be rewritten as (33) and in this case the visibility v of the interference fringes is $|\gamma_{12}(\tau = 0)|$ (see Eq. (34)), I_{max} and I_{min} representing the brightest and weakest fringe intensities.

$$I_q = I + I + 2I\,|\gamma_{12}(\tau = 0)|\,cos(\beta_{12} - 2\pi\nu\tau) \tag{33}$$

and

$$v = \left(\frac{I_{\text{max}} - I_{\text{min}}}{I_{\text{max}} + I_{\text{min}}}\right) = |\gamma_{12}(\tau = 0)|. \tag{34}$$

We will see in the next section that the module of $\gamma_{12}(\tau = 0)$ is directly related to the structure of the source that we are observing.

Light coherence: visibility of the interference fringes

We propose hereafter to the reader to answer the two following questions:

Light coherence: visibility of the interference fringes

We propose hereafter to the reader to answer the two following questions:

What is the value of $|\gamma_{12}(\tau = 0)|$ in the Young's holes experiment for the case of a monochromatic wave, two point-like holes and an infinitely small point-like source?

Light coherence: visibility of the interference fringes

We propose hereafter to the reader to answer the two following questions:

What is the value of $|\gamma_{12}(\tau = 0)|$ in the Young's holes experiment for the case of a monochromatic wave, two point-like holes and an infinitely small point-like source?

And what can we say about the source when $|\gamma_{12}(\tau = 0)| = 0$?

Light coherence: visibility of the interference fringes

We propose hereafter to the reader to answer the two following questions:

What is the value of $|\gamma_{12}(\tau = 0)|$ in the Young's holes experiment for the case of a monochromatic wave, two point-like holes and an infinitely small point-like source?

And what can we say about the source when $|\gamma_{12}(\tau = 0)| = 0$?

Let us now evaluate what $\gamma_{12}(\tau = 0)$ is for the case we are interested in, namely an extended source emitting quasi-monochromatic light. This leads us directly to study the notion of the spatial coherence of light.

Light coherence: spatial coherence

Let us thus evaluate Eq. (30) for the case $\tau = 0$.

Light coherence: spatial coherence

Let us thus evaluate Eq. (30) for the case $\tau = 0$.
We find

$$\gamma_{12}(\tau = 0) = \langle V_1^*(t) V_2(t) \rangle / I, with \tag{35}$$

$$V_1(t) = \sum_{i=1}^{N} V_{i1}(t), V_2(t) = \sum_{i=1}^{N} V_{i2}(t). \tag{36}$$

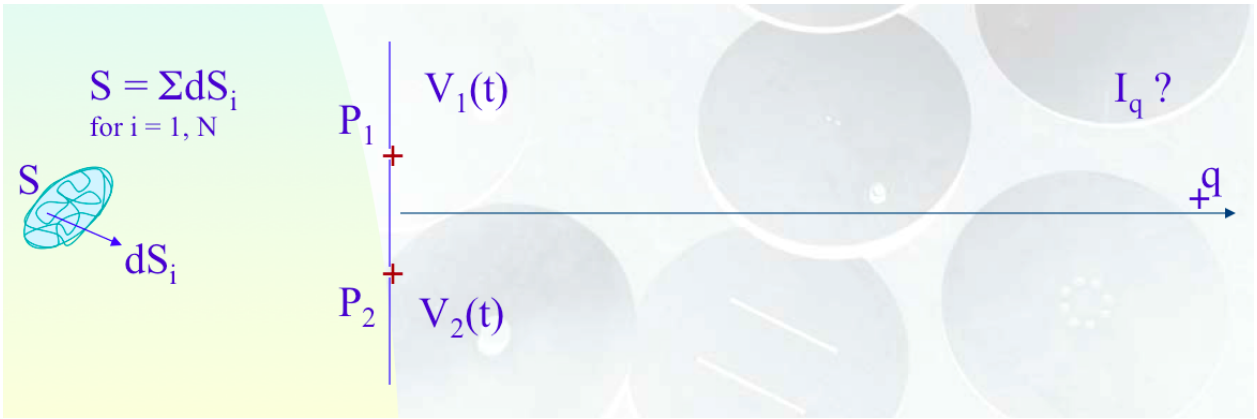

Figure: The extended source S is assumed to be composed of a large number of infinitesimal surface elements dS_i.

Light coherence: spatial coherence

It is assumed that the distinct points i of the source are separated by small distances compared to the wavelength λ of the light they emit in a mutually incoherent manner.

It is assumed that the distinct points i of the source are separated by small distances compared to the wavelength λ of the light they emit in a mutually incoherent manner. Obtaining the expression (37) for $\gamma_{12}(0)$ is then immediate

$$\gamma_{12}(0) = \left[\sum_{i=1}^{N} \langle V_{i1}^* V_{i2} \rangle + \sum_{i \neq j}^{N} \langle V_{i1}^* V_{j2} \rangle \right] / I. \tag{37}$$

It is assumed that the distinct points i of the source are separated by small distances compared to the wavelength λ of the light they emit in a mutually incoherent manner. Obtaining the expression (37) for $\gamma_{12}(0)$ is then immediate

$$\gamma_{12}(0) = \left[\sum_{i=1}^{N} \langle V_{i1}^{*} V_{i2} \rangle + \sum_{i \neq j}^{N} \langle V_{i1}^{*} V_{j2} \rangle \right] / I. \tag{37}$$

For an incoherent light source, the second summation appearing in (37) is obviously equal to zero.

It is assumed that the distinct points i of the source are separated by small distances compared to the wavelength λ of the light they emit in a mutually incoherent manner. Obtaining the expression (37) for $\gamma_{12}(0)$ is then immediate

$$\gamma_{12}(0) = \left[\sum_{i=1}^{N} \langle V_{i1}^* V_{i2} \rangle + \sum_{i \neq j}^{N} \langle V_{i1}^* V_{j2} \rangle \right] / I. \tag{37}$$

For an incoherent light source, the second summation appearing in (37) is obviously equal to zero. As a reminder, the contributions $V_{ij}(t)$ can be expressed as

$$\begin{aligned} V_{i1}(t) &= \frac{a_i(t - r_{i1}/c)}{r_{i1}} \exp[i2\pi\nu(t - r_{i1}/c)], \\ V_{i2}(t) &= \frac{a_i(t - r_{i2}/c)}{r_{i2}} \exp[i2\pi\nu(t - r_{i2}/c)]. \end{aligned} \tag{38}$$

The products $V_{i1}^*(t)V_{i2}(t)$ simplify themselves as

$$V_{i1}^*(t)V_{i2}(t) = \frac{|a_i(t - r_{i1}/c)|^2}{r_{i1}\,r_{i2}} \exp[-i2\pi\nu(r_{i2} - r_{i1})/c)], \tag{39}$$

as long as the following condition is verified

$$|r_{i1} - r_{i2}| \leq c/\Delta\nu = \lambda^2/\Delta\lambda = \ell. \tag{40}$$

The products $V_{i1}^*(t)V_{i2}(t)$ simplify themselves as

$$V_{i1}^*(t)V_{i2}(t) = \frac{|a_i(t - r_{i1}/c)|^2}{r_{i1}\,r_{i2}} \exp[-i2\pi\nu(r_{i2} - r_{i1})/c)], \tag{39}$$

as long as the following condition is verified

$$|r_{i1} - r_{i2}| \leq c/\Delta\nu = \lambda^2/\Delta\lambda = \ell. \tag{40}$$

We thus see how to naturally introduce the coherence length ℓ which characterizes the precision with which we must obtain the equality between the optical paths in order to be able to observe interference fringes (typically 2.5 microns in the visible for $\Delta\lambda = 1000$ Å).

Light coherence: Zernicke-vanCittert theorem

To obtain the mutual intensity due to the whole source, it suffices to insert in the expression (37), the relation (39) using (41).

To obtain the mutual intensity due to the whole source, it suffices to insert in the expression (37), the relation (39) using (41).
The result is Eq. (42), also known as the Zernicke-van Cittert Theorem.

$$I(s)ds = |a_i(t - r/c)|^2, \tag{41}$$

$$\gamma_{12}(0) = \int_S \frac{I(s)}{r_1 r_2} \exp[-i2\pi(r_2 - r_1)/\lambda)]ds/I. \tag{42}$$

To obtain the mutual intensity due to the whole source, it suffices to insert in the expression (37), the relation (39) using (41).
The result is Eq. (42), also known as the Zernicke-van Cittert Theorem.

$$I(s)ds = |a_i(t - r/c)|^2, \tag{41}$$

$$\gamma_{12}(0) = \int_S \frac{I(s)}{r_1 r_2} \exp[-i2\pi(r_2 - r_1)/\lambda)]ds/I. \tag{42}$$

When the distance between the source and the screen is very large, the expression of this theorem can be simplified as follows.

By means of a relation analogous to (15), we find that

$$|r_2 - r_1| = |P_2P_i - P_1P_i| = |-\frac{(X^2 + Y^2)}{2Z'} + (X\zeta + Y\eta)| \tag{43}$$

where

$$\zeta = \frac{X'}{Z'}, \eta = \frac{Y'}{Z'} \tag{44}$$

represent the angular coordinates of the source measured from the interferometer. Using the two last relations, one can easily transform the expression (42) into (45).

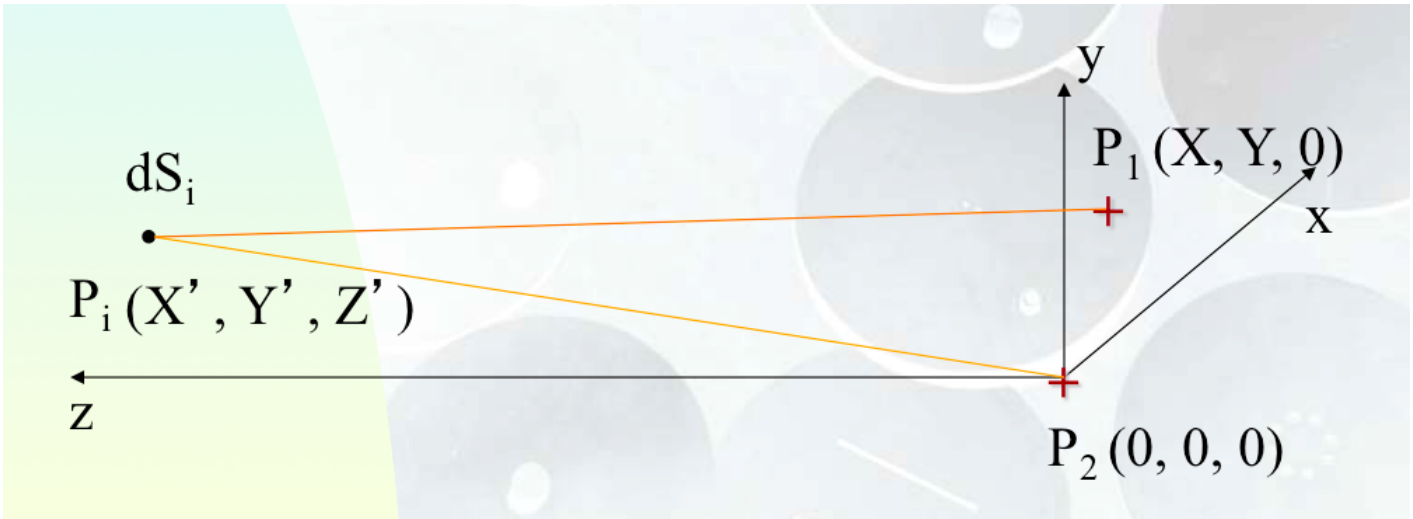

Figure: Positions of the two elements P_1 and P_2 of the interferometer and of the infinitesimal element P_i of the source assuming that the distance $Z' >> |X'|, |Y'|, |X|$ or $|Y|$.

Apart from a multiplicative factor, we thus find that the visibility of the fringes (the function $|\gamma_{12}(\tau = 0)|$) is simply the modulus of the Fourier transform of the normalized surface brightness I' of the source (Eq. (46)).

$$\gamma_{12}(0, X/\lambda, Y/\lambda) = \exp(-i\phi_{X,Y}) \int\int_S I'(\zeta, \eta) \exp[-i2\pi(X\zeta + Y\eta)/\lambda] d\zeta d\eta \qquad (45)$$

with

$$I'(\zeta, \eta) = \frac{I(\zeta, \eta)}{\int\int_S I(\zeta', \eta') d\zeta' d\eta'}. \qquad (46)$$

Apart from a multiplicative factor, we thus find that the visibility of the fringes (the function $|\gamma_{12}(\tau = 0)|$) is simply the modulus of the Fourier transform of the normalized surface brightness I' of the source (Eq. (46)).

$$\gamma_{12}(0, X/\lambda, Y/\lambda) = \exp(-i\phi_{X,Y}) \int\int_S I'(\zeta, \eta) \exp[-i2\pi(X\zeta + Y\eta)/\lambda] d\zeta d\eta \qquad (45)$$

with

$$I'(\zeta, \eta) = \frac{I(\zeta, \eta)}{\int\int_S I(\zeta', \eta') d\zeta' d\eta'}. \qquad (46)$$

Defining the angular space frequencies $u = X/\lambda$, $v = Y/\lambda$, Eq. (45) becomes

$$\gamma_{12}(0,u,v) = \exp(-i\phi_{u,v}) \int\int_S I'(\zeta,\eta)\, \exp[-i2\pi(u\zeta + v\eta)] d\zeta d\eta. \quad (47)$$

$$\gamma_{12}(0,u,v) = \exp(-i\phi_{u,v}) \int\int_S I'(\zeta,\eta)\, \exp[-i2\pi(u\zeta + v\eta)] d\zeta d\eta. \quad (47)$$

By a simple inverse Fourier transform, it is then possible to recover the surface (normalized) brightness of the source with an angular resolution equivalent to that of a telescope whose effective diameter would be equal to the baseline of the interferometer consisting of two independent telescopes

$$I'(\zeta,\eta) = \int\int \gamma_{12}(0,u,v)\, \exp(i\phi_{u,v})\, \exp[i2\pi(\zeta u + \eta v)] du dv. \quad (48)$$

$$\gamma_{12}(0,u,v) = \exp(-i\phi_{u,v}) \int\int_S I'(\zeta,\eta)\, \exp[-i2\pi(u\zeta + v\eta)] d\zeta d\eta. \quad (47)$$

By a simple inverse Fourier transform, it is then possible to recover the surface (normalized) brightness of the source with an angular resolution equivalent to that of a telescope whose effective diameter would be equal to the baseline of the interferometer consisting of two independent telescopes

$$I'(\zeta,\eta) = \int\int \gamma_{12}(0,u,v)\, \exp(i\phi_{u,v})\, \exp[i2\pi(\zeta u + \eta v)] du dv. \quad (48)$$

Equations (47) and (48) thus clearly highlight the power of the complex degree of mutual coherence since they make it possible to link the visibility and the normalized intensity distribution of the source by means of the Fourier transform $v = |\gamma_{12}(0)| = |TF_-(I')|$, and its inverse.

$$\gamma_{12}(0,u,v) = \exp(-i\phi_{u,v}) \int\int_S I'(\zeta,\eta)\, \exp[-i2\pi(u\zeta + v\eta)] d\zeta d\eta. \quad (47)$$

By a simple inverse Fourier transform, it is then possible to recover the surface (normalized) brightness of the source with an angular resolution equivalent to that of a telescope whose effective diameter would be equal to the baseline of the interferometer consisting of two independent telescopes

$$I'(\zeta,\eta) = \int\int \gamma_{12}(0,u,v)\, \exp(i\phi_{u,v})\, \exp[i2\pi(\zeta u + \eta v)] du dv. \quad (48)$$

Equations (47) and (48) thus clearly highlight the power of the complex degree of mutual coherence since they make it possible to link the visibility and the normalized intensity distribution of the source by means of the Fourier transform $v = |\gamma_{12}(0)| = |TF_-(I')|$, and its inverse.
Aperture synthesis consists in observing a maximum number of visibilities of the source, thus trying to cover as well as possible the (u,v) plane from which we shall try, sometimes with some additional assumptions, to determine the structure of the source from the inverse Fourier transform (48) in which the integrant is not the visibility (i.e. the module of the complex degree of mutual coherence) but the complex degree of mutual coherence itself, within the factor $exp(i\phi_{x,y})$.

It is now good to remind some specific properties of the Fourier transform. The Fourier transform of the function $f(x)$, denoted $FT\_f(s)$, where $x \in \Re$, is the function

$$FT\_f(s) = \int_{-\infty}^{\infty} f(x) \exp(-2i\pi sx)dx \tag{49}$$

where $s \in \Re$.

It is now good to remind some specific properties of the Fourier transform. The Fourier transform of the function $f(x)$, denoted $FT\_f(s)$, where $x \in \Re$, is the function

$$FT\_f(s) = \int_{-\infty}^{\infty} f(x) \exp(-2i\pi sx)dx \tag{49}$$

where $s \in \Re$.
The functions f and FT_f form a Fourier pair. The function $FT\_f(s)$ exists if the function $f(x)$ is bounded, summable and has a finite number of extrema and discontinuities.

It is now good to remind some specific properties of the Fourier transform. The Fourier transform of the function $f(x)$, denoted $FT\_f(s)$, where $x \in \Re$, is the function

$$FT\_f(s) = \int_{-\infty}^{\infty} f(x) \exp(-2i\pi sx)dx \tag{49}$$

where $s \in \Re$.
The functions f and FT_f form a Fourier pair. The function $FT\_f(s)$ exists if the function $f(x)$ is bounded, summable and has a finite number of extrema and discontinuities.
This does not necessarily imply that the inverse Fourier transform, denoted $FT\_^{-1}FT\_f$ transform is f. For the Fourier transformation to be reciprocal,

$$f(x) = \int_{-\infty}^{\infty} FT\_f(s) \exp(2i\pi xs)ds, \tag{50}$$

it suffices f to be of summable square, i.e. that the following integral exists

$$\int_{-\infty}^{\infty} |f(x)|^2 dx. \tag{51}$$

We can generalize the FT to several dimensions, by defining f on the space $\Re^n$. Let $\mathbf{r}$, $\mathbf{w} \in \Re^{\mathbf{n}}$, we then have

$$FT\_f(\mathbf{w}) = \int_{-\infty}^{\infty} f(\mathbf{r}) \exp(-2i\pi \mathbf{wr}) d\mathbf{r}. \tag{52}$$

We can generalize the FT to several dimensions, by defining f on the space $\Re^n$. Let $\mathbf{r}$, $\mathbf{w} \in \Re^{\mathbf{n}}$, we then have

$$FT\_f(\mathbf{w}) = \int_{-\infty}^{\infty} f(\mathbf{r}) \exp(-2i\pi \mathbf{wr}) d\mathbf{r}. \tag{52}$$

As a reminder, if $f(t)$ designates a function of time, $FT\_f(s)$ represents its content as a function of time frequencies.

We can generalize the FT to several dimensions, by defining f on the space $\Re^n$. Let $\mathbf{r}$, $\mathbf{w} \in \Re^{\mathbf{n}}$, we then have

$$FT\_f(\mathbf{w}) = \int_{-\infty}^{\infty} f(\mathbf{r}) \exp(-2i\pi \mathbf{w}\mathbf{r}) d\mathbf{r}. \tag{52}$$

As a reminder, if $f(t)$ designates a function of time, $FT\_f(s)$ represents its content as a function of time frequencies. Similarly, if $f(\mathbf{r})$ is defined on $\Re^2$, where $\Re^2$ represents a two-dimensional space, the function $FT\_f(\mathbf{w})$ represents the spatial frequency content of $f(\mathbf{r})$, where $\mathbf{w} \in \Re^{\mathbf{2}}$.

We can generalize the FT to several dimensions, by defining f on the space $\Re^n$. Let $\mathbf{r}$, $\mathbf{w} \in \Re^{\mathbf{n}}$, we then have

$$FT\_f(\mathbf{w}) = \int_{-\infty}^{\infty} f(\mathbf{r}) \exp(-2i\pi \mathbf{w}\mathbf{r}) d\mathbf{r}. \tag{52}$$

As a reminder, if $f(t)$ designates a function of time, $FT\_f(s)$ represents its content as a function of time frequencies. Similarly, if $f(\mathbf{r})$ is defined on $\Re^2$, where $\Re^2$ represents a two-dimensional space, the function $FT\_f(\mathbf{w})$ represents the spatial frequency content of $f(\mathbf{r})$, where $\mathbf{w} \in \Re^{\mathbf{2}}$.
Among the interesting properties of the Fourier transform, let us first remind the **linearity properties**:

$$FT\_(af) = a\, FT\_f, \tag{53}$$

with the constant $a \in \Re$,

$$FT\_(f + g) = FT\_f + FT\_g. \tag{54}$$

The symmetry and parity properties:
The considerations of symmetry are very useful during the study of the Fourier transform.

The symmetry and parity properties:
The considerations of symmetry are very useful during the study of the Fourier transform. Let $P(x)$ and $I(x)$ be the even and odd parts of $f(x)$ such that

$$f(x) = P(x) + I(x), \tag{55}$$

we find that

$$FT\_f(s) = 2\int_0^\infty P(x)\cos(2\pi xs)dx - 2i\int_0^\infty I(x)\sin(2\pi xs)dx. \tag{56}$$

The symmetry and parity properties:
The considerations of symmetry are very useful during the study of the Fourier transform. Let $P(x)$ and $I(x)$ be the even and odd parts of $f(x)$ such that

$$f(x) = P(x) + I(x), \tag{55}$$

we find that

$$FT\_f(s) = 2\int_0^\infty P(x)\cos(2\pi xs)dx - 2i\int_0^\infty I(x)\sin(2\pi xs)dx. \tag{56}$$

From this result, we can deduce for instance that if $f(x)$ is real, the real part of $FT\_f(s)$ will be even and its imaginary part will be odd whereas if $f(x)$ is complex, the imaginary part of $FT\_f(s)$ will be even and its real part will be odd.

The similarity property: the relationship of similarity is the following one

$$FT_{-}(f(x/a))(s) = |a|\, FT_{-}(f(x))(as) \tag{57}$$

where $a \in \Re$, is a constant.

The similarity property: the relationship of similarity is the following one

$$FT_{-}(f(x/a))(s) = |a|\, FT_{-}(f(x))(as) \tag{57}$$

where $a \in \Re$, is a constant. The dilation of a function causes a contraction of its Fourier transform. This very visual property is very useful to understand that a function whose support is very compact, has a very spread transform.

The similarity property: the relationship of similarity is the following one

$$FT_{-}(f(x/a))(s) = |a|\, FT_{-}(f(x))(as) \tag{57}$$

where $a \in \Re$, is a constant. The dilation of a function causes a contraction of its Fourier transform. This very visual property is very useful to understand that a function whose support is very compact, has a very spread transform. In the analysis of temporal frequencies, one would state that a pulse of very short duration results in a very broad frequency spectrum, that is to say, contains frequencies all the higher as the pulse is brief. This is the classical relation of the spectrum of a wave packet, according to which the knowledge of the properties of a signal cannot be arbitrarily precise both in time and in frequency.

The similarity property: the relationship of similarity is the following one

$$FT_{-}(f(x/a))(s) = |a|\, FT_{-}(f(x))(as) \tag{57}$$

where $a \in \Re$, is a constant. The dilation of a function causes a contraction of its Fourier transform. This very visual property is very useful to understand that a function whose support is very compact, has a very spread transform. In the analysis of temporal frequencies, one would state that a pulse of very short duration results in a very broad frequency spectrum, that is to say, contains frequencies all the higher as the pulse is brief. This is the classical relation of the spectrum of a wave packet, according to which the knowledge of the properties of a signal cannot be arbitrarily precise both in time and in frequency.

The translation property: the translation relation is written as

$$FT_{-}(f(x-a))(s) = \exp(-2i\pi as)\, FT_{-}(f(x))(s). \tag{58}$$

The similarity property: the relationship of similarity is the following one

$$FT_{-}(f(x/a))(s) = |a|\, FT_{-}(f(x))(as) \tag{57}$$

where $a \in \Re$, is a constant. The dilation of a function causes a contraction of its Fourier transform. This very visual property is very useful to understand that a function whose support is very compact, has a very spread transform. In the analysis of temporal frequencies, one would state that a pulse of very short duration results in a very broad frequency spectrum, that is to say, contains frequencies all the higher as the pulse is brief. This is the classical relation of the spectrum of a wave packet, according to which the knowledge of the properties of a signal cannot be arbitrarily precise both in time and in frequency.

The translation property: the translation relation is written as

$$FT_{-}(f(x-a))(s) = \exp(-2i\pi as)\, FT_{-}(f(x))(s). \tag{58}$$

A translation of the function in its original space corresponds to a phase rotation of its Fourier transform in the transformed space.

The **door function**, denoted $\Pi(x)$, is defined by (see Fig. 26)

$$\Pi(x) = 1 \quad \text{if } x \in [-0.5, 0.5], \quad \text{and} \quad \Pi(x) = 0 \quad \text{otherwise.} \tag{59}$$

The **door function**, denoted $\Pi(x)$, is defined by (see Fig. 26)

$$\Pi(x) = 1 \quad \text{if } x \in [-0.5, 0.5], \quad \text{and} \quad \Pi(x) = 0 \quad \text{otherwise.} \tag{59}$$

It is easy to find that

$$FT_{-}(\Pi(x))(s) = sinc(s) = \frac{sin(\pi s)}{\pi s}. \tag{60}$$

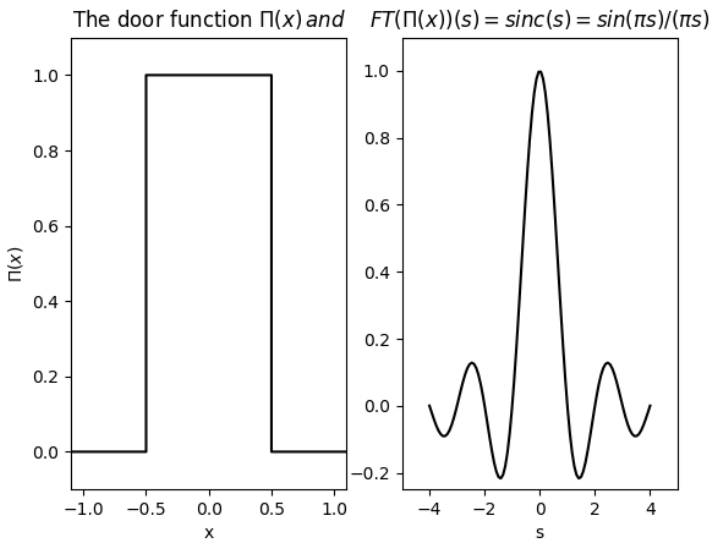

Figure: The door function and its Fourier transform (cardinal sine).

Applying the similarity relation, we also find that

$$FT_{-}(\Pi(x/a))(s) = |a|\, sinc(as) = |a|\, \frac{sin(\pi as)}{\pi as}. \tag{61}$$

Applying the similarity relation, we also find that

$$FT_{-}(\Pi(x/a))(s) = |a|\, sinc(as) = |a|\, \frac{sin(\pi as)}{\pi as}. \tag{61}$$

The door function is also sometimes called the window function or simply window.

Applying the similarity relation, we also find that

$$FT_{-}(\Pi(x/a))(s) = |a|\, sinc(as) = |a|\, \frac{sin(\pi as)}{\pi as}. \tag{61}$$

The door function is also sometimes called the window function or simply window. The **Dirac distribution**, also called Dirac peak, is noted $\delta(x)$. It is defined by the following integral, which exists only in the sense of the distributions

$$\delta(x) = \int_{-\infty}^{\infty} \exp(2i\pi xs)ds. \tag{62}$$

Its Fourier transform is therefore 1 in the interval $]-\infty, +\infty[$ since $\delta(x)$ appears above as the inverse Fourier transform of 1.

Some applications: we propose hereafter several astrophysical applications that make use of the previous remarkable properties of the Fourier transform.

Light coherence: some remarkable properties of the Fourier transform and applications

Some applications: we propose hereafter several astrophysical applications that make use of the previous remarkable properties of the Fourier transform.

Let us first consider the case of a double star which two point-like components are equally bright and separated by an angle $2\zeta_0$. Making use of Eqs. (34), (46) and (47), one may easily establish using the properties (58) and (62) that the normalized intensity $I'(\zeta)$ takes the simple form

Some applications: we propose hereafter several astrophysical applications that make use of the previous remarkable properties of the Fourier transform.

Let us first consider the case of a double star which two point-like components are equally bright and separated by an angle $2\zeta_0$. Making use of Eqs. (34), (46) and (47), one may easily establish using the properties (58) and (62) that the normalized intensity $I'(\zeta)$ takes the simple form

$$I'(\zeta) = \frac{\delta(\zeta - \zeta_0) + \delta(\zeta + \zeta_0)}{2} \tag{63}$$

Some applications: we propose hereafter several astrophysical applications that make use of the previous remarkable properties of the Fourier transform.

Let us first consider the case of a double star which two point-like components are equally bright and separated by an angle $2\zeta_0$. Making use of Eqs. (34), (46) and (47), one may easily establish using the properties (58) and (62) that the normalized intensity $I'(\zeta)$ takes the simple form

$$I'(\zeta) = \frac{\delta(\zeta - \zeta_0) + \delta(\zeta + \zeta_0)}{2} \tag{63}$$

and that the visibility v measured with an interferometer composed of 2 telescopes separated by the baseline X is given by the expression

$$v = |\gamma_{12}(u, 0)| = |cos(2\pi\zeta_0 u)| \tag{64}$$

where $u = X/\lambda$.

A second nice application consists in deriving the visibility of the interference fringes measured with the same interferometer of a $1-D$ Gaussian star which intensity $I(\zeta)$ distribution is given by the following expression

$$I(\zeta) = \exp\left(\frac{-4\ln(2)\zeta^2}{\mathrm{FWHM}^2}\right) \tag{65}$$

where *FWHM* represents the angular full width at half maximum of the $1-D$ Gaussian star.

A second nice application consists in deriving the visibility of the interference fringes measured with the same interferometer of a $1-D$ Gaussian star which intensity $I(\zeta)$ distribution is given by the following expression

$$I(\zeta) = \exp\left(\frac{-4\ln(2)\zeta^2}{\mathrm{FWHM}^2}\right) \tag{65}$$

where *FWHM* represents the angular full width at half maximum of the $1-D$ Gaussian star.

Tricks!!!, $\int \exp(-ax^2)dx = \sqrt{\pi/a}$, $FT_-(\exp(-ax^2))(s) = \sqrt{\pi/a}\exp(-\pi^2 s^2/a)$

A second nice application consists in deriving the visibility of the interference fringes measured with the same interferometer of a $1-D$ Gaussian star which intensity $I(\zeta)$ distribution is given by the following expression

$$I(\zeta) = \exp\left(\frac{-4\ln(2)\zeta^2}{\mathrm{FWHM}^2}\right) \tag{65}$$

where *FWHM* represents the angular full width at half maximum of the $1-D$ Gaussian star.
Tricks!!!, $\int \exp(-ax^2)dx = \sqrt{\pi/a}$, $FT_-(\exp(-ax^2))(s) = \sqrt{\pi/a}\exp(-\pi^2 s^2/a)$

The expression of the corresponding visibility is then easily found to be

$$v = |\gamma_{12}(0,u)| = \exp\left(\frac{-\pi^2 u^2\ \mathrm{FWHM}^2}{4\ln(2)}\right), \tag{66}$$

and we notice that narrower is the angular size of the star, broader is its visibility content in angular space frequencies.

Light coherence: some remarkable properties of the Fourier transform and applications

In the third proposed application, we ask to establish the expression of the visibility of a $2-D$ uniformly bright square star which each angular side is ζ_0,

In the third proposed application, we ask to establish the expression of the visibility of a $2-D$ uniformly bright square star which each angular side is ζ_0,

i.e. $I(\zeta) = Cte\Pi(\zeta/\zeta_0)\Pi(\eta/\zeta_0)$.

In the third proposed application, we ask to establish the expression of the visibility of a $2-D$ uniformly bright square star which each angular side is ζ_0,

i.e. $I(\zeta) = Cte\Pi(\zeta/\zeta_0)\Pi(\eta/\zeta_0)$.

The expression to be derived is the following one

$$v = |\gamma_{12}(0, u, v)| = |\frac{sin(\pi\zeta_0 u)}{\pi\zeta_0 u}\frac{sin(\pi\zeta_0 v)}{\pi\zeta_0 v}|. \quad (67)$$

Light coherence: some remarkable properties of the Fourier transform and applications

In the third proposed application, we ask to establish the expression of the visibility of a $2-D$ uniformly bright square star which each angular side is ζ_0,

i.e. $I(\zeta) = Cte\Pi(\zeta/\zeta_0)\Pi(\eta/\zeta_0)$.

The expression to be derived is the following one

$$v = |\gamma_{12}(0, u, v)| = |\frac{sin(\pi\zeta_0 u)}{\pi\zeta_0 u}\frac{sin(\pi\zeta_0 v)}{\pi\zeta_0 v}|. \quad (67)$$

Remark:

To check whether your original function $I(\zeta, (and/or\ \eta))$ has been properly normalized, see whether its Fourier Transform for u=0 (and/or v=0) is equal to unity! Why?

Finally, a generalization of the previous application consists in deriving the visibility of a star which is seen as a projected $2-D$ uniform circular disk which angular radius is ρ_{UD} and its angular diameter θ_{UD}.

Finally, a generalization of the previous application consists in deriving the visibility of a star which is seen as a projected $2-D$ uniform circular disk which angular radius is ρ_{UD} and its angular diameter θ_{UD}.
Due to the circular symmetry of the problem, it is convenient to make use of polar coordinates in Eq. (45) as follows:

$$\begin{aligned} u &= X/\lambda = R\cos(\psi)/\lambda \\ v &= Y/\lambda = R\sin(\psi)/\lambda, \end{aligned} \tag{68}$$

where R denotes the baseline between the two telescopes of the interferometer, and

$$\begin{aligned} \zeta &= \theta\cos(\phi) \\ \eta &= \theta\sin(\phi). \end{aligned} \tag{69}$$

Finally, a generalization of the previous application consists in deriving the visibility of a star which is seen as a projected $2-D$ uniform circular disk which angular radius is ρ_{UD} and its angular diameter θ_{UD}.
Due to the circular symmetry of the problem, it is convenient to make use of polar coordinates in Eq. (45) as follows:

$$\begin{aligned} u &= X/\lambda = R\cos(\psi)/\lambda \\ v &= Y/\lambda = R\sin(\psi)/\lambda, \end{aligned} \tag{68}$$

where R denotes the baseline between the two telescopes of the interferometer, and

$$\begin{aligned} \zeta &= \theta\cos(\phi) \\ \eta &= \theta\sin(\phi). \end{aligned} \tag{69}$$

Eq. (45) then transforms into

$$|\gamma_{12}(0, R/\lambda, \psi)| = |\frac{1}{\pi\rho_{UD}^2}\int_0^{\rho_{UD}} \theta \int_0^{2\pi} \exp\left[-i2\pi\theta R/\lambda(\cos(\phi)\cos(\psi) + \sin(\phi)\sin(\psi))\right] d\phi d\theta| \tag{70}$$

$$|\gamma_{12}(0, R/\lambda, \psi)| = |\frac{1}{\pi\rho_{UD}^2}\int_0^{\rho_{UD}} \theta \int_0^{2\pi} \exp\left[-i2\pi\theta R/\lambda(\cos(\phi)\cos(\psi) + \sin(\phi)\sin(\psi))\right] d\phi d\theta| \tag{70}$$

Making use of the additional changes of variables

$$\begin{aligned} z &= 2\pi\theta R/\lambda \\ \Phi &= \pi/2 - \phi + \psi, \end{aligned} \tag{71}$$

Eq. (70) becomes

$$|\gamma_{12}(0, R/\lambda, \psi)| = |(\frac{\lambda}{2\pi R})^2 \frac{1}{\pi\rho_{UD}^2}\int_0^{2\pi\rho_{UD}R/\lambda} \theta \int_{-3\pi/2+\psi}^{\pi/2+\psi} \cos(z\sin(\Phi)) d\Phi d\theta|. \tag{72}$$

$$|\gamma_{12}(0, R/\lambda, \psi)| = |\frac{1}{\pi\rho_{UD}^2}\int_0^{\rho_{UD}} \theta \int_0^{2\pi} \exp\left[-i2\pi\theta R/\lambda(\cos(\phi)\cos(\psi) + \sin(\phi)\sin(\psi))\right] d\phi d\theta| \tag{70}$$

Making use of the additional changes of variables

$$\begin{aligned} z &= 2\pi\theta R/\lambda \\ \Phi &= \pi/2 - \phi + \psi, \end{aligned} \tag{71}$$

Eq. (70) becomes

$$|\gamma_{12}(0, R/\lambda, \psi)| = |(\frac{\lambda}{2\pi R})^2 \frac{1}{\pi\rho_{UD}^2}\int_0^{2\pi\rho_{UD}R/\lambda} \theta \int_{-3\pi/2+\psi}^{\pi/2+\psi} \cos(z\sin(\Phi)) d\Phi d\theta|. \tag{72}$$

Reminding the definition of the zero order Bessel function $J_0(x)$

$$J_0(x) = \frac{1}{\pi}\int_0^{\pi} \cos[x\sin(\theta)] d\theta, \tag{73}$$

and the relation existing between $J_0(x)$ and the first order Bessel function $J_1(x)$, namely

$$xJ_1(x) = \int x' J_0(x')dx', \tag{74}$$

Eq. (72) successively reduces to

$$|\gamma_{12}(0, R/\lambda)| = |(\frac{\lambda}{2\pi R})^2 \frac{1}{\pi\rho_{UD}^2} 2\pi \int_0^{2\pi\rho_{UD}R/\lambda} zJ_0(z)dz| \tag{75}$$

and the relation existing between $J_0(x)$ and the first order Bessel function $J_1(x)$, namely

$$xJ_1(x) = \int x' J_0(x')dx', \tag{74}$$

Eq. (72) successively reduces to

$$|\gamma_{12}(0, R/\lambda)| = |(\frac{\lambda}{2\pi R})^2 \frac{1}{\pi\rho_{UD}^2} 2\pi \int_0^{2\pi\rho_{UD}R/\lambda} zJ_0(z)dz| \tag{75}$$

and

$$|\gamma_{12}(0, R/\lambda)| = |2\frac{J_1(2\pi\rho_{UD}R/\lambda)}{2\pi\rho_{UD}R/\lambda}|. \tag{76}$$

and the relation existing between $J_0(x)$ and the first order Bessel function $J_1(x)$, namely

$$xJ_1(x) = \int x' J_0(x')dx', \tag{74}$$

Eq. (72) successively reduces to

$$|\gamma_{12}(0, R/\lambda)| = |(\frac{\lambda}{2\pi R})^2 \frac{1}{\pi\rho_{UD}^2} 2\pi \int_0^{2\pi\rho_{UD}R/\lambda} zJ_0(z)dz| \tag{75}$$

and

$$|\gamma_{12}(0, R/\lambda)| = |2\frac{J_1(2\pi\rho_{UD}R/\lambda)}{2\pi\rho_{UD}R/\lambda}|. \tag{76}$$

We thus find that the expression (34) of the fringe visibility for the case of a star seen as a projected $2-D$ uniform circular disk with an angular dimater $\theta_{UD} = 2\rho_{UD}$ is

$$v = \left(\frac{I_{max} - I_{min}}{I_{max} + I_{min}}\right) = |\gamma_{12}(0, u)| = \left|\frac{2J_1(\pi\theta_{UD}u)}{\pi\theta_{UD}u}\right|, \tag{77}$$

where we have set $u = R/\lambda$.

As a reminder, the Bessel function has the following properties

$$J_1(x = 3.8317...) = 0$$
$$\lim_{x \to 0} \frac{J_1(x)}{x} = 1/2, \tag{78}$$

which allow us to easily understand the behavior of the visibility function illustrated in Fig. 27.

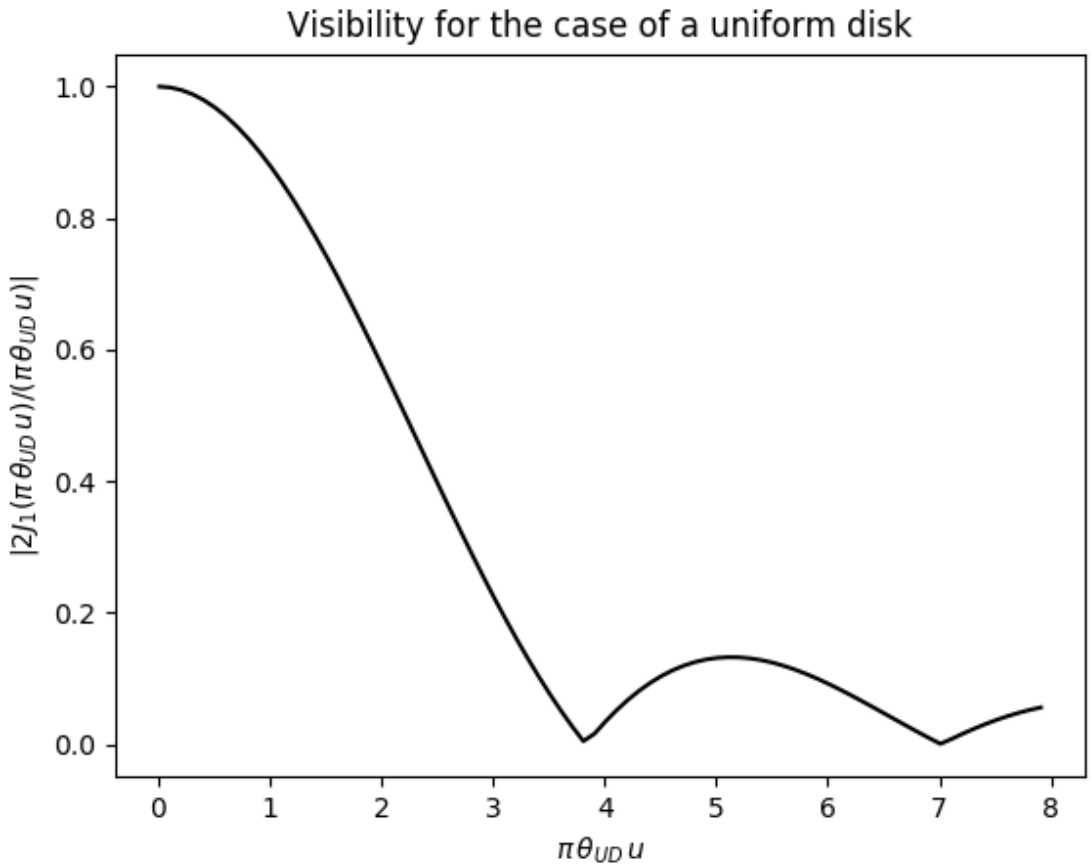

Figure: Visibility function expected for a star consisting of a uniformly bright circular disk with an angular diameter θ_{UD}.

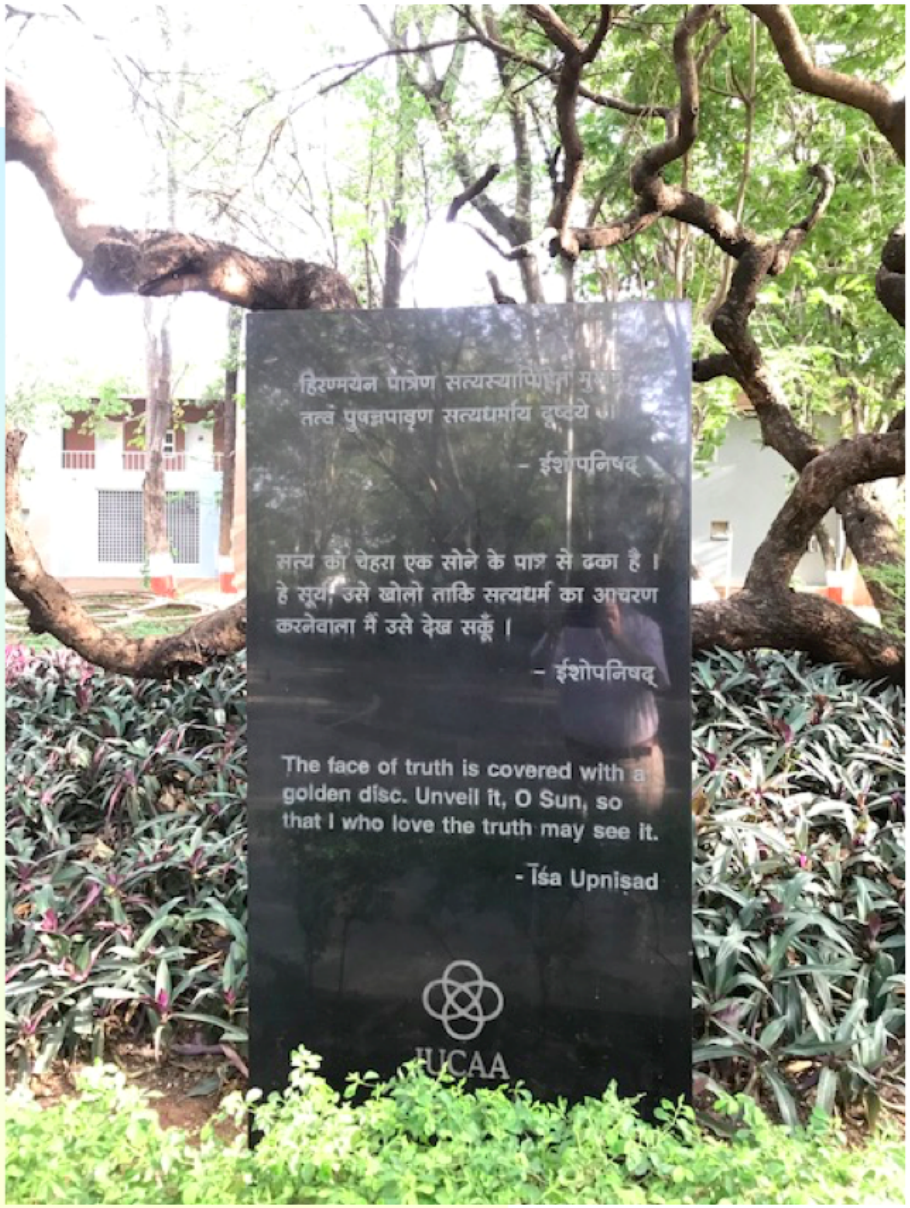

Figure: Face of the Truth and the Golden Disk.

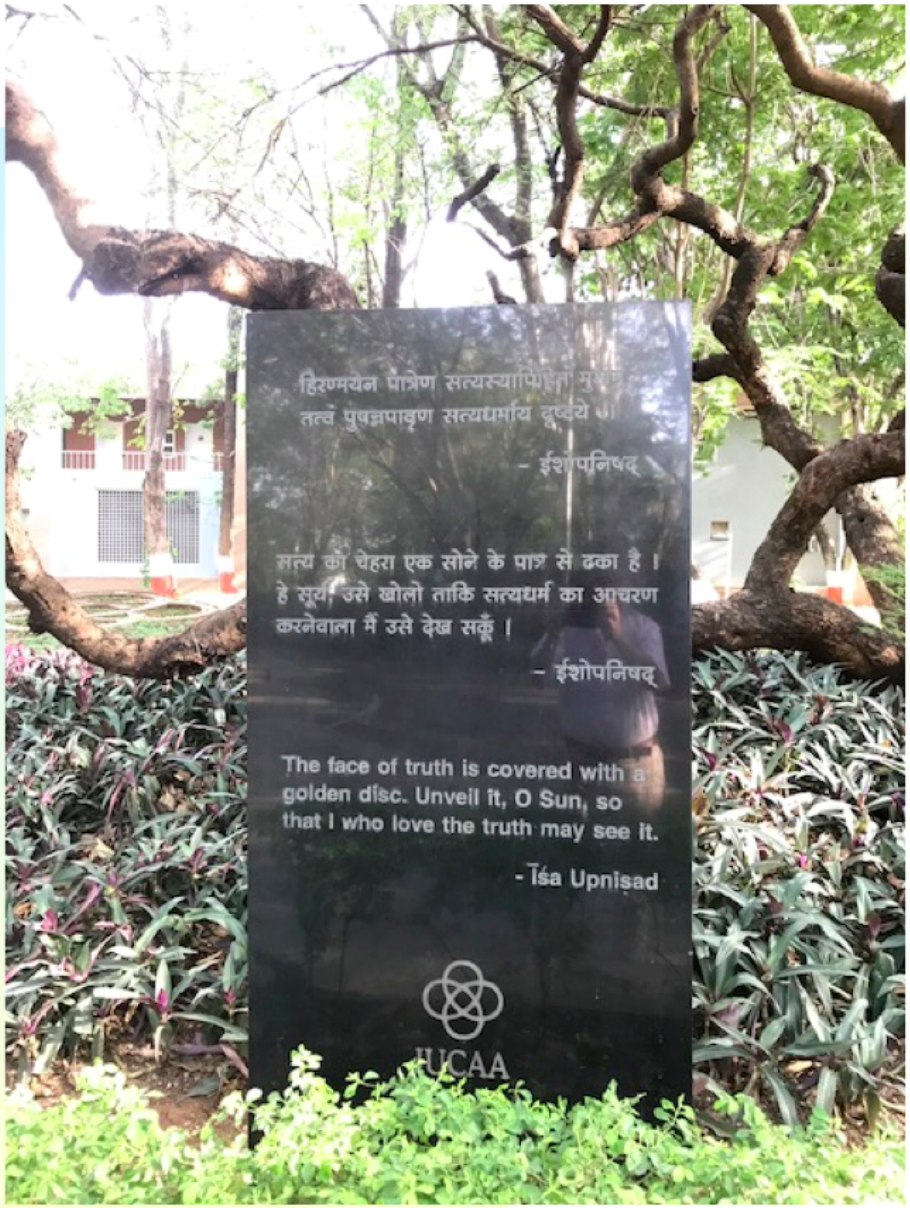

Figure: Face of the Truth and the Golden Disk.

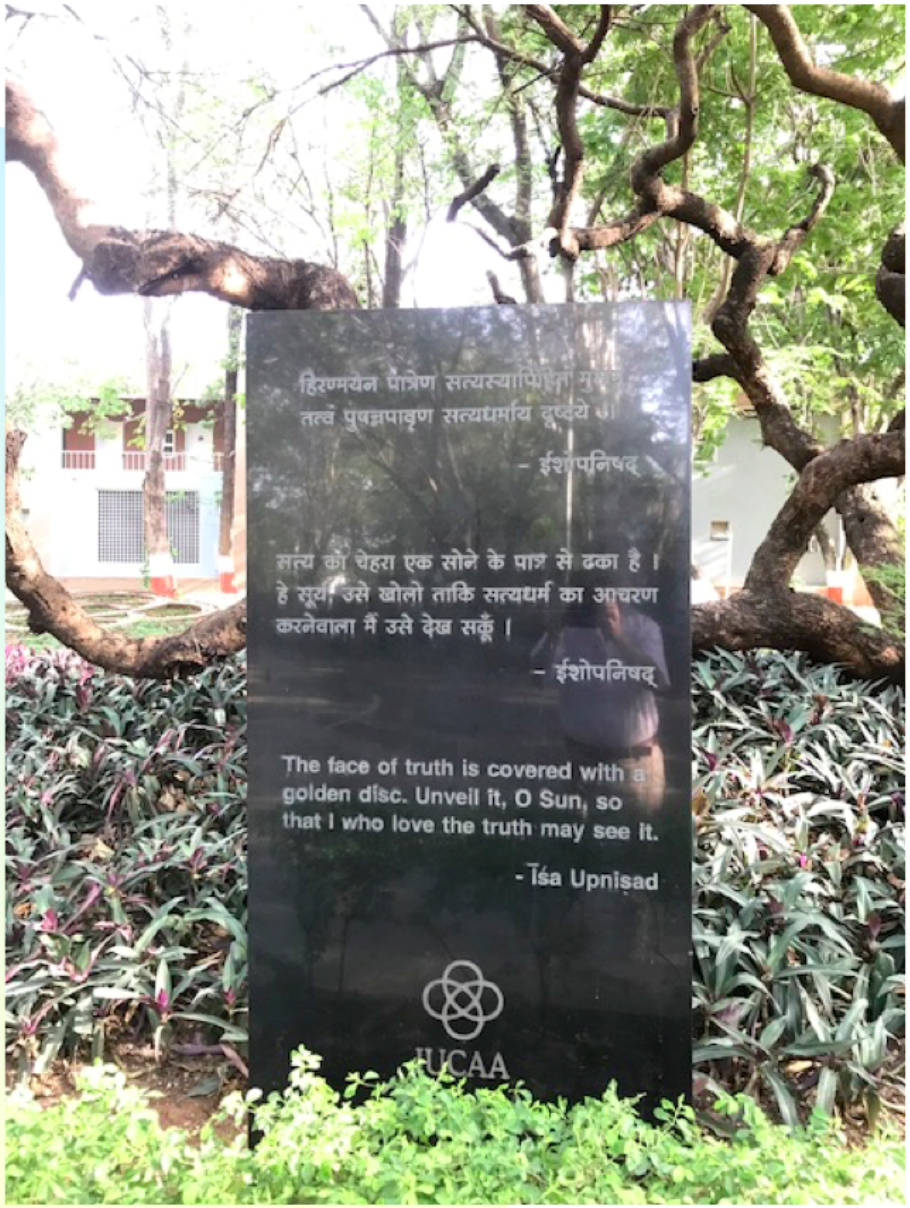

$$v = |\gamma_{12}| = \frac{2|J_1(\pi\theta_{UD}u)|}{(\pi\theta_{UD}u)}$$

Figure: Face of the Truth and the Golden Disk.

One could then wonder whether it is possible to observe interferometric fringes from our nearest star, i.e. the Sun?

One could then wonder whether it is possible to observe interferometric fringes from our nearest star, i.e. the Sun? Figure 31 illustrates such fringes in while light obtained on 9th of April 2010 using a micro interferometer consisting of 2 holes with a diameter of 11.8 μ separated by a baseline of 29.4 μ. This micro-interferometer was placed in front of the objective of an EOS 5D Canon camera. Since the picture was taken in white light, it is possible to see the effects due to color dispersion. It is then easy to get an estimate of the fringe visibility, using Eq. (77), assuming that the Sun is a uniform disk with an angular diameter of 30'.

Figure: Solar fringes photographed with an EOS 5D Canon camera in front of which was set a micro-interferometer consisting of two holes having a diameter of 11.8μ separated by a baseline of 29.4μ.

Table of Contents

LIÈGE université

Some examples of interferometers

One of the most respected sanctuaries of optical interferometry is located on the plateau of Caussols, north of Grasse, in the south of France. The I2T (in French, "Interféromètre à 2 Télescopes"), made of 2 telescopes with an aperture of 26cm each and separated by a baseline of up to 144m was characterized by an angular resolution $\Phi \sim 0.001''$ attainable for objects with an apparent magnitude brighter than $V_{lim} \sim 6$ (see Figure 32, left).

Some examples of interferometers

One of the most respected sanctuaries of optical interferometry is located on the plateau of Caussols, north of Grasse, in the south of France. The I2T (in French, "Interféromètre à 2 Télescopes"), made of 2 telescopes with an aperture of 26cm each and separated by a baseline of up to 144m was characterized by an angular resolution $\Phi \sim 0.001''$ attainable for objects with an apparent magnitude brighter than $V_{lim} \sim 6$ (see Figure 32, left). First interference fringes were obtained on Vega in 1975 (Fig. 32, right).

Some examples of interferometers

One of the most respected sanctuaries of optical interferometry is located on the plateau of Caussols, north of Grasse, in the south of France. The I2T (in French, "Interféromètre à 2 Télescopes"), made of 2 telescopes with an aperture of 26cm each and separated by a baseline of up to 144m was characterized by an angular resolution $\Phi \sim 0.001''$ attainable for objects with an apparent magnitude brighter than $V_{lim} \sim 6$ (see Figure 32, left). First interference fringes were obtained on Vega in 1975 (Fig. 32, right). About twenty angular diameters of stars have been measured using the same I2T by Prof. Antoine Labeyrie and his close collaborators.

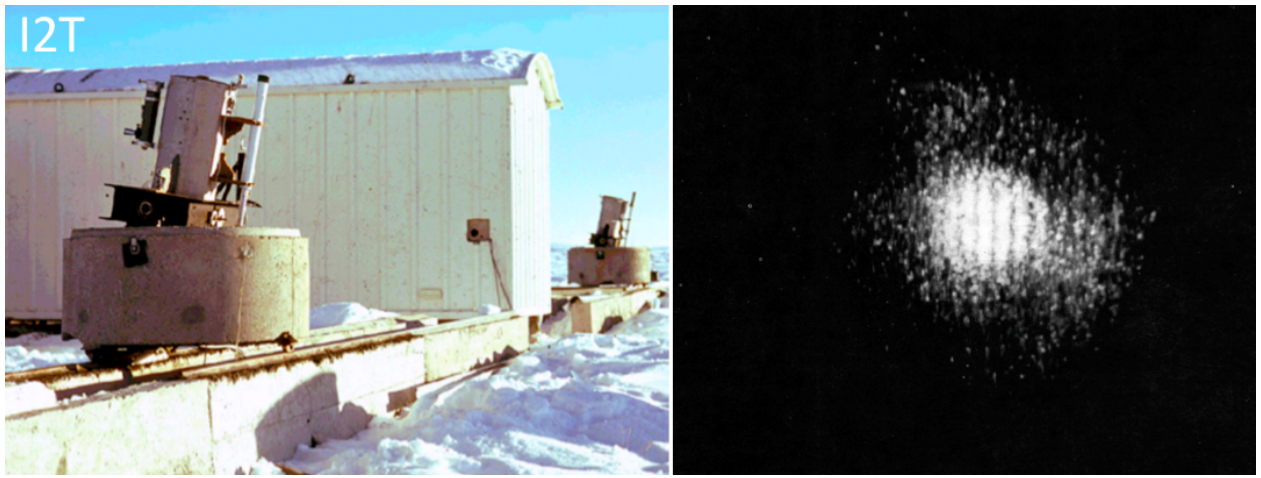

Figure: First fringes obtained with the I2T on Vega (Labeyrie et al. 1975, © Observatoire de la Côte d'Azur).

Some examples of interferometers

In order to equalize the light paths collected from the stars passing through the two telescopes, optical delay lines are mandatory. These have been successfully used for the first time in 1975 (see Fig. 33 for an illustration of how delay lines work).

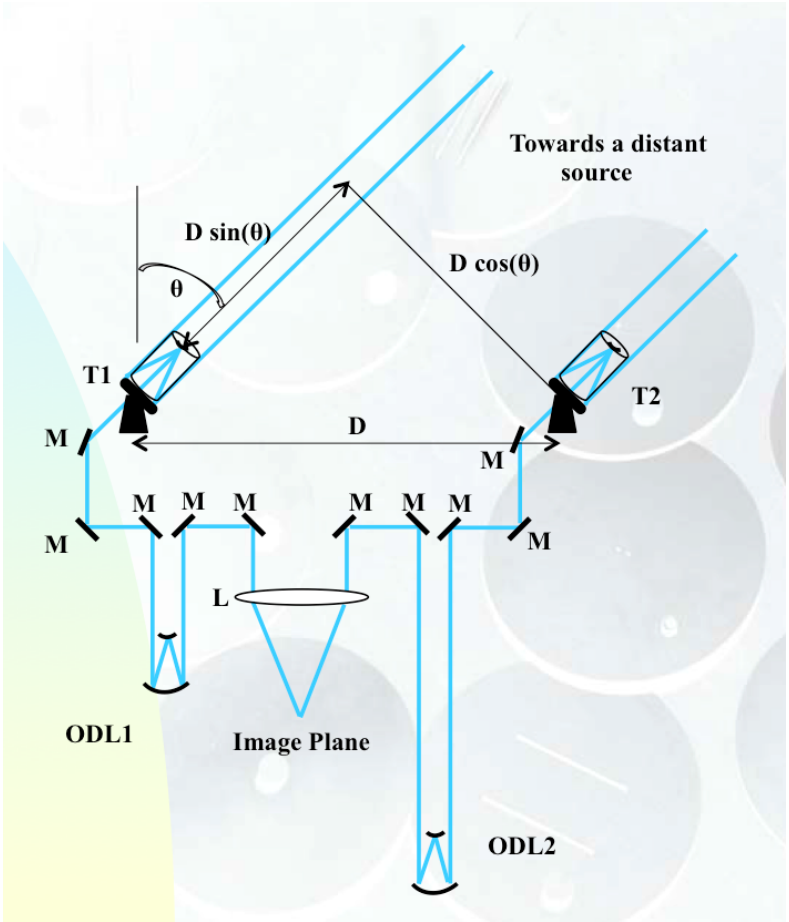

Figure: Use of optical delay lines to compensate for the continuous change in the lengths of the two light paths as the Earth rotates.

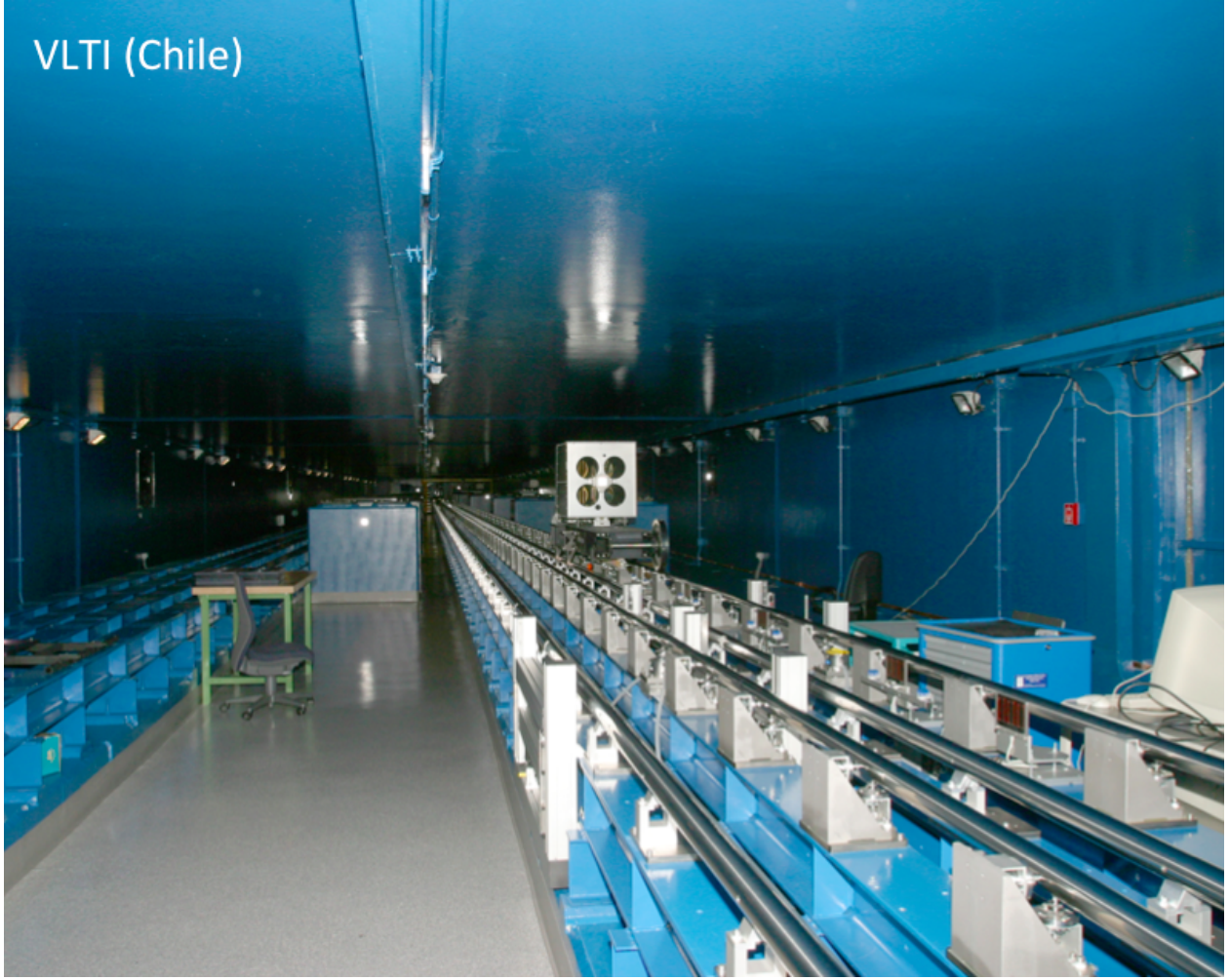

Figure: Optical delay lines at VLTI. © ESO.

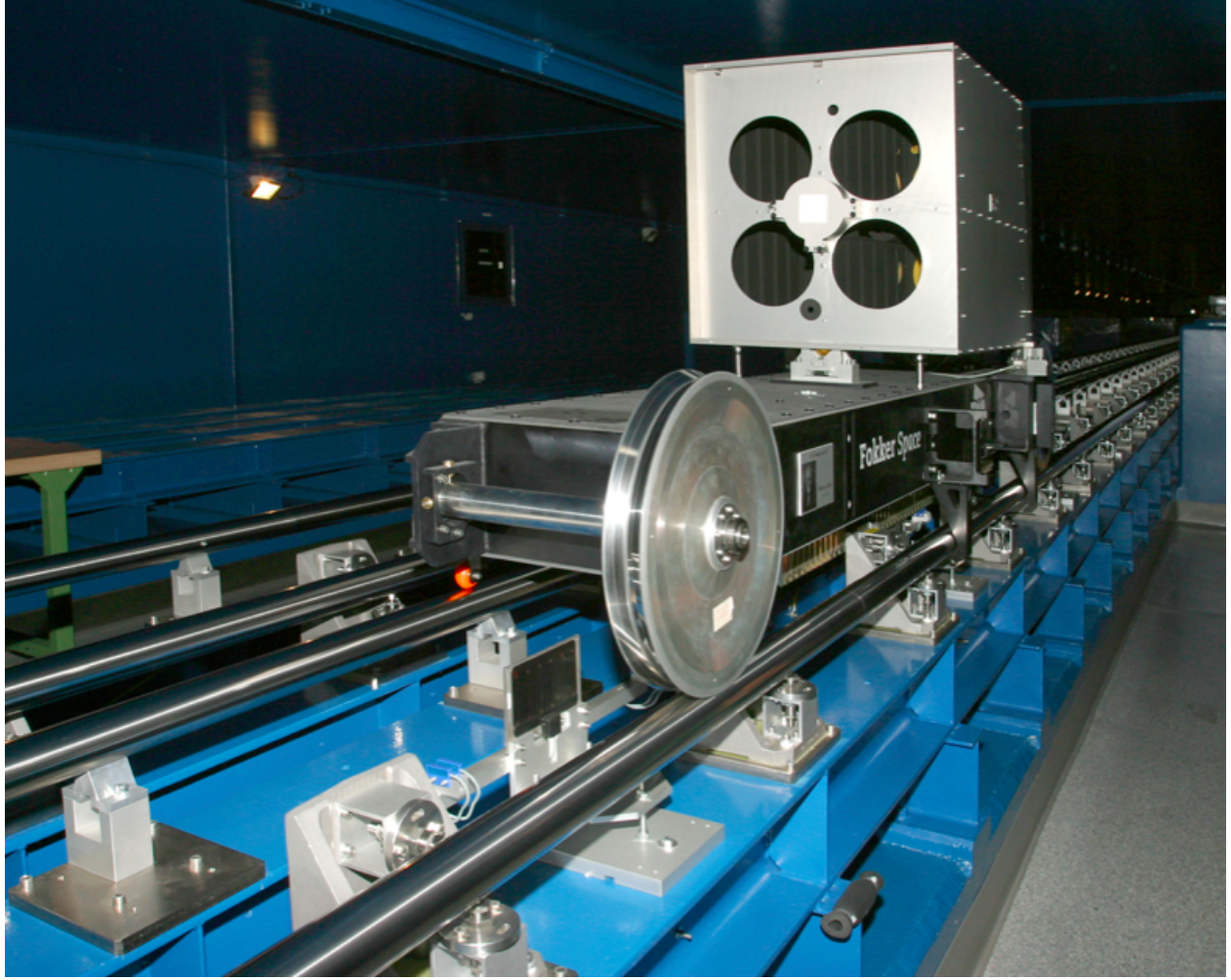

Figure: Optical delay lines at VLTI. © ESO.

Some examples of interferometers

The GI2T (in French, "Grand Interféromètre à 2 Télescopes") composed of two 1.5m telescopes was subsequently used by the same team. The two big telescopes could in principle be set 2 km apart, corresponding to an angular resolution $\Phi \sim 0.0001''$ for V_{lim} = 15-17 (see Fig. 36). Prof. A. Labeyrie also proposed to build a large network of ($\sim$ 27) optical telescopes whose individual diameters would be of the order of 10m.

Figure: The GI2T constructed by Antoine Labeyrie and his close collaborators on the plateau of Caussols, north of Grasse, near Nice (France, © Observatoire de la Côte d'Azur).

Some examples of interferometers

Since the beginning of the 21^{st} century, the modern sanctuary of stellar interferometry and aperture synthesis is undoubtedly the Very Large Telescope Interferometer (VLTI) of ESO (Southern European Observatory), located in Chile on Mount Paranal (see Fig. 37).

Some examples of interferometers

Since the beginning of the 21^{st} century, the modern sanctuary of stellar interferometry and aperture synthesis is undoubtedly the Very Large Telescope Interferometer (VLTI) of ESO (Southern European Observatory), located in Chile on Mount Paranal (see Fig. 37). The VLTI is a European interferometer that can re-combine the signal from 2, 3 or 4 telescopes depending on the instrument used. It has 4 telescopes of 8.2m and 4 mobile telescopes of 1.8m. Only telescopes of the same size can be re-combined together. The auxiliary telescopes of 1.8m can be easily moved allowing a better coverage of the u, v plane. The maximum base length of this interferometer is about 200m.

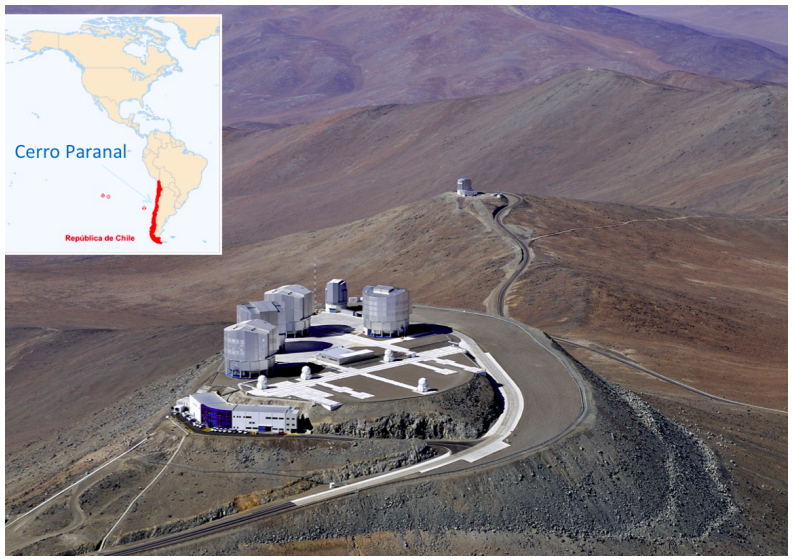

Figure: The Very Large Telescope Interferometer (VLTI) at the top ofParanal (Chile, © ESO).

Some examples of interferometers

CHARA is another very performing interferometer located on the heights of Los Angeles, California (see Fig. 38). It is installed on the historic observatory of Mount Wilson. Remember that it was with the 2.5m telescope of this observatory that the first measurement of a stellar diameter was made by Michelson and Pease by installing a beam of 7m at the top of the telescope.

Some examples of interferometers

CHARA is another very performing interferometer located on the heights of Los Angeles, California (see Fig. 38). It is installed on the historic observatory of Mount Wilson. Remember that it was with the 2.5m telescope of this observatory that the first measurement of a stellar diameter was made by Michelson and Pease by installing a beam of 7m at the top of the telescope.
The CHARA interferometric array, operational since 1999 is composed of 6 telescopes of 1m in diameter. These 6 telescopes can be either re-combined by 2, by 3 since 2008 and very soon the 6 together. The maximum base length of this interferometer is 330m allowing to achieve an angular resolution of 200μarcsec.

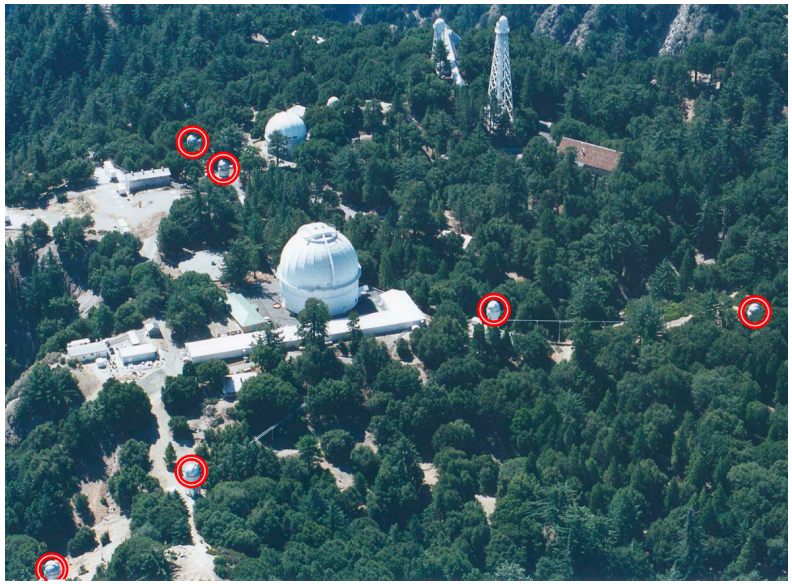

Figure: The CHARA interferometer composed of six 1m telescopes at Mount Wilson Observatory (California, USA). © The Observatories of the Carnegie Institution.

Some examples of interferometers

It is mainly used for angular diameter measurements but also for the detection and characterization of tight binary stars as well as for the detection of exo-zodiacal clouds (clouds of dust gravitating around the stars).

Some examples of interferometers

It is mainly used for angular diameter measurements but also for the detection and characterization of tight binary stars as well as for the detection of exo-zodiacal clouds (clouds of dust gravitating around the stars).
Another famous optical/IR interferometer is the Keck Interferometer made of two 10m telescopes separated by a fixed baseline of 85m (see Fig. 39) on top of Mauna Kea (Hawaii, USA).

Figure: The Keck interferometer on top of Mauna Kea (Hawaii, USA). © Ethan Tweedie.

Table of Contents

LIÈGE université

Three important theorems and some applications: the fundamental theorem

When we previously established the relation existing between the structure of an extended celestial source and the visibility of the fringes observed with an interferometer, we implicitly assumed that the size of the apertures was infinitely small (hole apertures).

Three important theorems and some applications: the fundamental theorem

When we previously established the relation existing between the structure of an extended celestial source and the visibility of the fringes observed with an interferometer, we implicitly assumed that the size of the apertures was infinitely small (hole apertures). Use of the fundamental theorem allows one to calculate the response function of an interferometer equipped with finite size apertures.

Three important theorems and some applications: the fundamental theorem

When we previously established the relation existing between the structure of an extended celestial source and the visibility of the fringes observed with an interferometer, we implicitly assumed that the size of the apertures was infinitely small (hole apertures). Use of the fundamental theorem allows one to calculate the response function of an interferometer equipped with finite size apertures.

The fundamental theorem that we shall demonstrate here merely stipulates that given a converging optical system which can be assimilated to the lens or to the mirror of a telescope, or of an optical interferometer, the complex amplitude distribution $a(p, q)$ of the electromagnetic field of radiation in the focal plane is the Fourier transform of the complex amplitude distribution $A(x, y)$ of the electromagnetic field in the pupil plane, i.e.

$$a(p, q) = \int_{R^2} A(x, y) \exp\left[-i2\pi(px + qy)\right] dxdy \tag{79}$$

Three important theorems and some applications: the fundamental theorem

When we previously established the relation existing between the structure of an extended celestial source and the visibility of the fringes observed with an interferometer, we implicitly assumed that the size of the apertures was infinitely small (hole apertures). Use of the fundamental theorem allows one to calculate the response function of an interferometer equipped with finite size apertures.

The fundamental theorem that we shall demonstrate here merely stipulates that given a converging optical system which can be assimilated to the lens or to the mirror of a telescope, or of an optical interferometer, the complex amplitude distribution $a(p,q)$ of the electromagnetic field of radiation in the focal plane is the Fourier transform of the complex amplitude distribution $A(x,y)$ of the electromagnetic field in the pupil plane, i.e.

$$a(p,q) = \int_{R^2} A(x,y) \exp\left[-i2\pi(px+qy)\right] dxdy \tag{79}$$

or in a more compact form

$$a(p,q) = FT_{-}(A(x,y))(p,q) \tag{80}$$

with

$$p = \frac{x'}{\lambda f} \quad \text{and} \quad q = \frac{y'}{\lambda f} \tag{81}$$

where x', y' refer to the Cartesian coordinates in the focal plane, λ to the wavelength of the monochromatic light under consideration and f the effective focal length of the converging system.

where x', y' refer to the Cartesian coordinates in the focal plane, λ to the wavelength of the monochromatic light under consideration and f the effective focal length of the converging system.

The figure on the next slide represents a convergent optical system, its focal point F', its principal planes P, P' and its principal points H and H'. The latter degenerate with the optical center in the case of a thin lens or with the bottom of the dish in the case of a single mirror.

where x', y' refer to the Cartesian coordinates in the focal plane, λ to the wavelength of the monochromatic light under consideration and f the effective focal length of the converging system.

The figure on the next slide represents a convergent optical system, its focal point F', its principal planes P, P' and its principal points H and H'. The latter degenerate with the optical center in the case of a thin lens or with the bottom of the dish in the case of a single mirror.

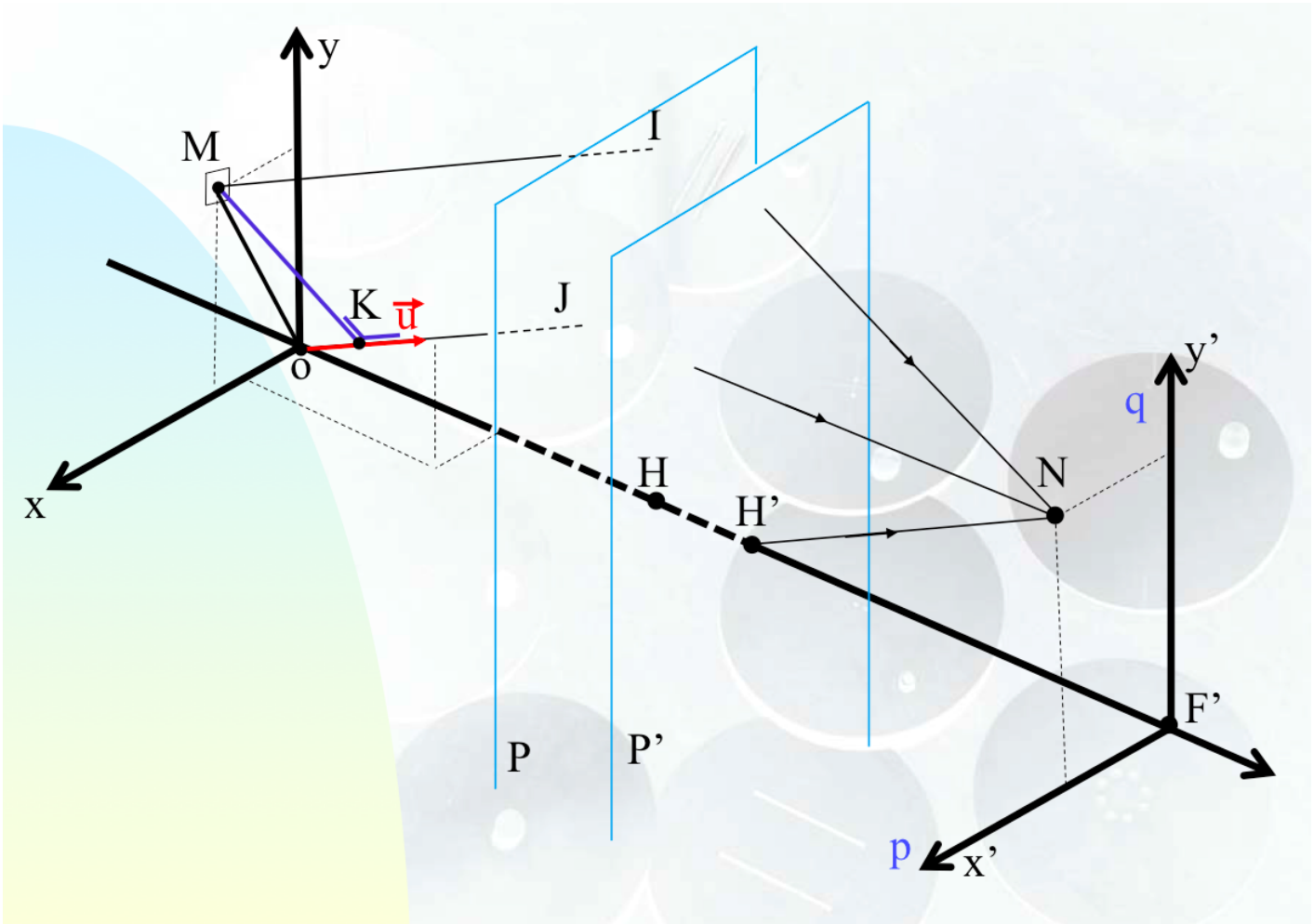

Figure: Fourier transform by a focusing optical system represented by its main planes P and P'. For the case of a thin lens, the latter would be degenerated into a single plane passing through its center.

The two orthonormal coordinate systems (O, x, y, z) and (F', x', y', z') make it possible to locate the input pupil plane and the image focal plane of the optical system. The pupil plane would normally be at the level of the primary mirror but, to simplify the calculations, we will arbitrarily shift it by placing it at the object focus F of the instrument.

The two orthonormal coordinate systems (O, x, y, z) and (F', x', y', z') make it possible to locate the input pupil plane and the image focal plane of the optical system. The pupil plane would normally be at the level of the primary mirror but, to simplify the calculations, we will arbitrarily shift it by placing it at the object focus F of the instrument.

For a mirror telescope, the planes O, x, y and F', x', y' are mathematically the same $(F = F')$ but in all cases, the term 'pupil plane' will serve as the support for the definition of the vibration state at the entrance of the collector while the 'focal plane' will serve as the support for the definition of the image that the collector gives of the source located at infinity. Defining the action of the collector is thus to establish the transformation that it operates on the radiation between these two planes.

The **hypotheses** underlying this theorem are:

- H1. The optical system is free from any geometric aberration.

The **hypotheses** underlying this theorem are:

- H1. The optical system is free from any geometric aberration.
- H2. The edges of the diaphragm do not disturb the electromagnetic field of radiation, that is to say that the diaphragm behaves as an "all (1) or nothing (0)" function with respect to this field. This is equivalent to assume that the wavelength of the light is small compared to the dimensions of the collecting aperture(s).

The **hypotheses** underlying this theorem are:

- H1. The optical system is free from any geometric aberration.
- H2. The edges of the diaphragm do not disturb the electromagnetic field of radiation, that is to say that the diaphragm behaves as an "all (1) or nothing (0)" function with respect to this field. This is equivalent to assume that the wavelength of the light is small compared to the dimensions of the collecting aperture(s).
- H3. No disturbance, other than those imposed by the optical system, intervenes between the pupil and the focal planes. The optical elements are thus assumed to be perfectly transparent or reflective.

The **hypotheses** underlying this theorem are:

- H1. The optical system is free from any geometric aberration.
- H2. The edges of the diaphragm do not disturb the electromagnetic field of radiation, that is to say that the diaphragm behaves as an "all (1) or nothing (0)" function with respect to this field. This is equivalent to assume that the wavelength of the light is small compared to the dimensions of the collecting aperture(s).
- H3. No disturbance, other than those imposed by the optical system, intervenes between the pupil and the focal planes. The optical elements are thus assumed to be perfectly transparent or reflective.
- H4. The light source is located at an infinite distance from the optical system and can thus be considered to be point-like.

The **hypotheses** underlying this theorem are:

- H1. The optical system is free from any geometric aberration.
- H2. The edges of the diaphragm do not disturb the electromagnetic field of radiation, that is to say that the diaphragm behaves as an "all (1) or nothing (0)" function with respect to this field. This is equivalent to assume that the wavelength of the light is small compared to the dimensions of the collecting aperture(s).
- H3. No disturbance, other than those imposed by the optical system, intervenes between the pupil and the focal planes. The optical elements are thus assumed to be perfectly transparent or reflective.
- H4. The light source is located at an infinite distance from the optical system and can thus be considered to be point-like.
- H5. The disturbances occurring between the source and the pupil plane are weak and have very long evolution times relative to the period (i.e. $T = 1/\nu = \lambda/c$) of the radiation.

The **hypotheses** underlying this theorem are:

- H1. The optical system is free from any geometric aberration.
- H2. The edges of the diaphragm do not disturb the electromagnetic field of radiation, that is to say that the diaphragm behaves as an "all (1) or nothing (0)" function with respect to this field. This is equivalent to assume that the wavelength of the light is small compared to the dimensions of the collecting aperture(s).
- H3. No disturbance, other than those imposed by the optical system, intervenes between the pupil and the focal planes. The optical elements are thus assumed to be perfectly transparent or reflective.
- H4. The light source is located at an infinite distance from the optical system and can thus be considered to be point-like.
- H5. The disturbances occurring between the source and the pupil plane are weak and have very long evolution times relative to the period (i.e. $T = 1/\nu = \lambda/c$) of the radiation.
- H6. The radiation is monochromatic and has a fixed polarization plane.

LIÈGE université

Theorem statement:
Within a multiplicative coefficient of the variables, the amplitude distribution in the focal plane is the Fourier transform of the amplitude distribution in the pupil plane.

Demonstration:
Consider the different points $(x,\ y)$ of the pupil plane. H6 (i.e. the previous hypothesis 6) makes it possible to represent the electrical component of the electromagnetic field by the real part of the vibration distribution

$$A(x,y)\exp\left(i2\pi\nu t\right), \tag{82}$$

with the very general representation of the expression of the complex amplitude $A(x,y)$

$$A(x,y)=\mathcal{A}(x,y)\exp\left(i\Phi(x,y)\right)P_0(x,y), \tag{83}$$

where $\mathcal{A}(x,y)$ and $\Phi(x,y)$ represent the amplitude and phase of the electric field and $P_0(x,y)$ the input pupil function which is 1 inside the pupil and 0 outside (in agreement with H2 and H3).

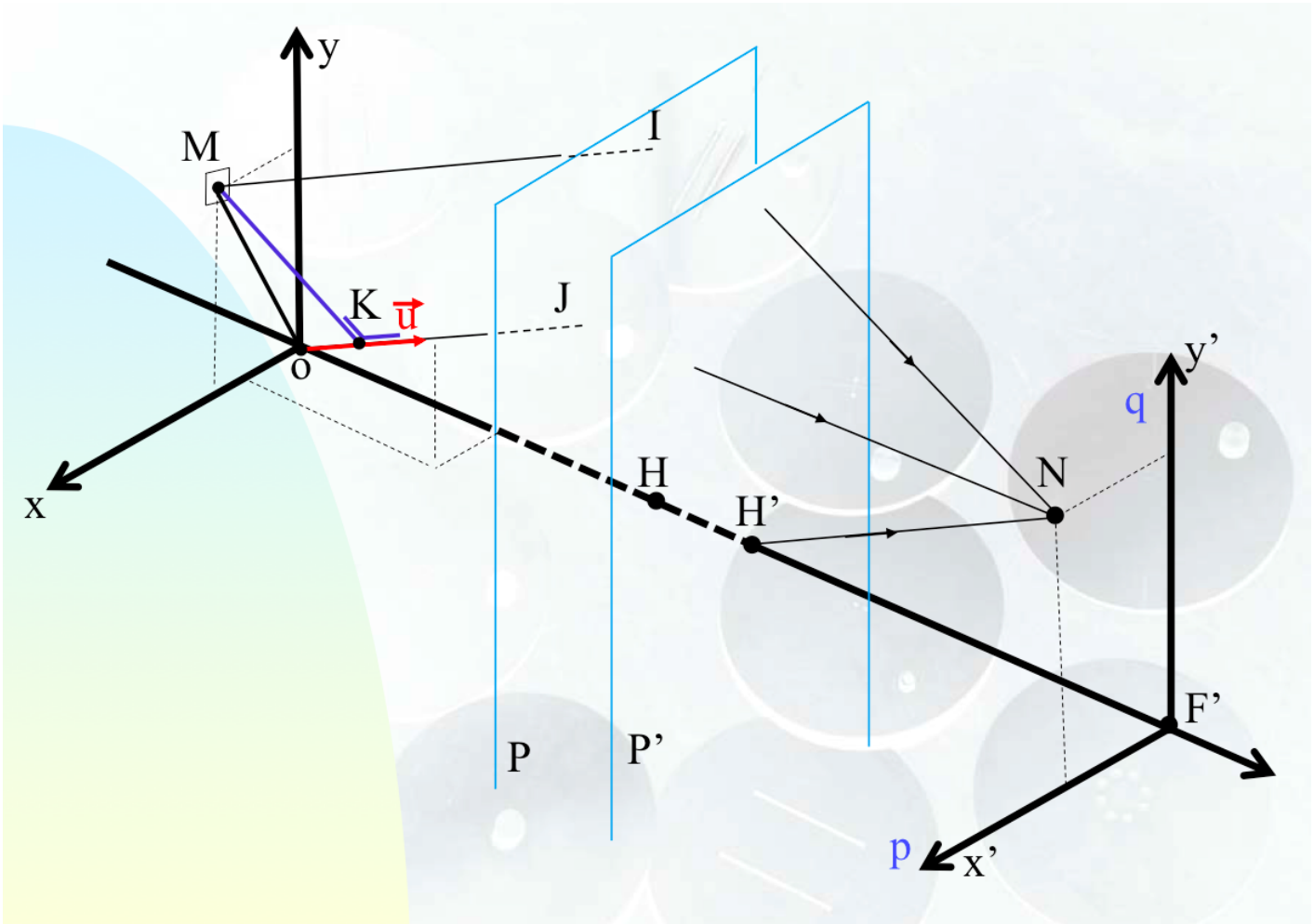

Figure: Fourier transform by a focusing optical system represented by its main planes P and P'. For the case of a thin lens, the latter would be degenerated into a single plane passing through its center.

Three important theorems and some applications: the fundamental theorem

In agreement with the Huygens-Fresnel principle, we will consider in the following that every point reached by a wave can be considered as a secondary source re-emitting a vibration with the same amplitude, the same frequency ν, the same polarization and the same phase (within a constant phase shift of $\pi/2$) as those of the incident vibration at this point.

Three important theorems and some applications: the fundamental theorem

In agreement with the Huygens-Fresnel principle, we will consider in the following that every point reached by a wave can be considered as a secondary source re-emitting a vibration with the same amplitude, the same frequency ν, the same polarization and the same phase (within a constant phase shift of $\pi/2$) as those of the incident vibration at this point.
The point $N(x',y')$ of the focal plane will thus receive vibrations emitted by all the points of the pupil plane. The laws of geometrical optics, deduced from the Fermat principle, make it possible to write that the rays which, after the optical system, converge at the point N of the image focal plane, were, before the optical system, parallel to $H'N$.
Having assumed that the source is at infinity, the amplitude will be preserved between the pupil plane and the focal plane.

In agreement with the Huygens-Fresnel principle, we will consider in the following that every point reached by a wave can be considered as a secondary source re-emitting a vibration with the same amplitude, the same frequency ν, the same polarization and the same phase (within a constant phase shift of $\pi/2$) as those of the incident vibration at this point.
The point $N(x',y')$ of the focal plane will thus receive vibrations emitted by all the points of the pupil plane. The laws of geometrical optics, deduced from the Fermat principle, make it possible to write that the rays which, after the optical system, converge at the point N of the image focal plane, were, before the optical system, parallel to $H'N$.
Having assumed that the source is at infinity, the amplitude will be preserved between the pupil plane and the focal plane. From the point $M(x,y)$ of the pupil plane, the point $N(x',y')$ of the focal plane will thus receive the vibration

$$A(x,y)\exp\left(i2\pi\nu t + i\Psi\right). \tag{84}$$

Let us take as the zero phase shift reference that of the ray passing through the point O along the direction OJN.

In agreement with the Huygens-Fresnel principle, we will consider in the following that every point reached by a wave can be considered as a secondary source re-emitting a vibration with the same amplitude, the same frequency ν, the same polarization and the same phase (within a constant phase shift of $\pi/2$) as those of the incident vibration at this point.
The point $N(x',y')$ of the focal plane will thus receive vibrations emitted by all the points of the pupil plane. The laws of geometrical optics, deduced from the Fermat principle, make it possible to write that the rays which, after the optical system, converge at the point N of the image focal plane, were, before the optical system, parallel to $H'N$.
Having assumed that the source is at infinity, the amplitude will be preserved between the pupil plane and the focal plane. From the point $M(x,y)$ of the pupil plane, the point $N(x',y')$ of the focal plane will thus receive the vibration

$$A(x,y)\exp\left(i2\pi\nu t + i\Psi\right). \tag{84}$$

Let us take as the zero phase shift reference that of the ray passing through the point O along the direction OJN. The phase shift Ψ can then be expressed using the difference between the optical paths

$$\delta = d(MIN) - d(OJN), \tag{85}$$

In agreement with the Huygens-Fresnel principle, we will consider in the following that every point reached by a wave can be considered as a secondary source re-emitting a vibration with the same amplitude, the same frequency ν, the same polarization and the same phase (within a constant phase shift of $\pi/2$) as those of the incident vibration at this point.
The point $N(x',y')$ of the focal plane will thus receive vibrations emitted by all the points of the pupil plane. The laws of geometrical optics, deduced from the Fermat principle, make it possible to write that the rays which, after the optical system, converge at the point N of the image focal plane, were, before the optical system, parallel to $H'N$.
Having assumed that the source is at infinity, the amplitude will be preserved between the pupil plane and the focal plane. From the point $M(x,y)$ of the pupil plane, the point $N(x',y')$ of the focal plane will thus receive the vibration

$$A(x,y)\exp\left(i2\pi\nu t + i\Psi\right). \tag{84}$$

Let us take as the zero phase shift reference that of the ray passing through the point O along the direction OJN. The phase shift Ψ can then be expressed using the difference between the optical paths

$$\delta = d(MIN) - d(OJN), \tag{85}$$

where $d()$ refers to the distance along the specified path, and the relation

$$\Psi = 2\pi\delta/\lambda. \tag{86}$$

Three important theorems and some applications: the fundamental theorem

If the point K corresponds to the orthogonal projection of M onto OJ, M and K belong to the same wave plane which, after the optical system, will converge at the N point of the focal plane.

If the point K corresponds to the orthogonal projection of M onto OJ, M and K belong to the same wave plane which, after the optical system, will converge at the N point of the focal plane.
The Fermat principle, according to which the optical path between a point and its image is constant (rigorous stigmatism) or extremum (approximate stigmatism) makes it possible to write that the difference in optical path $(MIN)-(KJN)$ behaves in the neighborhood of zero as an infinitely small second order with respect to the $d(I,J)$ and thus also with respect to $d(O,M)$ and $d(O,K)$, which are of the same order as $d(I,J)$. As a result (see Fig. 40),

$$\delta = -d(O,K) = -|(\mathbf{OM}\,\mathbf{u})|, \tag{87}$$

$\mathbf{u}$ designating the unit vector along the direction $H'N$ and $(\mathbf{OM}\,\mathbf{u})$ the scalar product between the vectors $\mathbf{OM}$ and $\mathbf{u}$.

If the point K corresponds to the orthogonal projection of M onto OJ, M and K belong to the same wave plane which, after the optical system, will converge at the N point of the focal plane.
The Fermat principle, according to which the optical path between a point and its image is constant (rigorous stigmatism) or extremum (approximate stigmatism) makes it possible to write that the difference in optical path $(MIN)-(KJN)$ behaves in the neighborhood of zero as an infinitely small second order with respect to the $d(I,J)$ and thus also with respect to $d(O,M)$ and $d(O,K)$, which are of the same order as $d(I,J)$. As a result (see Fig. 40),

$$\delta = -d(O,K) = -|(\mathbf{OM}\,\mathbf{u})|, \tag{87}$$

$\mathbf{u}$ designating the unit vector along the direction $H'N$ and $(\mathbf{OM}\,\mathbf{u})$ the scalar product between the vectors $\mathbf{OM}$ and $\mathbf{u}$.
If the angle that $H'N$ makes with the optical axis is small, the vector of components $(x'/f,\ y'/f,\ 1)$ is the vector director of $H'N$ and has a norm close to 1 (at first order because $f >> |x'|, |y'|$).

If the point K corresponds to the orthogonal projection of M onto OJ, M and K belong to the same wave plane which, after the optical system, will converge at the N point of the focal plane.
The Fermat principle, according to which the optical path between a point and its image is constant (rigorous stigmatism) or extremum (approximate stigmatism) makes it possible to write that the difference in optical path $(MIN)-(KJN)$ behaves in the neighborhood of zero as an infinitely small second order with respect to the $d(I,J)$ and thus also with respect to $d(O,M)$ and $d(O,K)$, which are of the same order as $d(I,J)$. As a result (see Fig. 40),

$$\delta = -d(O,K) = -|(\mathbf{OM}\,\mathbf{u})|, \tag{87}$$

$\mathbf{u}$ designating the unit vector along the direction $H'N$ and $(\mathbf{OM}\,\mathbf{u})$ the scalar product between the vectors $\mathbf{OM}$ and $\mathbf{u}$.
If the angle that $H'N$ makes with the optical axis is small, the vector of components $(x'/f,\ y'/f,\ 1)$ is the vector director of $H'N$ and has a norm close to 1 (at first order because $f >> |x'|, |y'|$).
Moreover, $\mathbf{OM}$ has for components $(x,\ y,\ 0)$.

If the point K corresponds to the orthogonal projection of M onto OJ, M and K belong to the same wave plane which, after the optical system, will converge at the N point of the focal plane.
The Fermat principle, according to which the optical path between a point and its image is constant (rigorous stigmatism) or extremum (approximate stigmatism) makes it possible to write that the difference in optical path $(MIN)-(KJN)$ behaves in the neighborhood of zero as an infinitely small second order with respect to the $d(I,J)$ and thus also with respect to $d(O,M)$ and $d(O,K)$, which are of the same order as $d(I,J)$. As a result (see Fig. 40),

$$\delta = -d(O,K) = -|(\mathbf{OM}\,\mathbf{u})|, \tag{87}$$

$\mathbf{u}$ designating the unit vector along the direction $H'N$ and $(\mathbf{OM}\,\mathbf{u})$ the scalar product between the vectors $\mathbf{OM}$ and $\mathbf{u}$.
If the angle that $H'N$ makes with the optical axis is small, the vector of components $(x'/f,\ y'/f,\ 1)$ is the vector director of $H'N$ and has a norm close to 1 (at first order because $f >> |x'|, |y'|$).
Moreover, $\mathbf{OM}$ has for components $(x,\ y,\ 0)$.
Using (Eq. (87) in (86), the expression (84) becomes

$$A(x,y)\exp\left(i2\pi\nu t - xx'/\lambda f - yy'/\lambda f\right). \tag{88}$$

Choosing as new variables in the focal plane those defined in (81), we get

$$A(x, y) \exp\left(-i2\pi(xp + yq) \exp\left(i2\pi\nu t\right).\right. \tag{89}$$

The resulting vibration at the point N will be the resultant of the vibrations transmitted towards N by all the points of the pupil plane.

Choosing as new variables in the focal plane those defined in (81), we get

$$A(x, y) \exp\left(-i2\pi(xp + yq)\right) \exp\left(i2\pi\nu t\right). \tag{89}$$

The resulting vibration at the point N will be the resultant of the vibrations transmitted towards N by all the points of the pupil plane.
The equi-phase wave surfaces which reach the pupil plane are not planes if the radiation has been disturbed between the source and the entrance pupil. But the hypotheses $H4$ and $H5$ make it possible to affirm that the pupil plane is spatially coherent, that is to say that at the time scale of the vibration periods, the relative phase shift of its different points is constant.

Choosing as new variables in the focal plane those defined in (81), we get

$$A(x, y) \exp\left(-i2\pi(xp + yq)\right) \exp\left(i2\pi\nu t\right). \tag{89}$$

The resulting vibration at the point N will be the resultant of the vibrations transmitted towards N by all the points of the pupil plane.
The equi-phase wave surfaces which reach the pupil plane are not planes if the radiation has been disturbed between the source and the entrance pupil. But the hypotheses $H4$ and $H5$ make it possible to affirm that the pupil plane is spatially coherent, that is to say that at the time scale of the vibration periods, the relative phase shift of its different points is constant. Consequently, to calculate the resulting vibration at the point $N(p,q)$ of the focal plane, it is necessary to sum the amplitudes that N receives from the different points of the pupil plane.

Choosing as new variables in the focal plane those defined in (81), we get

$$A(x, y) \exp\left(-i2\pi(xp + yq)\right) \exp\left(i2\pi\nu t\right). \tag{89}$$

The resulting vibration at the point N will be the resultant of the vibrations transmitted towards N by all the points of the pupil plane.
The equi-phase wave surfaces which reach the pupil plane are not planes if the radiation has been disturbed between the source and the entrance pupil. But the hypotheses $H4$ and $H5$ make it possible to affirm that the pupil plane is spatially coherent, that is to say that at the time scale of the vibration periods, the relative phase shift of its different points is constant. Consequently, to calculate the resulting vibration at the point $N(p,q)$ of the focal plane, it is necessary to sum the amplitudes that N receives from the different points of the pupil plane. The amplitude distribution $a(p, q)$ in the focal plane then becomes

$$a(p, q) = \int_{R^2} A(x, y) \exp\left(-i2\pi(xp + yq)dxdy, \right. \tag{90}$$

Choosing as new variables in the focal plane those defined in (81), we get

$$A(x, y) \exp(-i2\pi(xp + yq) \exp(i2\pi\nu t). \tag{89}$$

The resulting vibration at the point N will be the resultant of the vibrations transmitted towards N by all the points of the pupil plane.
The equi-phase wave surfaces which reach the pupil plane are not planes if the radiation has been disturbed between the source and the entrance pupil. But the hypotheses $H4$ and $H5$ make it possible to affirm that the pupil plane is spatially coherent, that is to say that at the time scale of the vibration periods, the relative phase shift of its different points is constant. Consequently, to calculate the resulting vibration at the point $N(p,q)$ of the focal plane, it is necessary to sum the amplitudes that N receives from the different points of the pupil plane. The amplitude distribution $a(p, q)$ in the focal plane then becomes

$$a(p, q) = \int_{R^2} A(x, y) \exp(-i2\pi(xp + yq) dxdy, \tag{90}$$

that is, the complex amplitude distribution in the focal plane $a(p, q)$ is the Fourier transform of the complex amplitude distribution $A(x, y)$ in the pupil plane, i.e.

$$a(p, q) = TF_{-}[A(x, y)](p, q). \tag{91}$$

Applications of the fundamental theorem: the case of a single square aperture

Considering first the case of a single square aperture as depicted in Fig. 42 (left) and a point-like source perfectly located at zenith, i.e. the plane wavefronts arrive parallel to the aperture with a constant and real amplitude $A(x, y) = A_0$, we find that the calculation of the amplitude in the focal plane is very simple

Applications of the fundamental theorem: the case of a single square aperture

Considering first the case of a single square aperture as depicted in Fig. 42 (left) and a point-like source perfectly located at zenith, i.e. the plane wavefronts arrive parallel to the aperture with a constant and real amplitude $A(x, y) = A_0$, we find that the calculation of the amplitude in the focal plane is very simple

$$a(p, q) = A_0 \, FT(\Pi(x/a)\Pi(y/a))(p, q). \tag{92}$$

Applications of the fundamental theorem: the case of a single square aperture

Considering first the case of a single square aperture as depicted in Fig. 42 (left) and a point-like source perfectly located at zenith, i.e. the plane wavefronts arrive parallel to the aperture with a constant and real amplitude $A(x, y) = A_0$, we find that the calculation of the amplitude in the focal plane is very simple

$$a(p, q) = A_0 \, FT(\Pi(x/a)\Pi(y/a))(p, q). \tag{92}$$

Making use of the separation of the variables x, y and of the relation (61), Eq. (80) successively transforms into

$$a(p, q) = A_0 \, FT(\Pi(x/a)(p)\Pi(y/a))(q), \tag{93}$$

$$a(p, q) = A_0 \, a^2 \, \frac{sin(\pi ap)}{\pi ap} \frac{sin(\pi aq)}{\pi aq}. \tag{94}$$

Applications of the fundamental theorem: the case of a single square aperture

Considering first the case of a single square aperture as depicted in Fig. 42 (left) and a point-like source perfectly located at zenith, i.e. the plane wavefronts arrive parallel to the aperture with a constant and real amplitude $A(x, y) = A_0$, we find that the calculation of the amplitude in the focal plane is very simple

$$a(p, q) = A_0 \, FT(\Pi(x/a)\Pi(y/a))(p, q). \tag{92}$$

Making use of the separation of the variables x, y and of the relation (61), Eq. (80) successively transforms into

$$a(p, q) = A_0 \, FT(\Pi(x/a)(p)\Pi(y/a))(q), \tag{93}$$

$$a(p, q) = A_0 \, a^2 \, \frac{sin(\pi ap)}{\pi ap} \frac{sin(\pi aq)}{\pi aq}. \tag{94}$$

This is the impulse response, in amplitude, for a square pupil and in the absence of any external disturbance.

Applications of the fundamental theorem: the case of a single square aperture

Adopting the definition (11) for the intensity of the vibrations, we find that (see Fig. 42, at right)

$$i(p,q) = a(p,q)\, a^*(p,q) = |a(p,q)|^2 = i_0\, a^4 \left(\frac{sin(\pi ap)}{\pi ap}\right)^2 \left(\frac{sin(\pi aq)}{\pi aq}\right)^2 . \qquad (95)$$

Applications of the fundamental theorem: the case of a single square aperture

Adopting the definition (11) for the intensity of the vibrations, we find that (see Fig. 42, at right)

$$i(p,q) = a(p,q)\, a^*(p,q) = |a(p,q)|^2 = i_0\, a^4 \left(\frac{sin(\pi ap)}{\pi ap}\right)^2 \left(\frac{sin(\pi aq)}{\pi aq}\right)^2 . \qquad (95)$$

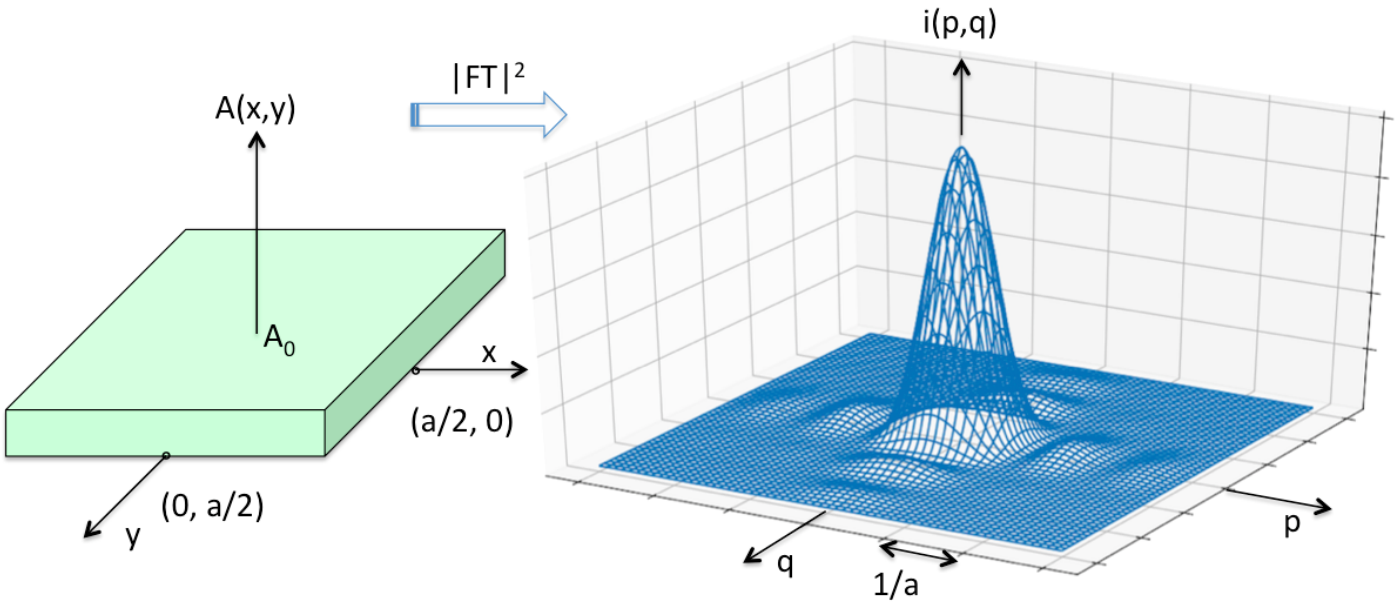

Figure: Complex amplitude distribution $A(x,y)$ in the plane of a single square aperture (left) and resulting response function in intensity $i(p,q)$ (right).

Applications of the fundamental theorem: the case of a single square aperture

Defining the angular resolution Φ of an optical system as being the angular width of the response function in intensity inside the first minima, we obtain for the values of $\pi pa = \pm\pi$ (resp. $\pi qa = \pm\pi$), i.e. $p = \pm 1/a$ (resp. $q = \pm 1/a$) and with the definition (81) for p, q

$$\frac{x'}{\lambda f} = \pm\frac{1}{a} \quad (\text{resp.} \quad \frac{y'}{\lambda f} = \pm\frac{1}{a}), \tag{96}$$

Applications of the fundamental theorem: the case of a single square aperture

Defining the angular resolution Φ of an optical system as being the angular width of the response function in intensity inside the first minima, we obtain for the values of $\pi pa = \pm\pi$ (resp. $\pi qa = \pm\pi$), i.e. $p = \pm 1/a$ (resp. $q = \pm 1/a$) and with the definition (81) for p, q

$$\frac{x'}{\lambda f} = \pm\frac{1}{a} \quad (\text{resp.} \quad \frac{y'}{\lambda f} = \pm\frac{1}{a}), \tag{96}$$

$$\Phi = \frac{\Delta x'}{f} = \frac{\Delta y'}{f} = \frac{2\lambda}{a}. \tag{97}$$

Applications of the fundamental theorem: the case of a single square aperture

Defining the angular resolution Φ of an optical system as being the angular width of the response function in intensity inside the first minima, we obtain for the values of $\pi pa = \pm\pi$ (resp. $\pi qa = \pm\pi$), i.e. $p = \pm 1/a$ (resp. $q = \pm 1/a$) and with the definition (81) for p, q

$$\frac{x'}{\lambda f} = \pm\frac{1}{a} \quad (\text{resp.} \quad \frac{y'}{\lambda f} = \pm\frac{1}{a}), \tag{96}$$

$$\Phi = \frac{\Delta x'}{f} = \frac{\Delta y'}{f} = \frac{2\lambda}{a}. \tag{97}$$

The angular resolution is thus inversely proportional to the size a of the square aperture, and proportional to the wavelength λ. Working at short wavelength with a big size aperture thus confers a better angular resolution.

Applications of the fundamental theorem: the case of a single square aperture

Defining the angular resolution Φ of an optical system as being the angular width of the response function in intensity inside the first minima, we obtain for the values of $\pi pa = \pm\pi$ (resp. $\pi qa = \pm\pi$), i.e. $p = \pm 1/a$ (resp. $q = \pm 1/a$) and with the definition (81) for p, q

$$\frac{x'}{\lambda f} = \pm\frac{1}{a} \quad (\text{resp.} \quad \frac{y'}{\lambda f} = \pm\frac{1}{a}), \tag{96}$$

$$\Phi = \frac{\Delta x'}{f} = \frac{\Delta y'}{f} = \frac{2\lambda}{a}. \tag{97}$$

The angular resolution is thus inversely proportional to the size a of the square aperture, and proportional to the wavelength λ. Working at short wavelength with a big size aperture thus confers a better angular resolution.

Applications of the fundamental theorem: the case of a single square aperture

Up to now, we have considered that the source S, assumed to be point-like and located at an infinite distance from the optical system, was on the optical axis of the instrument.

Applications of the fundamental theorem: the case of a single square aperture

Up to now, we have considered that the source S, assumed to be point-like and located at an infinite distance from the optical system, was on the optical axis of the instrument. Suppose now that it is slightly moved away from the zenith direction by a small angle. Let $(b/f,\ c/f,\ 1)$ be the unit vector representing the new direction of the source, the previous one being $(0,\ 0,\ 1)$. The plane wavefront falling on the square aperture will not have anymore a constant amplitude A_0 because each point of the pupil touched by such a wavefront will experience a phase shift given by the angle

$$\Psi = \frac{2\pi\delta}{\lambda} = \frac{2\pi(xb/f + yc/f)}{\lambda} \tag{98}$$

Applications of the fundamental theorem: the case of a single square aperture

Up to now, we have considered that the source S, assumed to be point-like and located at an infinite distance from the optical system, was on the optical axis of the instrument. Suppose now that it is slightly moved away from the zenith direction by a small angle. Let $(b/f,\ c/f,\ 1)$ be the unit vector representing the new direction of the source, the previous one being $(0,\ 0,\ 1)$. The plane wavefront falling on the square aperture will not have anymore a constant amplitude A_0 because each point of the pupil touched by such a wavefront will experience a phase shift given by the angle

$$\Psi = \frac{2\pi\delta}{\lambda} = \frac{2\pi(xb/f + yc/f)}{\lambda} \tag{98}$$

and consequently the correct expression of the complex amplitude $A(x, y)$ to be inserted in Eq. (80) becomes

$$A(x, y) = A_0\, \Pi(x/a)\Pi(y/a)\, \exp[\frac{i2\pi(xb/f + yc/f)}{\lambda}]. \tag{99}$$

Applications of the fundamental theorem: the case of a single square aperture

Up to now, we have considered that the source S, assumed to be point-like and located at an infinite distance from the optical system, was on the optical axis of the instrument. Suppose now that it is slightly moved away from the zenith direction by a small angle. Let $(b/f,\ c/f,\ 1)$ be the unit vector representing the new direction of the source, the previous one being $(0,\ 0,\ 1)$. The plane wavefront falling on the square aperture will not have anymore a constant amplitude A_0 because each point of the pupil touched by such a wavefront will experience a phase shift given by the angle

$$\Psi = \frac{2\pi\delta}{\lambda} = \frac{2\pi(xb/f + yc/f)}{\lambda} \tag{98}$$

and consequently the correct expression of the complex amplitude $A(x, y)$ to be inserted in Eq. (80) becomes

$$A(x, y) = A_0\, \Pi(x/a)\Pi(y/a)\, \exp[\frac{i2\pi(xb/f + yc/f)}{\lambda}]. \tag{99}$$

Proceeding as previously, we easily find that

Applications of the fundamental theorem: the case of a single square aperture

$$a(p,q) = A_0\, FT(\Pi(\frac{x}{a}))(p - \frac{b}{\lambda f}) FT(\Pi(\frac{y}{a}))(q - \frac{c}{\lambda f}), \tag{100}$$

Applications of the fundamental theorem: the case of a single square aperture

$$a(p,q) = A_0\, FT(\Pi(\frac{x}{a}))(p - \frac{b}{\lambda f}) FT(\Pi(\frac{y}{a}))(q - \frac{c}{\lambda f}), \tag{100}$$

and finally

$$i(p,q) = a(p,q)\, a^*(p,q) = |a(p,q)|^2 = i_0\, a^4 \left[\frac{sin(\pi a(p - \frac{b}{\lambda f}))}{\pi a(p - \frac{b}{\lambda f})}\right]^2 \left[\frac{sin(\pi a(q - \frac{c}{\lambda f}))}{\pi a(q - \frac{c}{\lambda f})}\right]^2. \tag{101}$$

Applications of the fundamental theorem: the case of a single square aperture

$$a(p,q) = A_0\, FT(\Pi(\frac{x}{a}))(p - \frac{b}{\lambda f}) FT(\Pi(\frac{y}{a}))(q - \frac{c}{\lambda f}), \tag{100}$$

and finally

$$i(p,q) = a(p,q)\, a^*(p,q) = |a(p,q)|^2 = i_0\, a^4 \left[\frac{sin(\pi a(p - \frac{b}{\lambda f}))}{\pi a(p - \frac{b}{\lambda f})}\right]^2 \left[\frac{sin(\pi a(q - \frac{c}{\lambda f}))}{\pi a(q - \frac{c}{\lambda f})}\right]^2. \tag{101}$$

The resulting intensity response function in the focal plane is nearly the same as the one previously calculated for the case $b = 0, c = 0$. It is being merely translated by a linear offset (b, c) in the x', y' focal plane and implies the invariance of the response function for a reference star that is being slightly offset from the optical axis of the system.

Three important theorems and some applications: the case of a circular aperture

Considering now a circular aperture with radius R, the complex amplitude $A(x, y)$ in the pupil plane may be represented as a circular symmetric distribution, i.e. $A(\rho, \varphi) = A_0$ for $\rho < R, \varphi \in [0, 2\pi]$ and $A(\rho, \varphi) = 0$ for $\rho > R$ (see Figure 43, at left).

Three important theorems and some applications: the case of a circular aperture

Considering now a circular aperture with radius R, the complex amplitude $A(x, y)$ in the pupil plane may be represented as a circular symmetric distribution, i.e. $A(\rho, \varphi) = A_0$ for $\rho < R, \varphi \in [0, 2\pi]$ and $A(\rho, \varphi) = 0$ for $\rho > R$ (see Figure 43, at left).

We naturally expect the distribution of the complex amplitude in the focal plane to be also circular symmetric, i.e.

$$a(\rho') = FT(A(\rho, \varphi))(\rho'). \tag{102}$$

Three important theorems and some applications: the case of a circular aperture

Considering now a circular aperture with radius R, the complex amplitude $A(x, y)$ in the pupil plane may be represented as a circular symmetric distribution, i.e. $A(\rho, \varphi) = A_0$ for $\rho < R, \varphi \in [0, 2\pi]$ and $A(\rho, \varphi) = 0$ for $\rho > R$ (see Figure 43, at left).

We naturally expect the distribution of the complex amplitude in the focal plane to be also circular symmetric, i.e.

$$a(\rho') = FT(A(\rho, \varphi))(\rho'). \tag{102}$$

It is here interesting to note that performing the above Fourier transform is quite alike deriving the expression of the visibility of a $2-D$ uniform circular disk star which angular diameter is θ_{UD} (see the last application in Section 4.5). We may just make use of the result (77) with appropriate changes of the corresponding variables. We easily find that

$$a(\rho') = A_0 \pi R^2 [2J_1(\frac{2\pi R\rho'/(\lambda f)}{2\pi R\rho'/(\lambda f)})]. \tag{103}$$

Three important theorems and some applications: the case of a circular aperture

Considering now a circular aperture with radius R, the complex amplitude $A(x, y)$ in the pupil plane may be represented as a circular symmetric distribution, i.e. $A(\rho, \varphi) = A_0$ for $\rho < R, \varphi \in [0, 2\pi]$ and $A(\rho, \varphi) = 0$ for $\rho > R$ (see Figure 43, at left).

We naturally expect the distribution of the complex amplitude in the focal plane to be also circular symmetric, i.e.

$$a(\rho') = FT(A(\rho, \varphi))(\rho'). \tag{102}$$

It is here interesting to note that performing the above Fourier transform is quite alike deriving the expression of the visibility of a $2-D$ uniform circular disk star which angular diameter is θ_{UD} (see the last application in Section 4.5). We may just make use of the result (77) with appropriate changes of the corresponding variables. We easily find that

$$a(\rho') = A_0 \pi R^2 [2J_1(\frac{2\pi R\rho'/(\lambda f)}{2\pi R\rho'/(\lambda f)})]. \tag{103}$$

The resulting intensity response function is thus given by

$$i(\rho') = a(\rho')^2 = A_0^2 (\pi R^2)^2 [2J_1(\frac{2\pi R\rho'/(\lambda f)}{2\pi R\rho'/(\lambda f)})]^2. \tag{104}$$

This is the very expression of the famous Airy disk (see Fig. 43, at right).

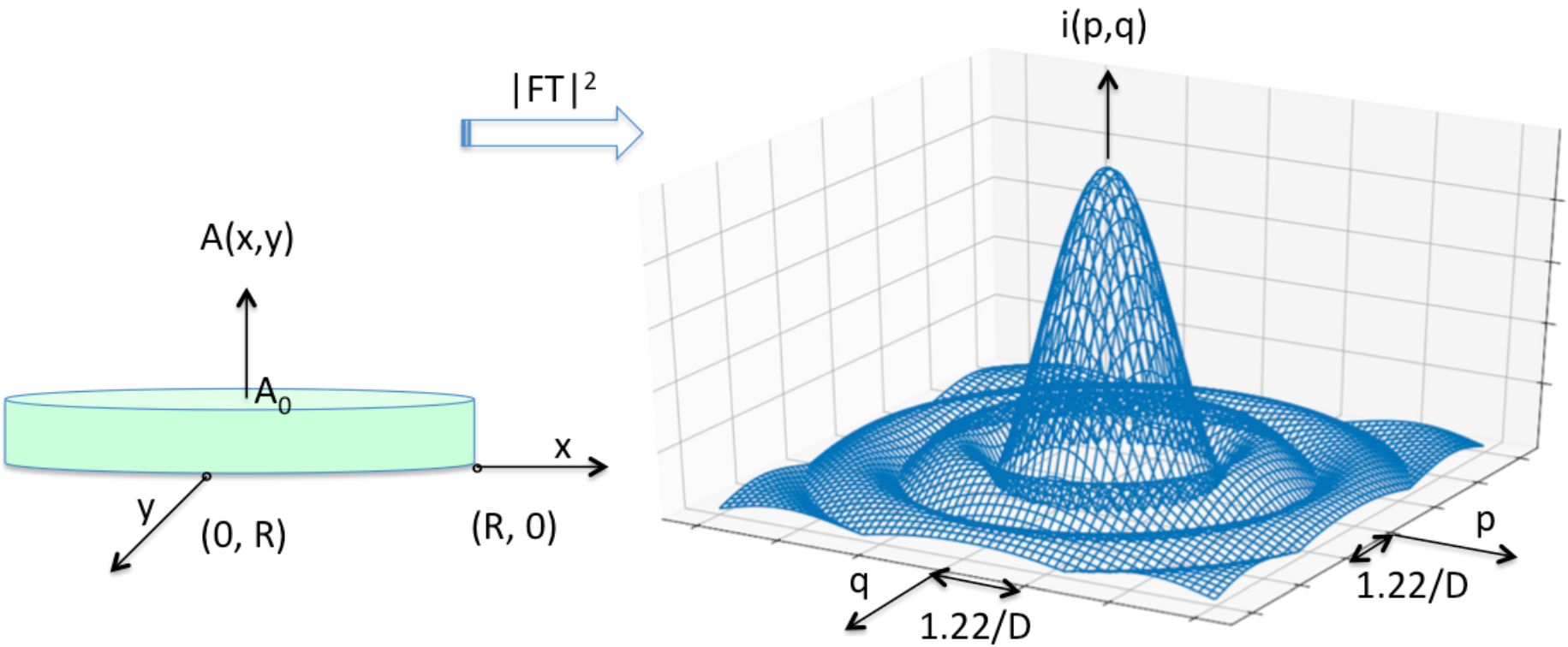

Figure: The Airy disk: complex amplitude distribution $A(\rho, \varphi) = A_0$ in the plane of a circular aperture (left) and the resulting response function in intensity $i(\rho')$ (right).

Three important theorems and some applications: the case of a circular aperture

Knowing that the first order Bessel function $J_1(x) = 0$ for $x \sim 3.96$, it is easy to deduce that the angular resolution Φ of a telescope equipped with a circular objective which diameter is $D = 2R$ is given by

$$\Phi = \frac{\Delta\rho'}{f} = \frac{2.44\,\lambda}{D}. \tag{105}$$

Three important theorems and some applications: the two telescope interferometer

Figure 44 (upper left) illustrates the principle of optically coupling two telescopes. Such a system is equivalent to a huge telescope in front of which would have been placed a screen pierced with two openings corresponding to the entrance pupils of the two telescopes. The pupil function $A(x, y)$ of this system is shown in that same Figure for the case of two square apertures.

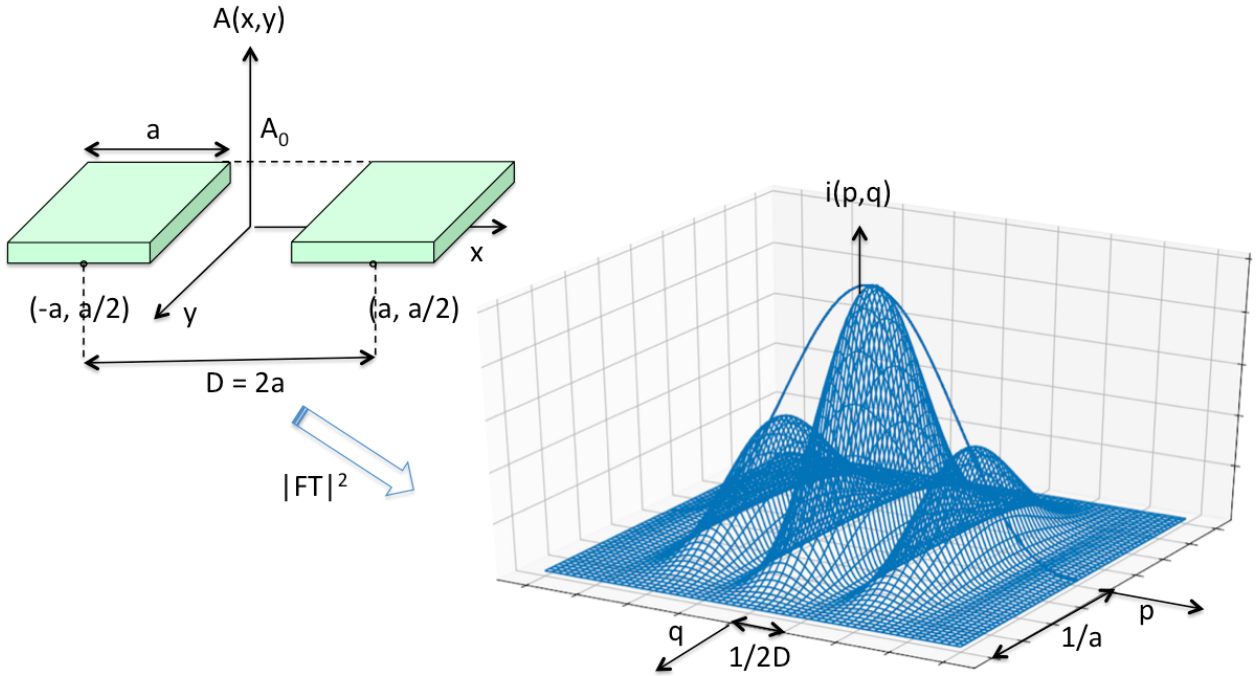

Figure: The two telescope interferometer: distribution of the complex amplitude for the case of two square apertures (upper left) and the corresponding impulse response function (lower right).

Three important theorems and some applications: the two telescope interferometer

Let us now calculate the impulse response function $a(p, q)$ of such a system.

Three important theorems and some applications: the two telescope interferometer

Let us now calculate the impulse response function $a(p, q)$ of such a system. Representing the distribution of the complex amplitude over each of the individual square apertures by means of the function $A_0(x, y)$ and assuming that the distance between their optical axes is D, we find that

$$a(p, q) = FT_{-}[A_0(x + D/2, y) + A_0(x - D/2, y)](p, q). \tag{106}$$

Three important theorems and some applications: the two telescope interferometer

Let us now calculate the impulse response function $a(p,q)$ of such a system. Representing the distribution of the complex amplitude over each of the individual square apertures by means of the function $A_0(x,y)$ and assuming that the distance between their optical axes is D, we find that

$$a(p,q) = FT_{-}[A_0(x+D/2,y) + A_0(x-D/2,y)](p,q). \tag{106}$$

Making use of the relation (58), the previous equation reduces to

$$a(p,q) = [\exp(i\pi pD) + \exp(-i\pi pD)]\, FT_{-}[A_0(x,y)](p,q), \tag{107}$$

$$a(p,q) = 2\,cos(\pi pD)\, FT_{-}[A_0(x,y)](p,q) \tag{108}$$

and finally

$$i(p,q) = a(p,q)a^{*}(p,q) = |a(p,q)|^2 = 4\,cos^2(\pi pD)\,\{FT_{-}[A_0(x,y)](p,q)\}^2. \tag{109}$$

Three important theorems and some applications: the two telescope interferometer

Let us now calculate the impulse response function $a(p,q)$ of such a system. Representing the distribution of the complex amplitude over each of the individual square apertures by means of the function $A_0(x,y)$ and assuming that the distance between their optical axes is D, we find that

$$a(p,q) = FT_{-}[A_0(x+D/2,y) + A_0(x-D/2,y)](p,q). \tag{106}$$

Making use of the relation (58), the previous equation reduces to

$$a(p,q) = [\exp(i\pi pD) + \exp(-i\pi pD)]\, FT_{-}[A_0(x,y)](p,q), \tag{107}$$

$$a(p,q) = 2\,cos(\pi pD)\, FT_{-}[A_0(x,y)](p,q) \tag{108}$$

and finally

$$i(p,q) = a(p,q)a^{*}(p,q) = |a(p,q)|^2 = 4\,cos^2(\pi pD)\,\{FT_{-}[A_0(x,y)](p,q)\}^2. \tag{109}$$

Three important theorems and some applications: the two telescope interferometer

Particularizing this intensity distribution to the case of two square apertures, or circular apertures, and making use of relations (95) or (104) leads to the respective results

$$i(p,q) = A_0^2\,(2a^2)^2\,[\frac{sin(\pi pa)}{\pi pa}]^2\,[\frac{sin(\pi qa)}{\pi qa}]^2\,cos^2(\pi pD) \tag{110}$$

or

$$i(p,\rho') = A_0^2(2\,\pi R^2)^2[\frac{2J_1(2\pi R\rho'/(\lambda f))}{2\pi R\rho'/(\lambda f)}]^2\,cos^2(\pi pD). \tag{111}$$

Three important theorems and some applications: the two telescope interferometer

Particularizing this intensity distribution to the case of two square apertures, or circular apertures, and making use of relations (95) or (104) leads to the respective results

$$i(p,q) = A_0^2\,(2a^2)^2\,[\frac{sin(\pi pa)}{\pi pa}]^2\,[\frac{sin(\pi qa)}{\pi qa}]^2\,cos^2(\pi pD) \tag{110}$$

or

$$i(p,\rho') = A_0^2(2\,\pi R^2)^2[\frac{2J_1(2\pi R\rho'/(\lambda f))}{2\pi R\rho'/(\lambda f)}]^2\,cos^2(\pi pD). \tag{111}$$

Figure 44 (lower right) illustrates the response function for the former case. We see that the impulse response of each individual telescope is modulated by the $\cos(2\pi pD)$ function and that the resulting impulse response function shows consequently a more detailed structure along the p axis, leading to a significantly improved angular resolution Φ along that direction.

Particularizing this intensity distribution to the case of two square apertures, or circular apertures, and making use of relations (95) or (104) leads to the respective results

$$i(p,q) = A_0^2\,(2a^2)^2\,[\frac{sin(\pi pa)}{\pi pa}]^2\,[\frac{sin(\pi qa)}{\pi qa}]^2\,cos^2(\pi pD) \tag{110}$$

or

$$i(p,\rho') = A_0^2(2\,\pi R^2)^2[\frac{2J_1(2\pi R\rho'/(\lambda f))}{2\pi R\rho'/(\lambda f)}]^2\,cos^2(\pi pD). \tag{111}$$

Figure 44 (lower right) illustrates the response function for the former case. We see that the impulse response of each individual telescope is modulated by the $\cos(2\pi pD)$ function and that the resulting impulse response function shows consequently a more detailed structure along the p axis, leading to a significantly improved angular resolution Φ along that direction.

The angular width Φ of the bright central fringe is equal to the angular width separating the two minima located on its two sides. We thus find successively

$$\pi pD = \pm\frac{\pi}{2}, \tag{112}$$

$$p = \pm \frac{1}{2D}, \tag{113}$$

$$\Delta p = \frac{1}{D} \tag{114}$$

and making use of relation (81)

$$\Phi = \frac{\Delta x'}{f} = \frac{\lambda}{D}. \tag{115}$$

$$p = \pm \frac{1}{2D}, \tag{113}$$

$$\Delta p = \frac{1}{D} \tag{114}$$

and making use of relation (81)

$$\Phi = \frac{\Delta x'}{f} = \frac{\lambda}{D}. \tag{115}$$

The angular resolution of the interferometer along the direction joining the two telescopes is approximately equivalent to that of a single dish telescope which diameter is equal to the baseline D separating them, and not any longer to the diameter of each single telescope (see Eqs. (97) or (105)).

The convolution theorem states that the convolution of two functions $f(x)$ and $g(x)$ is given by the following expression

$$f(x) * g(x) = (f * g)(x) = \int_R f(x-t)g(t)dt. \tag{116}$$

Figure 45 illustrates such a convolution product for the case of two rectangular functions $f(x) = \Pi(x/a)$ and $g(x) = \Pi(x/b)$ having the widths a and b, respectively.

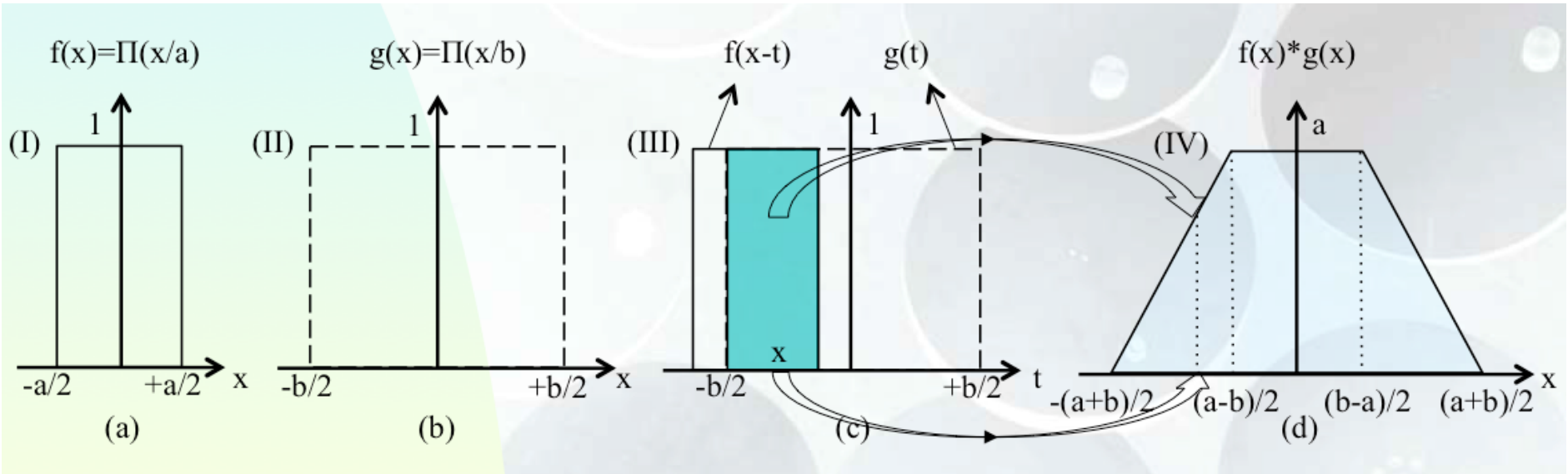

Figure: Convolution product of two 1-D rectangular functions. (a) $f(x)$, (b) $g(x)$, (c) $g(t)$ and $f(x-t)$. The dashed area represents the integral of the product of $f(x-t)$ and $g(t)$ for the given x offset, (d) $f(x) * g(x) = (f * g)(x)$ represents the previous integral as a function of x.

Three important theorems and some applications: the convolution theorem

Every day when the Sun is shining, it is possible to see nice illustrations of the convolution product while looking at the projected images of the Sun on the ground which are actually produced through small holes in the foliage of the trees (see the illustration in Fig. 46). It is a good exercise to establish the relation existing between the observed surface brightness of those Sun images, the shape of the holes in the foliage of the trees, their distance from the ground and the intrinsic surface brightness distribution of the Sun.

Figure: Projected images of the Sun on the ground actually produced through small holes in the foliage of trees (bamboo trees at IUCAA, Pune, India, June 2016). These images actually result from the convolution of the intrinsic Sun intensity distribution and the shapes of the holes in the trees.

The convolution theorem: application to the two telescope interferometer

We have previously seen that for the case of a point-like source having an intrinsic surface brightness distribution $O(p,q) = \delta(p)\delta(q)$, there results the formation of an image $e(p,q)$ in the focal plane which is the impulse response $e(p,q) = i(p,q) = |a(p,q)|^2$ of the optical instrument (see Eqs. (95), (104), (110), (111) for the case of a single square aperture, a single circular aperture, an interferometer composed of two square or circular apertures, respectively).

The convolution theorem: application to the two telescope interferometer

We have previously seen that for the case of a point-like source having an intrinsic surface brightness distribution $O(p,q) = \delta(p)\delta(q)$, there results the formation of an image $e(p,q)$ in the focal plane which is the impulse response $e(p,q) = i(p,q) = |a(p,q)|^2$ of the optical instrument (see Eqs. (95), (104), (110), (111) for the case of a single square aperture, a single circular aperture, an interferometer composed of two square or circular apertures, respectively).
Considering now an extended source represented by its intrinsic surface brightness distribution $O(p,q)$, application of the convolution theorem in two dimensions directly leads to the expression of its brightness distribution $e(p,q)$ in the focal plane of the optical system

$$e(p,q) = O(p,q) * |a(p,q)|^2 \tag{117}$$

or more explicitly

$$e(p,q) = \int_{R^2} O(r,s)|a(p-r,q-s)|^2 drds. \tag{118}$$

The convolution theorem: application to the two telescope interferometer

Since the Fourier transform of the convolution product of two functions is equal to the product of their Fourier transforms, we find that

$$FT_{-}[e(p,q)] = FT_{-}[O(p,q)]\, FT_{-}[|a(p,q)|^2] \tag{119}$$

and also that the inverse Fourier transform of $FT_{-}(O(p,q))$ leads to the result

$$O(p,q) = FT_{-}^{-1}[FT_{-}(O(p,q))] = FT_{-}^{-1}[\frac{FT_{-}[e(p,q)]}{FT_{-}[|a(p,q)|^2]}], \tag{120}$$

namely, that it should be possible to recover interesting information on the intrinsic surface brightness distribution of the source $O(p,q)$ at high angular resolution provided that we get sufficient information at high frequencies in the u, v plane on the object $FT_{-}(e(p,q))$ itself as well as on a reference point-like object $FT_{-}(|a(p,q)|2)$.

The convolution theorem: interferometric observations of a circular symmetric source

Considering the case of a symmetric source around the Y axis observed by means of an interferometer composed of two square apertures which size of their sides is d separated along the X axis by the baseline D, we find by means of Eqs. (95), (110) and (117) that

$$e(p) = 2d^2 \left(\frac{\sin(\pi p d)}{\pi p d} \right)^2 \left[O(p) * \cos^2(\pi p D) \right] . \tag{121}$$

The convolution theorem: interferometric observations of a circular symmetric source

Considering the case of a symmetric source around the Y axis observed by means of an interferometer composed of two square apertures which size of their sides is d separated along the X axis by the baseline D, we find by means of Eqs. (95), (110) and (117) that

$$e(p) = 2d^2 \left(\frac{\sin(\pi p d)}{\pi p d} \right)^2 \left[O(p) * \cos^2(\pi p D) \right]. \tag{121}$$

Making use of the relation $\cos(2x) = 2\cos 2(x) - 1$, Eq. (121) reduces to

$$e(p) = 2d^2 \left(\frac{\sin(\pi p d)}{\pi p d} \right)^2 \left[\frac{1}{2} \int_R O(p) dp + \frac{1}{2} O(p) * \cos(2\pi p D) \right]. \tag{122}$$

The convolution theorem: interferometric observations of a circular symmetric source

Considering the case of a symmetric source around the Y axis observed by means of an interferometer composed of two square apertures which size of their sides is d separated along the X axis by the baseline D, we find by means of Eqs. (95), (110) and (117) that

$$e(p) = 2d^2 \left(\frac{\sin(\pi p d)}{\pi p d} \right)^2 \left[O(p) * \cos^2(\pi p D) \right]. \tag{121}$$

Making use of the relation $\cos(2x) = 2\cos 2(x) - 1$, Eq. (121) reduces to

$$e(p) = 2d^2 \left(\frac{\sin(\pi p d)}{\pi p d} \right)^2 \left[\frac{1}{2} \int_R O(p) dp + \frac{1}{2} O(p) * \cos(2\pi p D) \right]. \tag{122}$$

Since the function $O(p)$ is real, the previous relation may rewritten in the form

$$e(p) = A \left[B + \frac{1}{2} Re[O(p) * \exp(i 2\pi p D)] \right] \tag{123}$$

where

$$A = 2d^2 \left(\frac{\sin(\pi p d)}{\pi p d} \right)^2 \quad \text{and} \quad B = \frac{1}{2} \int_R O(p) dp. \tag{124}$$

The convolution theorem: interferometric observations of a circular symmetric source

Given the definition of the convolution product (cf. Eq. (116)), relation (123) can be rewritten as

$$e(p) = A\left[B + \frac{1}{2}Re[\int_R O(r)\ \exp(i2\pi(p-r)D)dr]\right], \tag{125}$$

or

$$e(p) = A\left[B + \frac{1}{2}cos(2\pi pD)\, FT_{-}[O(r)](D)\right], \tag{126}$$

because $O(p)$ being real and even, its Fourier transform is also real.

The convolution theorem: interferometric observations of a circular symmetric source

Given the definition of the convolution product (cf. Eq. (116)), relation (123) can be rewritten as

$$e(p) = A\left[B + \frac{1}{2}Re[\int_R O(r)\ \exp(i2\pi(p-r)D)dr]\right], \tag{125}$$

or

$$e(p) = A\left[B + \frac{1}{2}cos(2\pi pD)\, FT_-[O(r)](D)\right], \tag{126}$$

because $O(p)$ being real and even, its Fourier transform is also real.
The visibility of the fringes being defined by (see Eq. (20))

$$v = |\gamma_{12}(D)| = \left(\frac{e_{\max} - e_{\min}}{e_{\max} + e_{\min}}\right), \tag{127}$$

we obtain

$$v = |\gamma_{12}(D)| = FT_-[\frac{O(r)}{2B}](D) = FT_-[\frac{O(r)}{\int O(p)dp}](D). \tag{128}$$

The convolution theorem: interferometric observations of a circular symmetric source

We have thus recovered the important result (47), first established for the case of two point-like apertures, according to which the visibility of the fringes is the Fourier transform of the normalized intensity distribution of the source. This result can be generalized to the case of a source that is not symmetric.

One example of stellar visibilities

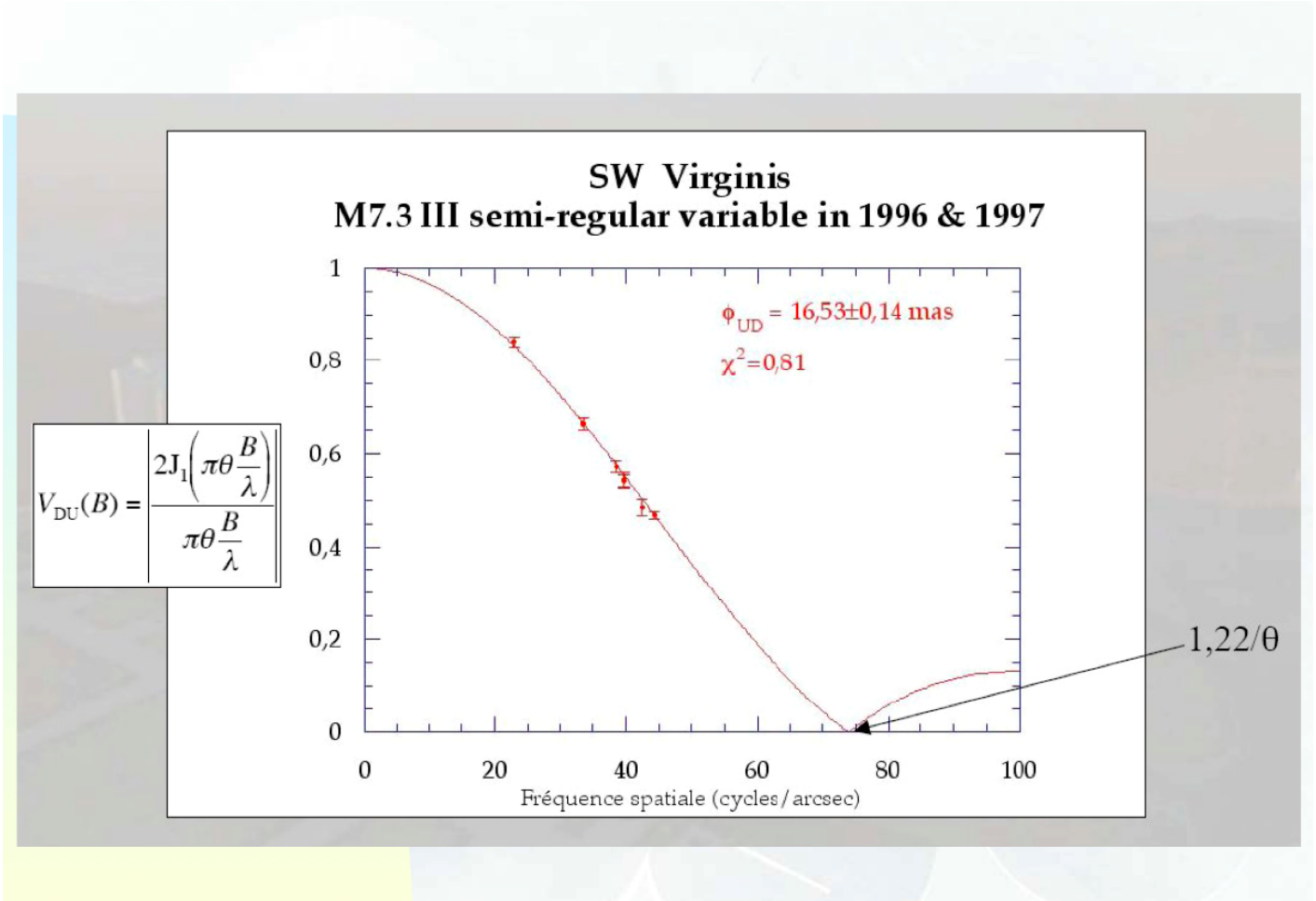

Figure: One example of stellar visibilities.

Using interferometric masks for didactical purposes

Interferometric observations on 10/4/2010 of Procyon, Mars and Saturn, using the 80cm telescope at Haute-Provence Observatory and adequate masks (coll. with Hervé le Coroller) …

Figure: Using interferometric masks for didactical purposes.

Using interferometric masks for didactical purposes

Figure: Using interferometric masks for didactical purposes.

Using interferometric masks for didactical purposes

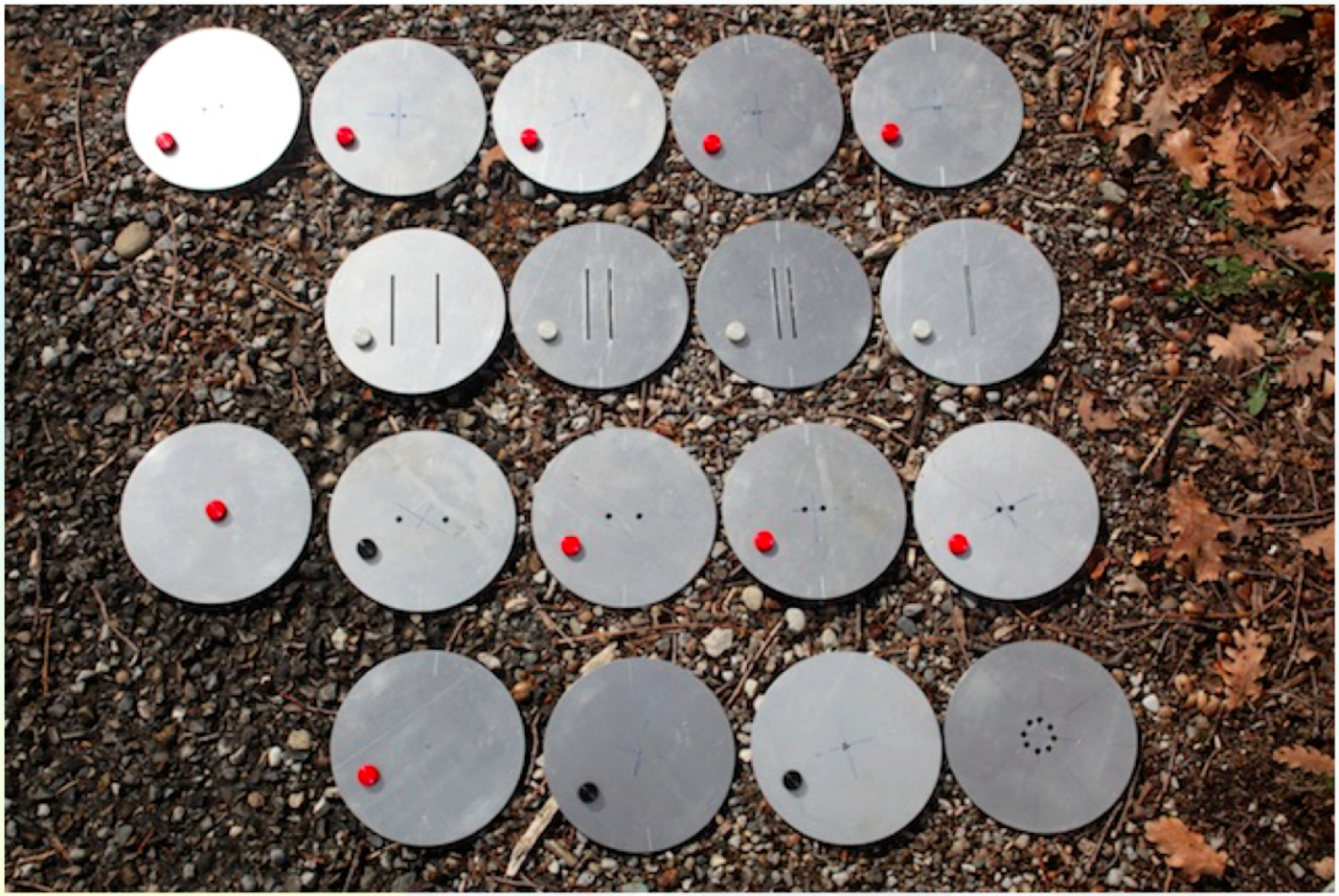

Figure: Using interferometric masks for didactical purposes.

Using interferometric masks for didactical purposes

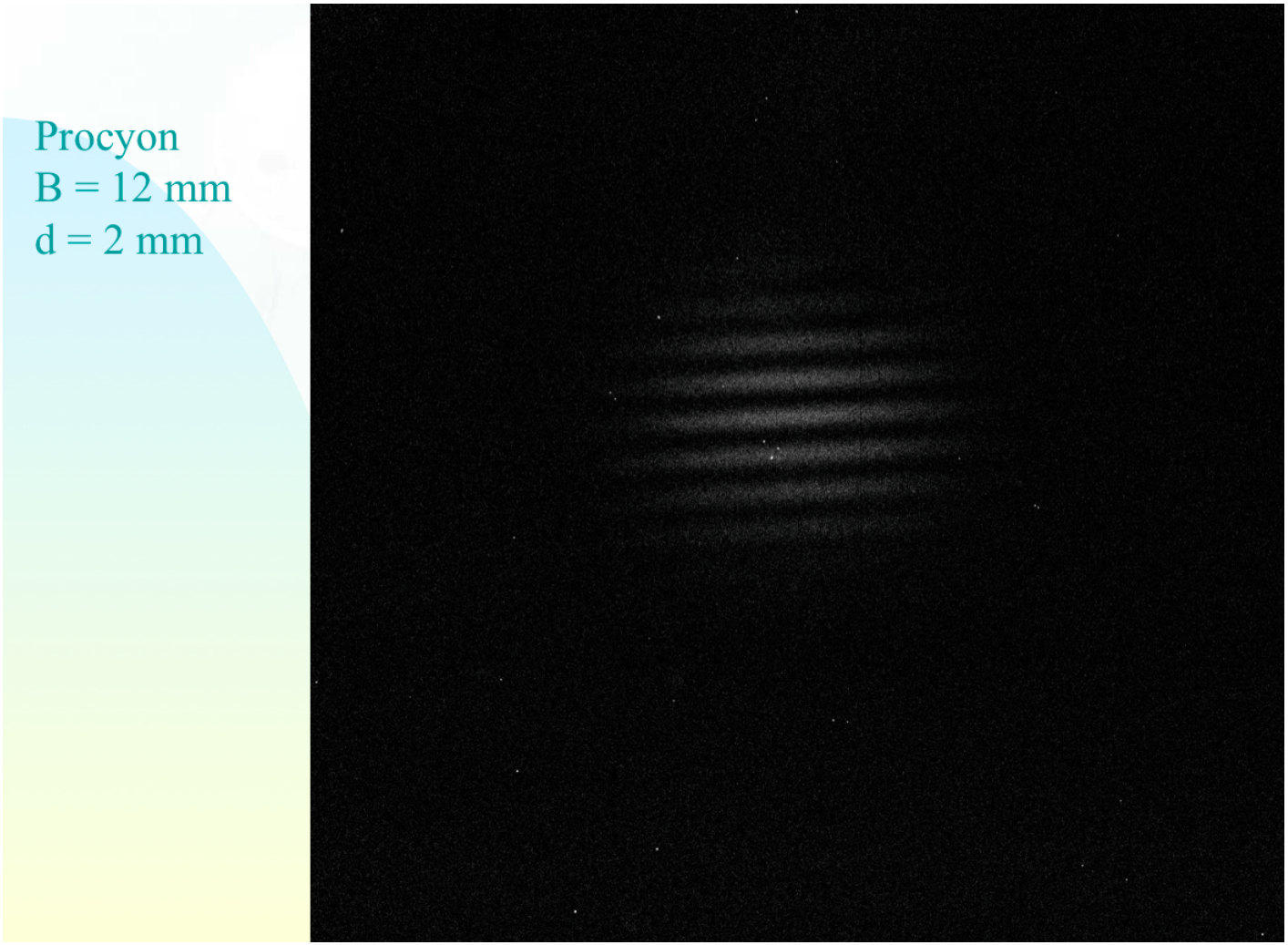

Figure: Using interferometric masks for didactical purposes.

Using interferometric masks for didactical purposes

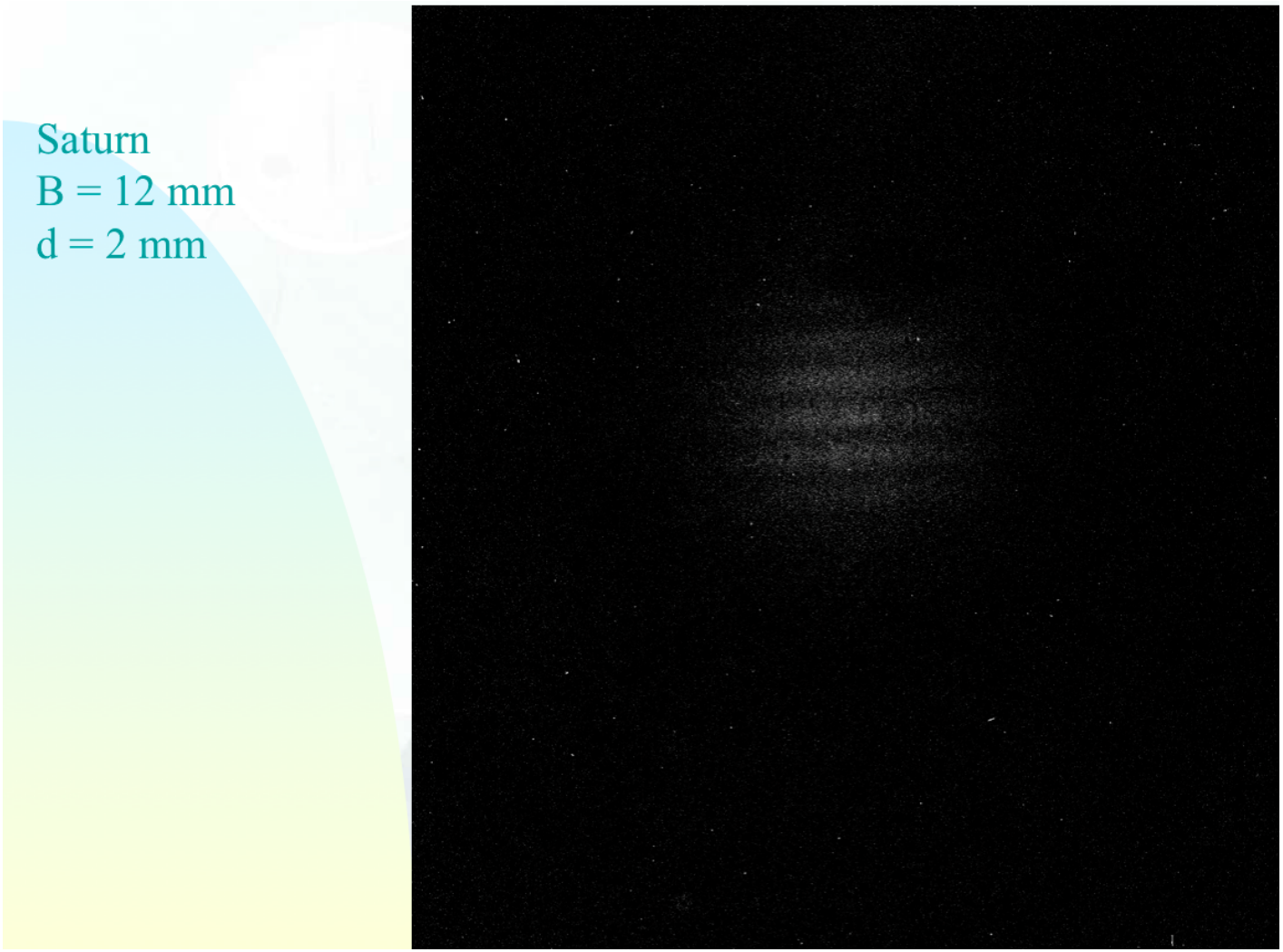

Figure: Using interferometric masks for didactical purposes.

More about VLTI

Figure: More about VLTI.

More about VLTI

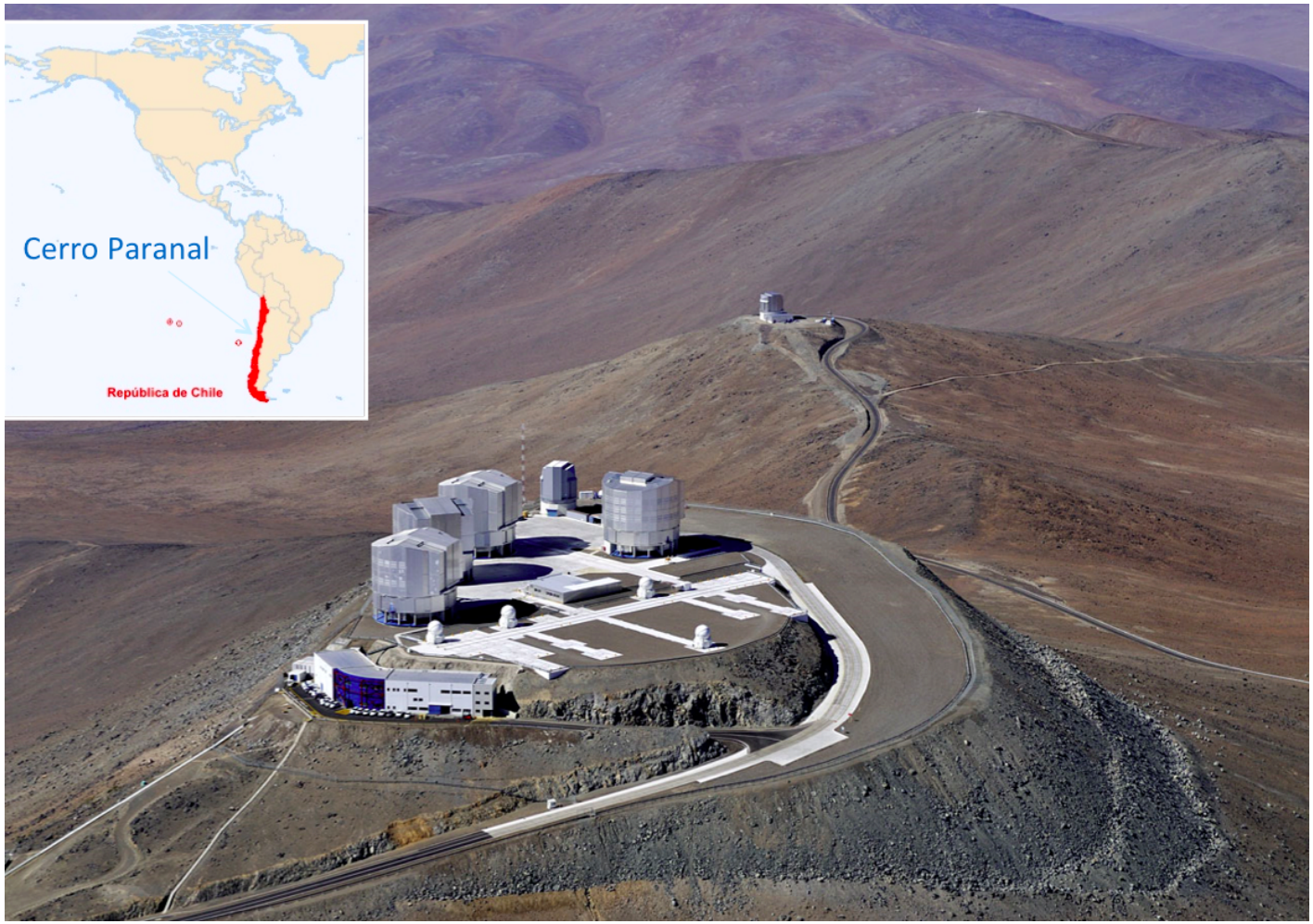

Figure: More about VLTI.

More about VLTI

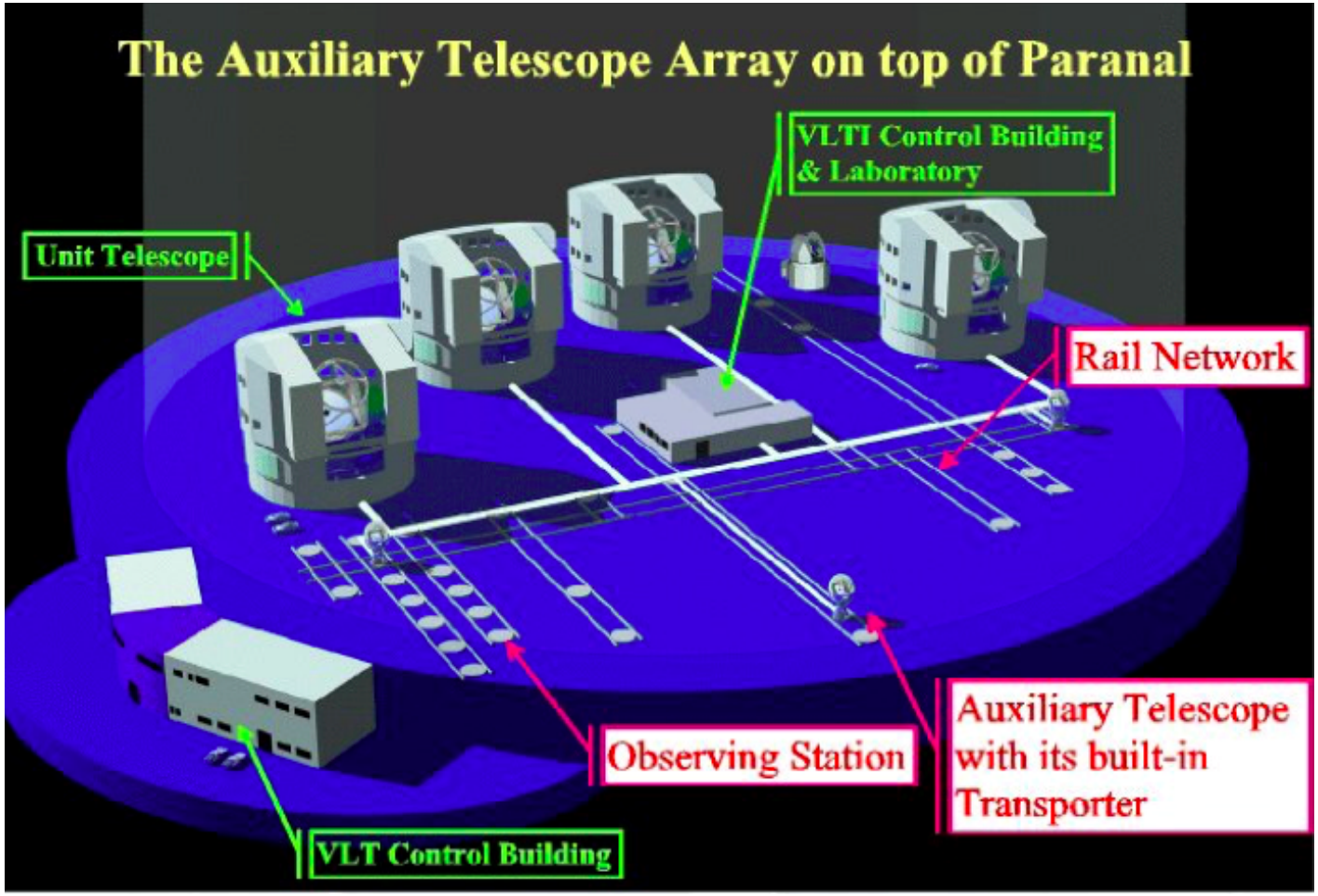

Figure: More about VLTI.

More about VLTI

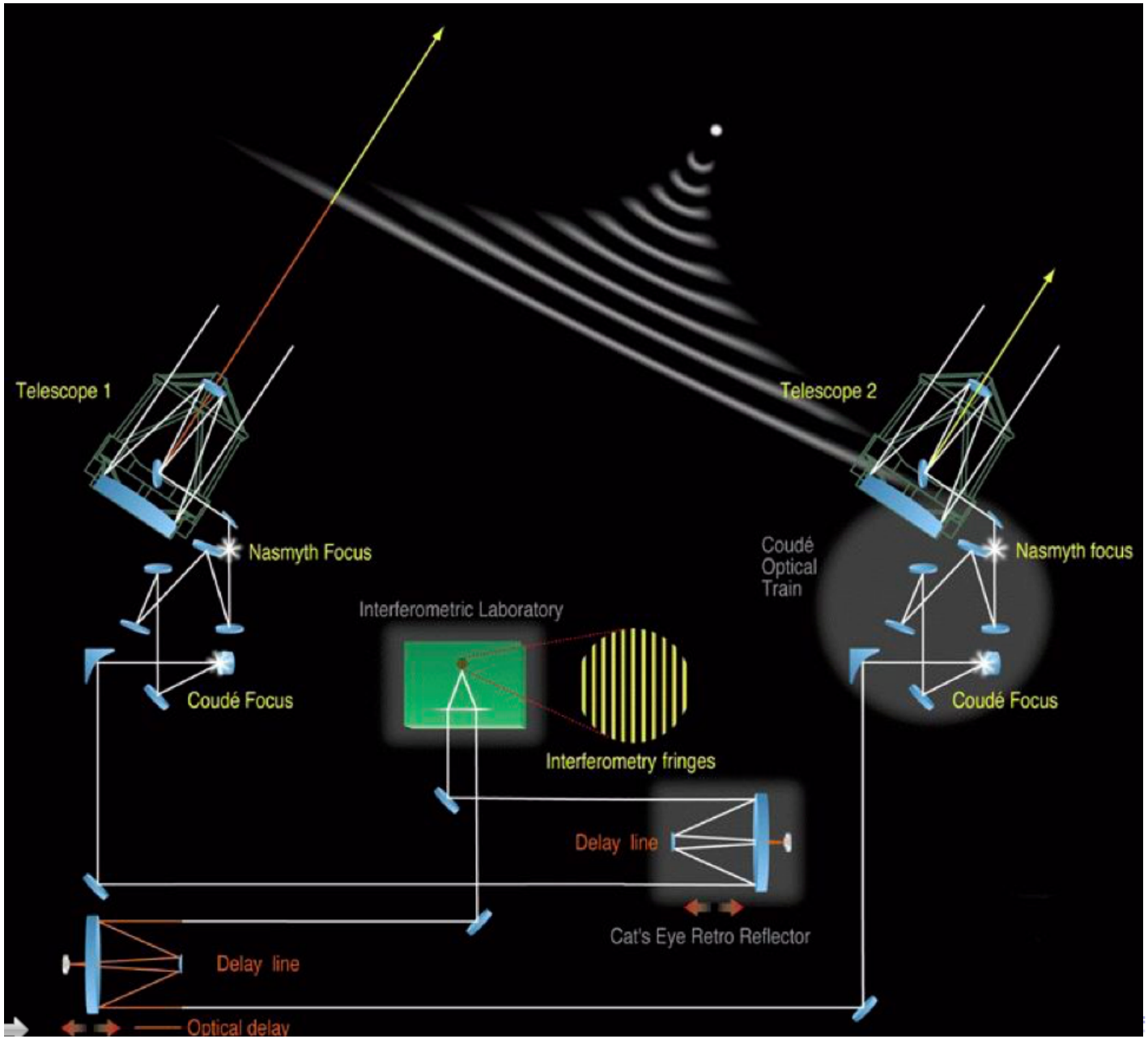

More about VLTI

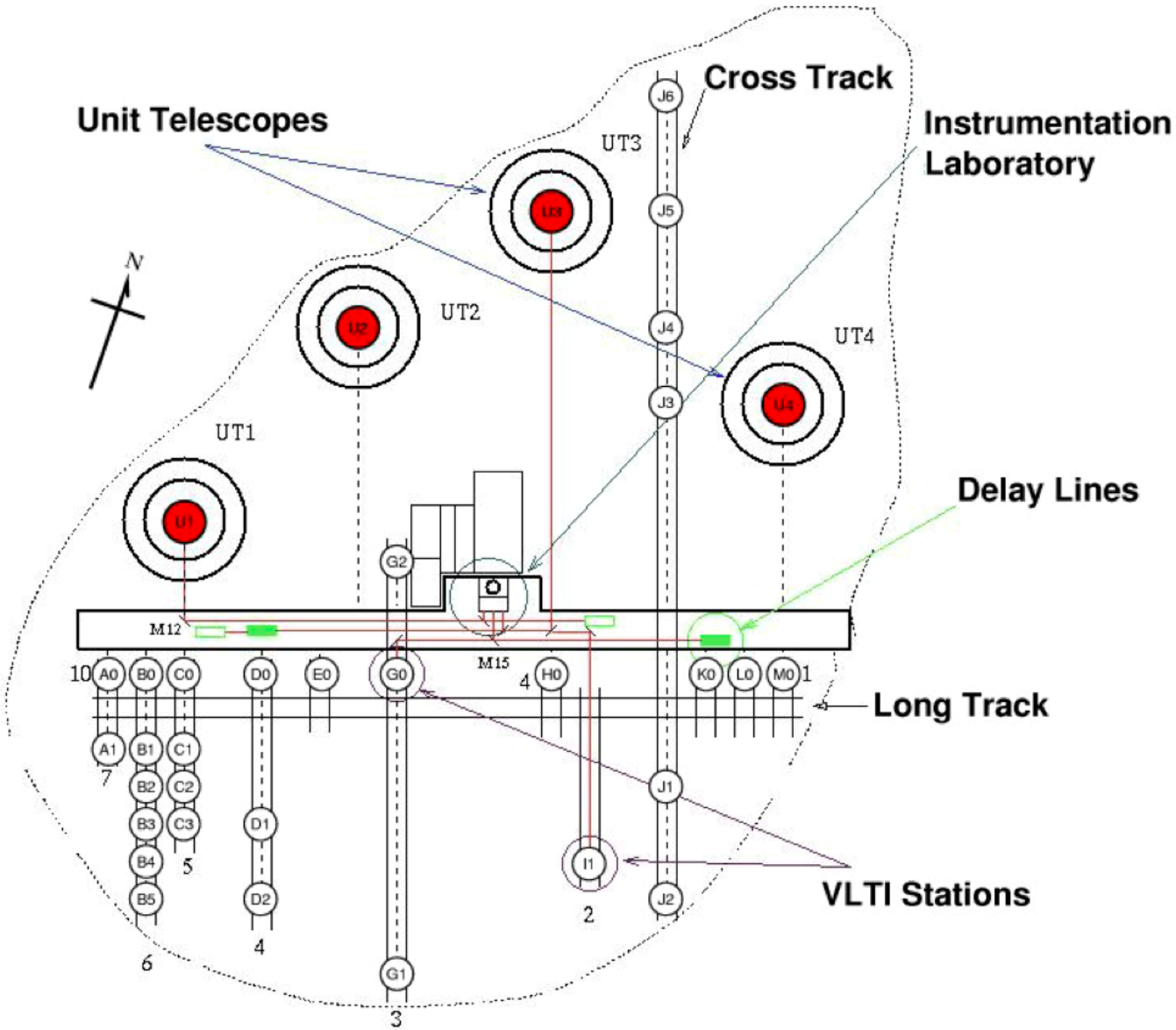

Figure: More about VLTI.

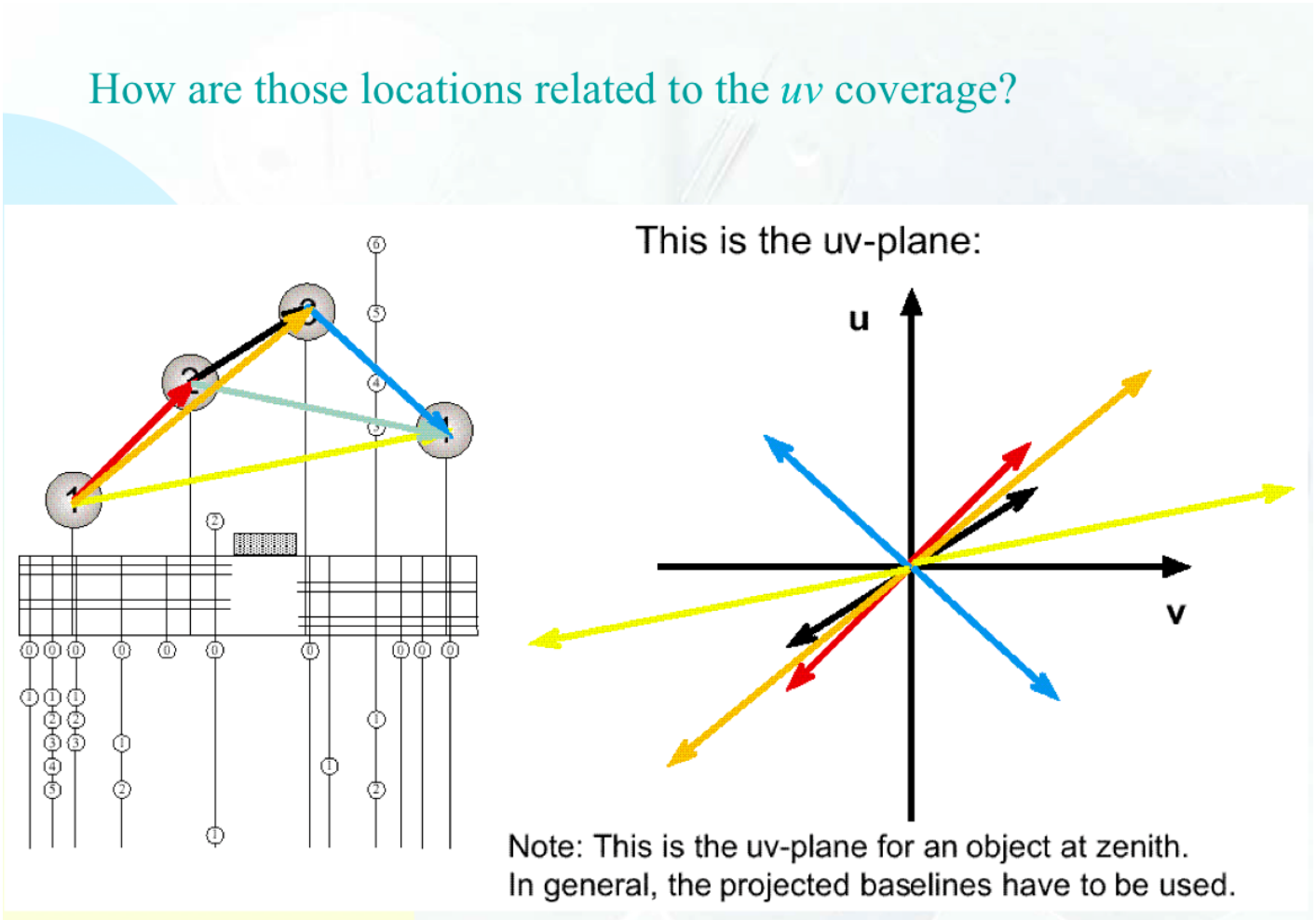

Figure: More about VLTI.

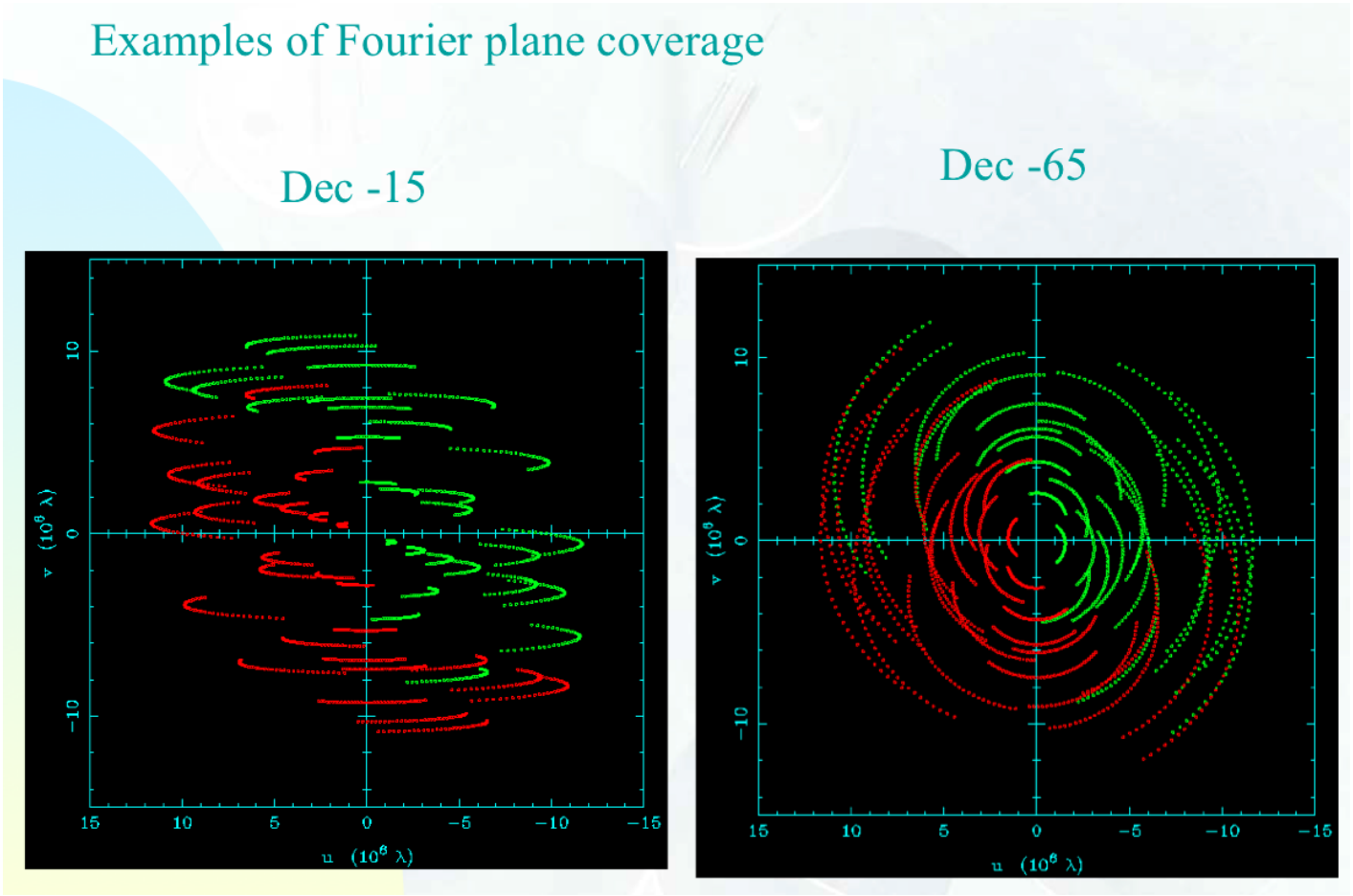

Figure: More about VLTI.

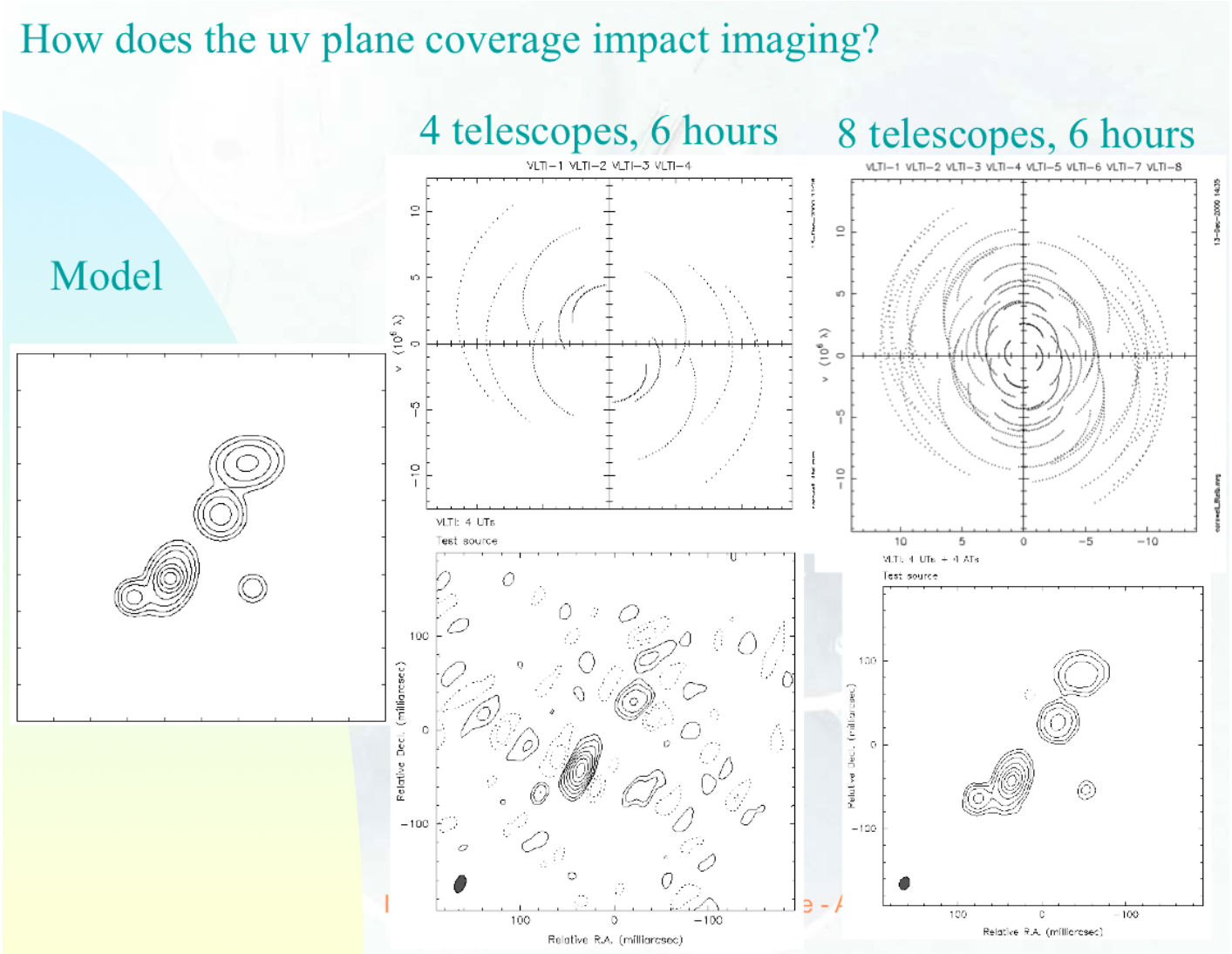

Figure: More about VLTI.

Closure phases – what are these?

• Measure visibility phase (Φ) on three baselines simultaneously.

• Each is perturbed from the true phase (ϕ) in a particular manner:

$$\Phi_{12} = \phi_{12} + \varepsilon_1 - \varepsilon_2$$
$$\Phi_{23} = \phi_{23} + \varepsilon_2 - \varepsilon_3$$
$$\Phi_{31} = \phi_{31} + \varepsilon_3 - \varepsilon_1$$

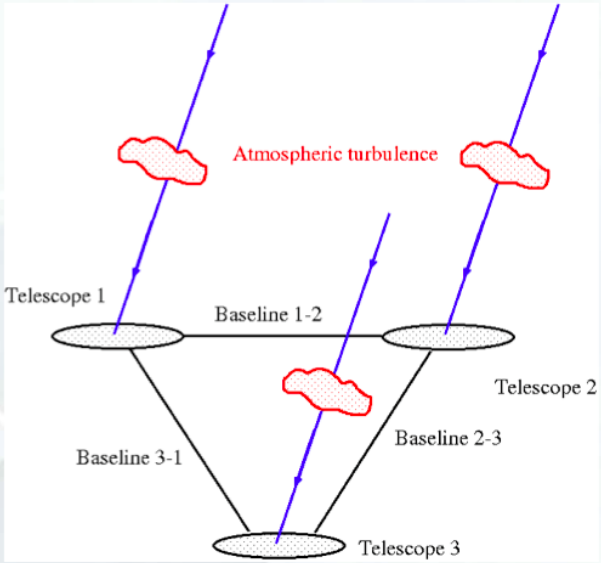

• Construct the linear combination of these:

$$\Phi_{12} + \Phi_{23} + \Phi_{31} = \phi_{12} + \phi_{23} + \phi_{31}$$

The error terms are antenna dependent – they vanish in the sum.
The source information is baseline dependent – it remains.
We still have to figure out how to use it!

Figure: About closure phases with an optical interferometer.

Closure phase is a peculiar linear combination of the true Fourier phases:

– In fact, it is the argument of the product of the visibilities on the baselines in question, hence the name triple product (or bispectrum):

$$V_{12}V_{23}V_{31} = |V_{12}|\,|V_{23}|\,|V_{31}| \exp(i2\pi[\Phi_{12} + \Phi_{23} + \Phi_{31}]) = T_{123}$$

– So we have to use the closure phases as additional constraints In some nonlinear iterative inversion scheme.

Figure: About closure phases with an optical interferometer.

Three important theorems and some applications: the Wiener-Khinchin theorem

The last theorem that we shall demonstrate during these lectures is the famous Wiener-Khinchin theorem according to which the Fourier transform of the response function of an optical system, i.e. the Fourier transform of the Point Spread Function in our case, is given by the auto-correlation of the distribution of the complex amplitude in the pupil plane. In mathematical terms, the theorem can be expressed as follows

$$FT_{-}(|a(p,q)|^2)(x,y) = FT_{-}(i(p,q))(x,y) = \int_{-\infty}^{+\infty}\int_{-\infty}^{+\infty} A^*(x'+x,y'+y)A(x',y')dx'dy'. \tag{129}$$

Three important theorems and some applications: the Wiener-Khinchin theorem

The last theorem that we shall demonstrate during these lectures is the famous Wiener-Khinchin theorem according to which the Fourier transform of the response function of an optical system, i.e. the Fourier transform of the Point Spread Function in our case, is given by the auto-correlation of the distribution of the complex amplitude in the pupil plane. In mathematical terms, the theorem can be expressed as follows

$$FT_{-}(|a(p,q)|^2)(x,y) = FT_{-}(i(p,q))(x,y) = \int_{-\infty}^{+\infty}\int_{-\infty}^{+\infty} A^*(x'+x,y'+y)A(x',y')dx'dy'. \tag{129}$$

When establishing the expression (120), we wrote that the quantity $FT_{-}(|a(p,q)|^2)$ appearing in its denominator could be retrieved from the observation of a point-like star. The Wiener-Khinchin theorem states that it can also be retrieved from the auto-correlation of the distribution of the complex amplitude $A(x,y)$ in the pupil plane.

Three important theorems and some applications: the Wiener-Khinchin theorem

The last theorem that we shall demonstrate during these lectures is the famous Wiener-Khinchin theorem according to which the Fourier transform of the response function of an optical system, i.e. the Fourier transform of the Point Spread Function in our case, is given by the auto-correlation of the distribution of the complex amplitude in the pupil plane. In mathematical terms, the theorem can be expressed as follows

$$FT_{-}(|a(p,q)|^2)(x,y) = FT_{-}(i(p,q))(x,y) = \int_{-\infty}^{+\infty}\int_{-\infty}^{+\infty} A^*(x'+x,y'+y)A(x',y')dx'dy'. \tag{129}$$

When establishing the expression (120), we wrote that the quantity $FT_{-}(|a(p,q)|^2)$ appearing in its denominator could be retrieved from the observation of a point-like star. The Wiener-Khinchin theorem states that it can also be retrieved from the auto-correlation of the distribution of the complex amplitude $A(x,y)$ in the pupil plane. Figure 63 illustrates the application of this theorem to the case of an interferometer composed of two circular apertures having a diameter a and separated by the baseline b. We see that the autocorrelation of an interferometer gives access to high spatial frequencies.

Three important theorems and some applications: the Wiener-Khinchin theorem

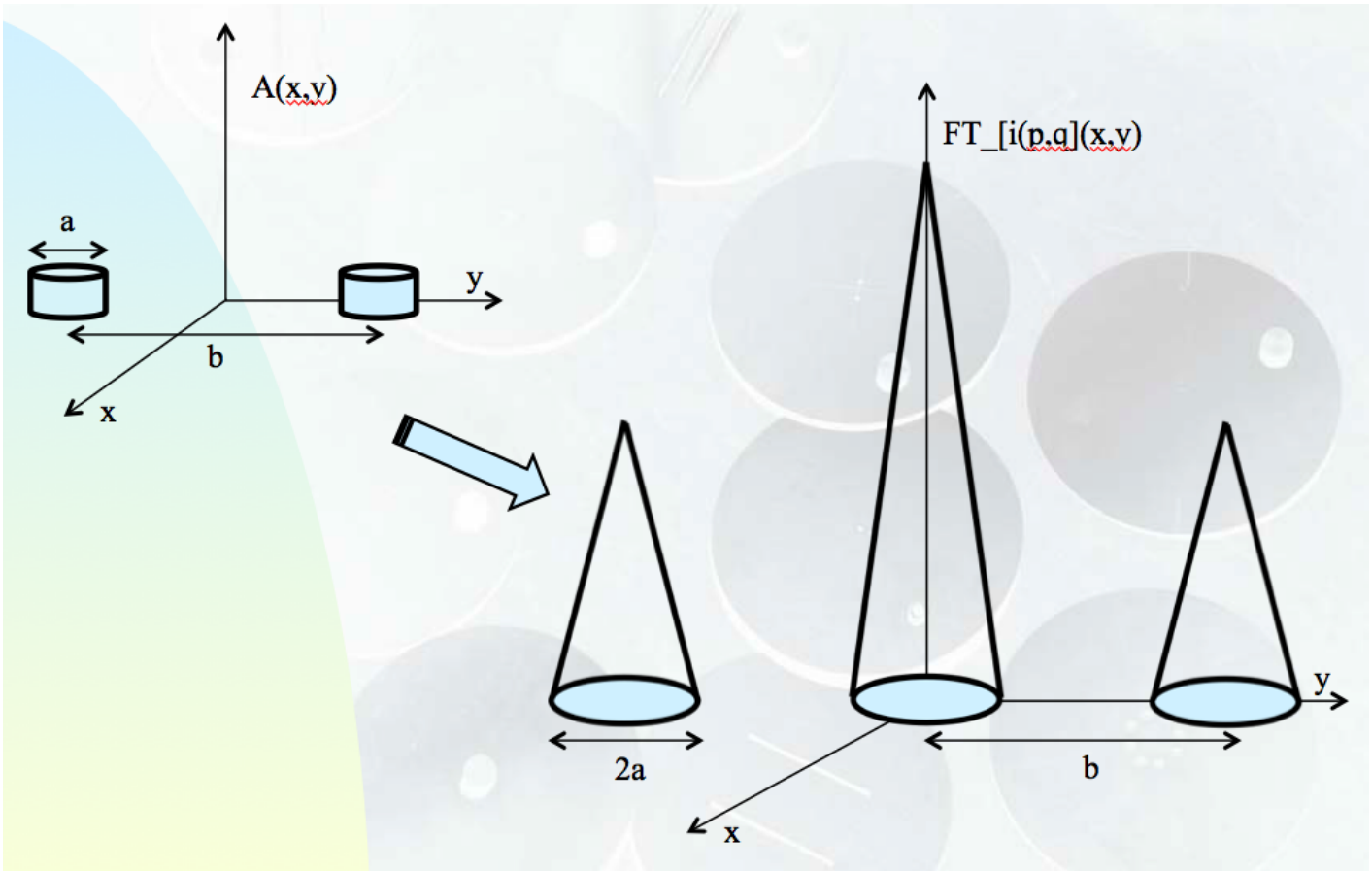

Figure: Diagram representing the autocorrelation function versus the space frequency, for a two telescope interferometer, each having a diameter a, separated by the baseline b.

Three important theorems and some applications: the Wiener-Khinchin theorem

A simple demonstration of the Wiener-Khinchin theorem (129) is given below.
We may successively establish that

$$FT_{-}(i(p,q))(x,y) = FT_{-}(|a(p,q)|^2)(x,y) = FT_{-}(a^*(p,q)a(p,q))(x,y), \tag{130}$$

$$FT_{-}[i(p,q)](x,y) = \int\int \exp[-2i\pi(px+qy)] \int\int A^*(x'',y'') \exp[2i\pi(px''+qy'')]\, dx''\, dy$$
$$\int\int A(x',y') \exp[-2i\pi(px'+qy')]\, dx'\, dy'\, dpa \tag{131}$$

Three important theorems and some applications: the Wiener-Khinchin theorem

A simple demonstration of the Wiener-Khinchin theorem (129) is given below.
We may successively establish that

$$FT_{-}(i(p,q))(x,y) = FT_{-}(|a(p,q)|^2)(x,y) = FT_{-}(a^*(p,q)a(p,q))(x,y), \tag{130}$$

$$FT_{-}[i(p,q)](x,y) = \int\int \exp[-2i\pi(px+qy)] \int\int A^*(x'',y'') \exp[2i\pi(px''+qy'')]\, dx''\, dy$$
$$\int\int A(x',y') \exp[-2i\pi(px'+qy')]\, dx'\, dy'\, dpq \tag{131}$$

$$FT_{-}[i(p,q)](x,y) = \int\int \exp[(2i\pi\{p[x''-(x'+x)]+q[y''-(y'+y)]\})] \tag{132}$$
$$\int\int A^*(x'',y'')\, dx''\, dy'' \int\int A(x',y')\, dx'\, dy'\, dpdq$$

and taking into account the definition (62) of the Dirac distribution

$$FT_{-}[i(p,q)](x,y) = \int\int\int\int \delta[x''-(x'+x)]\,\delta[y''-(y'+y)]\,A^{*}(x'',y'')\,A(x',y')\,dx'\,dy'\,dx \tag{133}$$

$$FT_{-}[i(p,q)](x,y) = \int\int\int\int \delta[x''-(x'+x)]\,\delta[y''-(y'+y)]\,A^{*}(x'',y'')\,A(x',y')\,dx'\,dy'\,dx \tag{133}$$

We finally find that

$$\begin{aligned} FT_{-}[i(p,q)](x,y) &= \int\int A^{*}(x'+x,y'+y)\,A(x',y')\,dx'\,dy'\,dx''\,dy'' = \\ &\int_{-\infty}^{+\infty}\int_{-\infty}^{+\infty} A^{*}(x'+x,y'+y)\,A(x',y')\,dx'\,dy'\,dx''\,dy'', \end{aligned} \tag{134}$$

i.e. the quoted result, namely that the Fourier transform of the impulse response function of an optical system can be represented by the autocorrelation of the distribution of the complex amplitude $A(x,y)$ in the pupil plane.

References

These lecture notes are based upon lectures on the same subject delivered by the author in French at the Liège University during the past ten years (see [1]). To get deeper into the field of interferometry, we highly recommend the following books: [2], [3], [4].

1. J. Surdej, see http://www.aeos.ulg.ac.be/teaching.php (2018)
2. P. Léna, D. Rouan, F., Lebrun, F. Mignard, D., Pelat, D., *Observational Astrophysics* (Astronomy and Astrophysics Library, 2012)
3. A. Glindemann, *Principles of Stellar Interferometry* (Astronomy and Astrophysics Library, 2011)
4. D. Buscher, *Practical Optical Interferometry: Imaging at Visible and Infrared Wavelengths* (Cambridge University Press, 2015)

N telescope interferometer

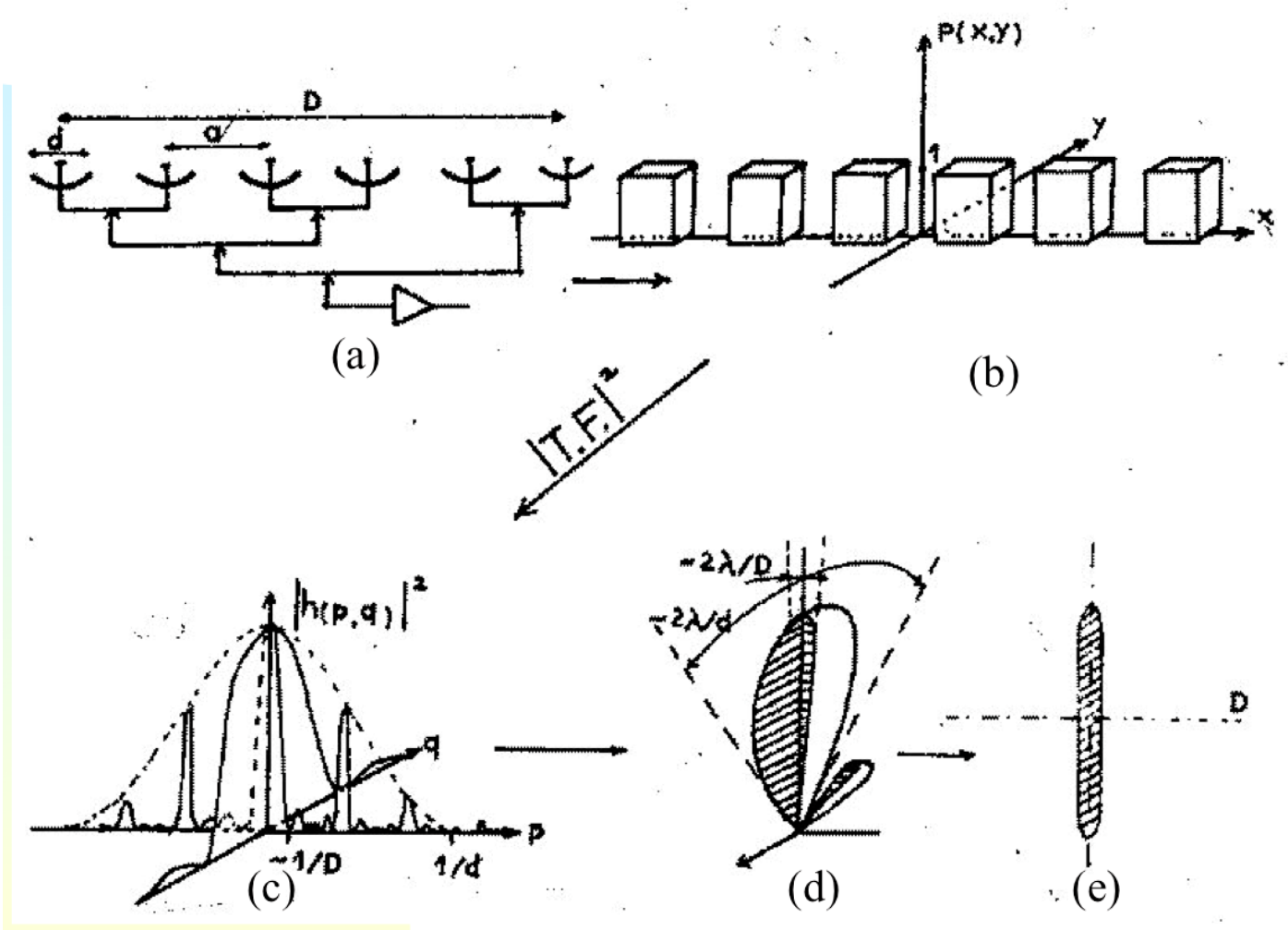

Figure: N telescope interferometer.

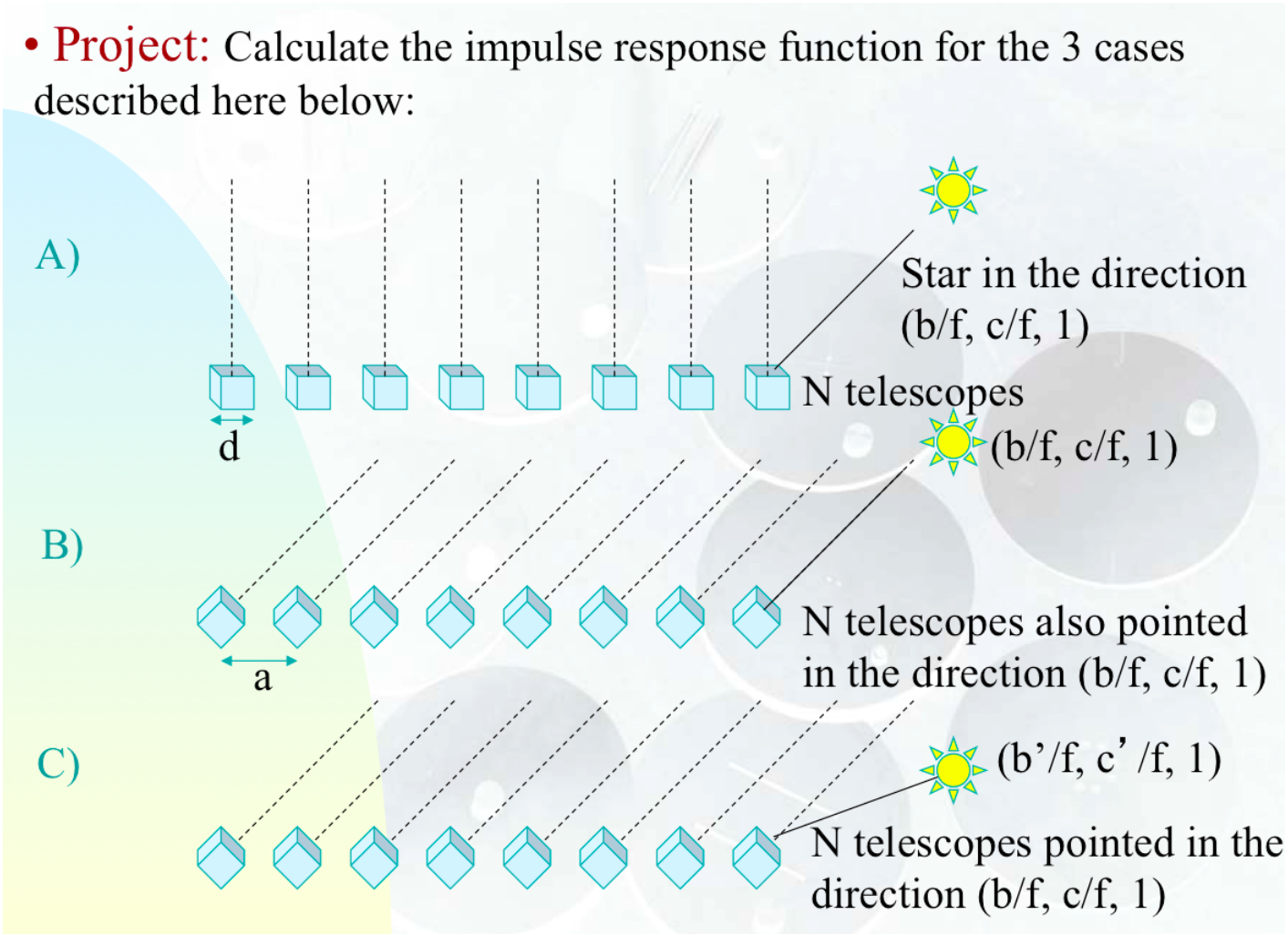

Figure: About closure phases with an optical interferometer.

Project for students

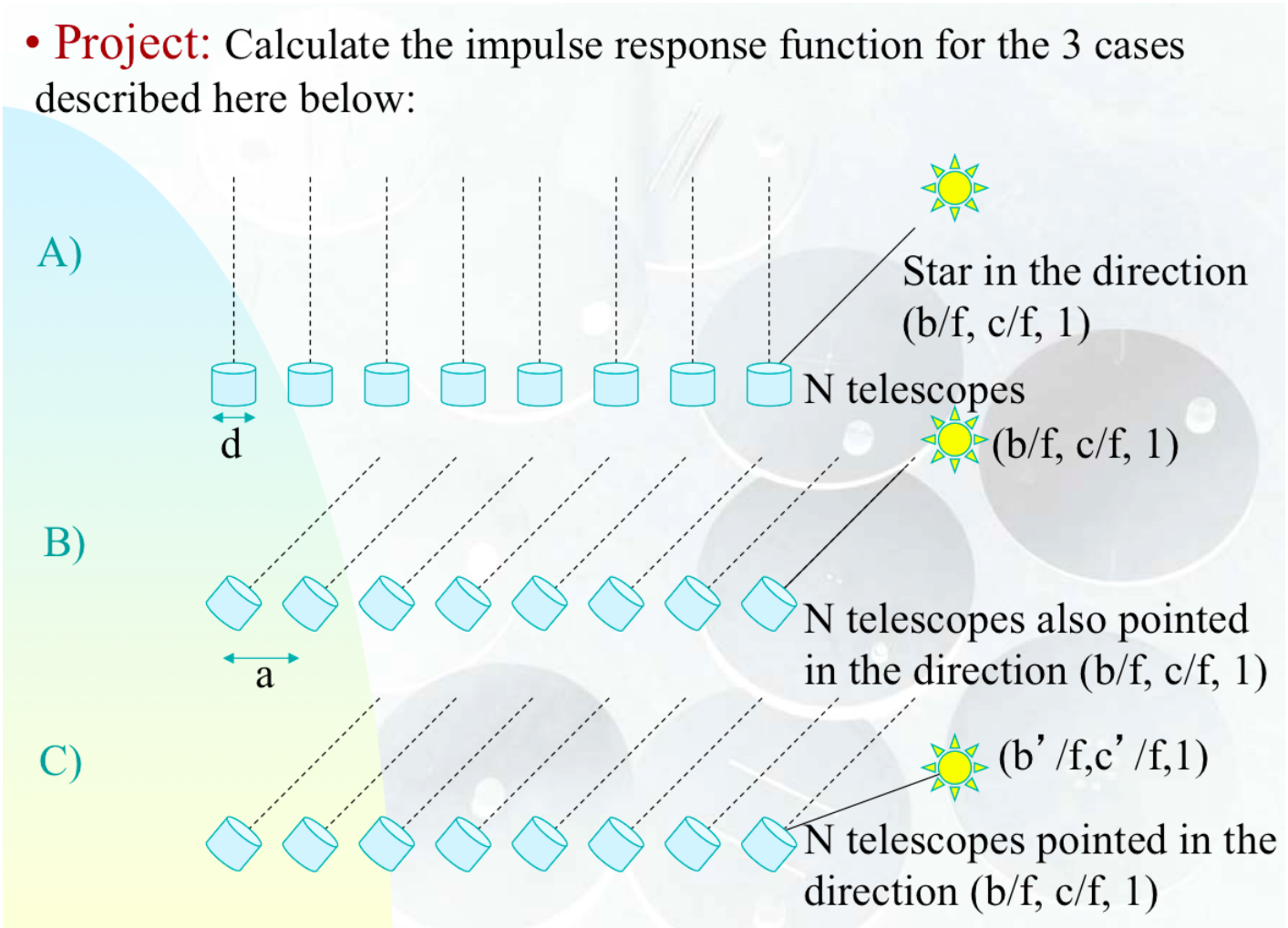

Figure: About closure phases with an optical interferometer.